Journal of the OPTICAL SOCIETY *of* AMERICA

VOLUME 28
No. 7

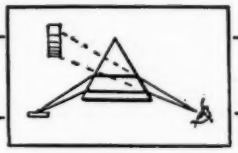

JULY
1938

Experimental Study of the Rate of a Moving Atomic Clock . . . . . HERBERT E. IVES AND G. R. STILWELL 215

Brightness of the Twilight Sky and the Density and Temperature of the Atmosphere . . . . . E. O. HULBURT 227

Tungsten, Mercury and Sodium Illuminants at Low Brightness Levels . . . . . MATTHEW LUCKIESH AND A. H. TAYLOR 237

Photometry of Colored Light Sources . . . . . W. E. FORSYTHE, B. T. BARNES AND ANN L. SHRIDER 241

Experimental Study of Latent-Image Formation by Means of Interrupted and Herschel Exposures at Low Temperature. Measurements of Reciprocity Law Failure at Low Temperature . J. H. WEBB AND C. H. EVANS 249

Apparatus for the Study of the Raman Effect . . . . . A. H. PFUND 264

Spring Suspended and Thermostated Littrow Spectrograph . . . . . NORTON A. KENT AND REGINALD G. LACOUNT 266

Adaptometer for Measuring Human Dark Adaptation . . . . . SELIG HECHT AND SIMON SHLAER 269

Note on an Optical Paradox . . . . . H. W. LEE 276

Published monthly
at Prince and Lemon Sts., Lancaster, Pa.
by the
AMERICAN INSTITUTE OF PHYSICS
Incorporated
175 Fifth Avenue, New York, N. Y.
FOR AND UNDER THE EDITORIAL SUPERVISION OF
THE OPTICAL SOCIETY OF AMERICA

THE OPTICAL SOCIETY OF AMERICA

Officers of the Society

R. C. GIBBS, *President*
Cornell University
Ithaca, New York

K. S. GIBSON, *Vice President*
National Bureau of Standards
Washington, D. C.

L. B. TUCKERMAN, *Secretary*
National Bureau of Standards
Washington, D. C.

HENRY F. KURTZ, *Treasurer*
Bausch & Lomb Optical Company
Rochester, New York

The Board of Directors consists of the above officers; the Editor of the Journal; the Past President; and five directors-at-large.

A. C. HARDY, *Past President*
Massachusetts Institute of Technology
Cambridge, Massachusetts

F. K. RICHTMYER, *Editor*
Cornell University
Ithaca, New York

Directors-at-Large

H. P. GAGE
Corning Glass Works
Corning, New York

G. R. HARRISON
Massachusetts Institute of Technology
Cambridge, Massachusetts

WILLIAM F. MEGGERS
National Bureau of Standards
Washington, D. C.

BRIAN O'BRIEN
University of Rochester
Rochester, New York

A. G. WORTHING
University of Pittsburgh
Pittsburgh, Pennsylvania

Rochester, New York, Section of the Optical Society of America

B. NOYES, *President* G. FASSIN, *Vice President* F. M. E. HOLMES, *Secretary* J. S. CAMPBELL, *Treasurer*
Councillors: F. C. FAIRBANKS, H. F. KURTZ, A. L. SCHOEN, J. H. WEBB, L. A. DUBRIDGE (*ex officio*)

Corporation Members of the Optical Society of America

American Optical Company, Southbridge, Massachusetts
Bausch & Lomb Optical Company, Rochester, New York
Bell Telephone Laboratories, Inc., New York, New York
Corning Glass Works, Corning, New York
Gaertner Scientific Corporation, Chicago, Illinois
Interchemical Corporation, New York, New York
Keuffel & Esser Company, Hoboken, New Jersey
Spencer Lens Company, Buffalo, New York
Arthur H. Thomas Company, Philadelphia, Pennsylvania

THE OPTICAL SOCIETY OF AMERICA was organized in 1916 "*to increase and diffuse the knowledge of optics in all its branches, pure and applied, to promote the mutual interests of investigators of optical problems, of designers, manufacturers and users of optical instruments and apparatus of all kinds and to encourage cooperation among them.*" It aims to serve the interests of all who are engaged in any branch of optics from fundamental research to the manufacture of optical goods.

MEMBERSHIP

Regular Members: "Any person who has contributed materially to the advancement of optics is eligible for regular membership."

Associate Members: "Any person who is interested in optics is eligible for associate membership."

Corporate Members: "Any corporation desirous of encouraging the work of the Society is eligible for corporation membership."

The Society cordially invites to membership all who are interested in any branch of optics, either in research, in instruction, in optical or illuminating engineering, in the manufacture and distribution of optical goods of all kinds or in physiological and medical optics.

ANNUAL DUES

Regular members, $7.50; Associate members, $5.00; Corporate members, $50.00. These dues include subscription to the Society's official journal, the *Journal of the Optical Society of America.*

MEETINGS

The Society holds two meetings per year: An annual meeting in the autumn and a midwinter meeting jointly with the American Physical Society.

For further information concerning the Optical Society of America address the Secretary, Dr. L. B. Tuckerman, National Bureau of Standards, Washington, D. C.

Journal of the
OPTICAL SOCIETY *of* AMERICA

VOLUME 28 JULY, 1938 NUMBER 7

An Experimental Study of the Rate of a Moving Atomic Clock

HERBERT E. IVES AND G. R. STILWELL
Bell Telephone Laboratories, Inc., New York, N. Y.
(Received April 12, 1938)

INTRODUCTION

IN previous papers in this series,[1] various consequences of the alteration of the rate of a clock in motion, which is an essential element in the theory of Larmor and Lorentz, have been discussed. In these papers, this change in clock rate has of necessity been treated as an assumption, since, up to the present time it has not been the subject of independent experimental verification. As was pointed out in these papers, the Michelson-Morley and Kennedy-Thorndyke experiments do not give the necessary information to establish the existence of this change of rate. An experimental search for this phenomenon is of particular interest, because the alteration of clock rate should be manifested as a *positive* effect, instead of the *null* effect characteristic of all other optical experiments.

The first suggestion as to a means by which this positive effect might be observed experimentally came from Einstein and from Ritz over thirty years ago, namely that the newly discovered Doppler effect in canal rays involved velocities of the moving particles high enough to show the expected effect. The experiment, whose crucial nature has been repeatedly emphasized, has been commonly imagined as performed by observing the canal rays at right angles to their direction of motion, and for that reason, has been referred to as "the transverse Doppler effect." For hydrogen canal rays for velocities obtainable without difficulty in the laboratory, namely about 0.005 the velocity of light, a separation of several hundredths of an Angstrom unit is to be expected in the lines due to laterally observed stationary and moving particles.

The experiment, although recognized as of fundamental importance, has commonly been described as beyond experimental feasibility, chiefly for the reason that the light emitted by the moving canal rays in a tube of the conventional design does not consist of a single narrow line, but of a diffuse band altogether too wide to permit the detection of the small displacement indicated by theory (Fig. 1a). Furthermore, in the experiment as usually imagined, where the canal rays are supposed to be observed from the side, it would be extremely difficult to be sure that observation was made exactly at right angles to the direction of the rays, and very small deviations from this direction would introduce shifts of the order of magnitude of the expected effect.

The first of these obstacles to the performance of the experiment has been removed by the development by Dempster[2] of a type of canal-ray tube in which the velocities of the positive par-

[1] Herbert E. Ives, J. Opt. Soc. Am. 27, 177 (1937); 27, 263 (1937); 27, 305 (1937); 27, 310 (1937); 27, 389 (1937).

[2] H. F. Batho and A. J. Dempster, Astrophys. J. 75, 34 (1932).

722 4864 4865
BOSTON UNIVERSITY
COLLEGE OF LIBERAL ARTS
LIBRARY

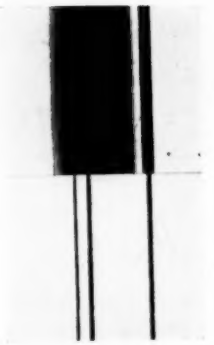

FIG. 1. Canal-ray spectra. (a) Undisplaced and displaced lines in tube of original type. (b) Undisplaced and displaced lines in tube of Dempster design.

ticles all lie within a very narrow range, so that the light emitted by them consists of a definite sharp line or lines (Fig. 1b). The second difficulty, above mentioned, can be avoided by observing not at right angles, but in two directions, with and against the motion of the particles; the observations being made simultaneously by the use of a mirror in the tube. Under these conditions the displaced Doppler lines are observed corresponding to motion toward and away from the observer, and the effect to be observed is a shift of the center of gravity of the displaced lines with respect to the undisplaced line. As shown in an earlier paper of this series[1] this shift of the center of gravity is expressed by the equation $\lambda=\lambda_0(1-V^2/c^2)^{\frac{1}{2}}$ where V is the observed or measured velocity of the positive particles.

APPARATUS AND METHODS OF OBSERVATION

The canal-ray tubes

The experimental test which forms the subject of this paper was performed with hydrogen canal rays, using the blue-green Hβ line, of wave-length 4861 angstroms. The canal-ray tubes were designed along the general lines described by Dempster, as shown in Figs. 2, 3, and 4. The positive particles were produced in a hydrogen arc between the oxide coated filaments F and the grounded element of the double electrode A_1, B_1, the discharge being constricted to the desired region by the shielding electrode D. The double electrode between which the accelerating field is

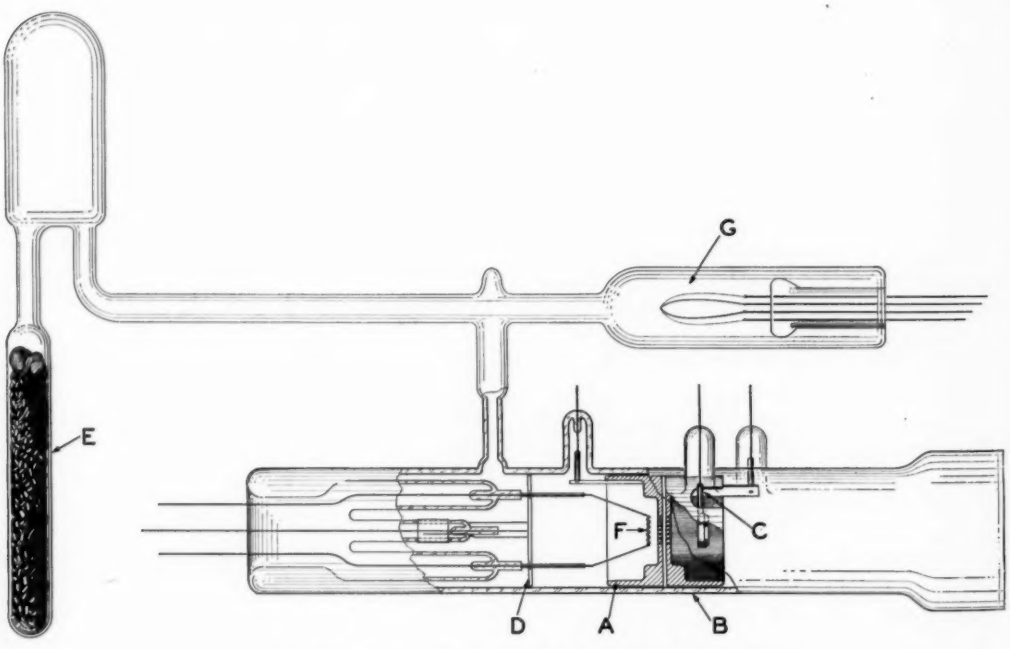

FIG. 2. Diagrammatic representation of canal-ray tube.

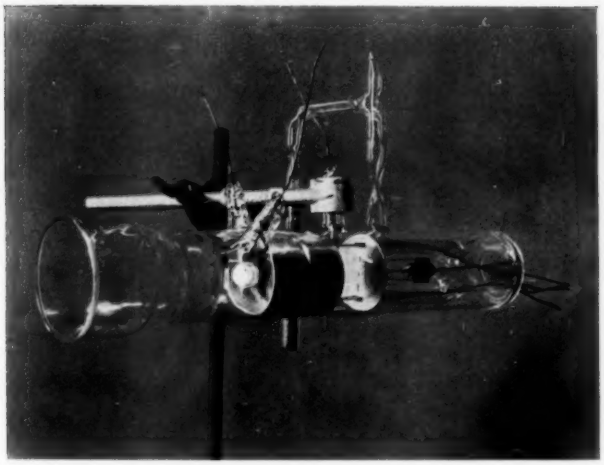

FIG. 3. Side view of canal-ray tube.

applied consists of two aluminum elements separated by 1.5 mm by quartz rod bushings which provide insulation and also hold the electrodes accurately parallel and in alignment. Both electrode units are drilled with 1 mm diameter holes to provide a positive ray beam approximately 1 cm square. The front surfaces and all edges of the accelerating plates are highly polished, to minimize the tendency to sparking which becomes quite bad when the higher accelerating potentials are used.

To one side of the perforations in the front electrode is placed a small concave mirror *C* made from an aluminum coated spectacle lens. The radius of curvature of this mirror is such that it will accurately image an object, such as the slit of the spectrograph, upon itself about 2 centimeters in front of the observation window. The observation window consists of a piece of plate glass fused onto the end of the tube. The small mirror is approximately 7° from the center of the perforations as viewed from its center of curvature. Because of the small rate of variation of the apparent velocity with angle near zero, no difference in apparent velocity of the canal rays as directly viewed and as seen in the mirror, as great as 1/100th of 1 percent can occur with the accuracy of imaging the spectrograph slit upon itself which was possible in the experiment.[3]

[3] With this arrangement the real image which the mirror forms of the discharge is not coincident with the discharge but falls on the other side of the spectrograph slit. It was not believed that this lack of optical symmetry was important when weighed against the accuracy of alignment rendered possible. However, to test this point a tube was constructed furnished with a concave mirror which, by the aid of cross hairs in the discharge path, could be adjusted to image the discharge upon itself. This tube while more difficult to align accurately, gave identical results, as did also a tube with a plane mirror, so that any suspicion that the phenomena observed could be ascribed to optical dissymmetry is untenable.

Hydrogen for the canal rays was stored in the side tube (*E*) containing activated charcoal. The gas pressure in the tube was controlled by the depth of immersion of the side tube in liquid air. The relative gas pressures were measured by the

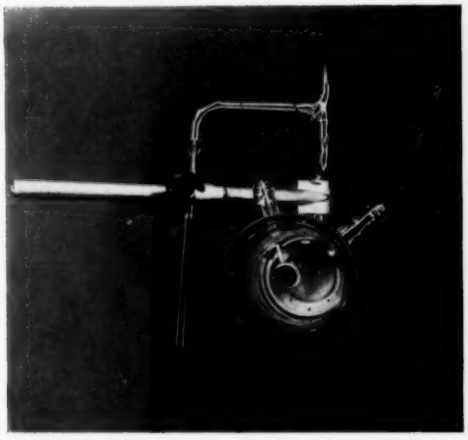

FIG. 4. End-on view of canal-ray tube.

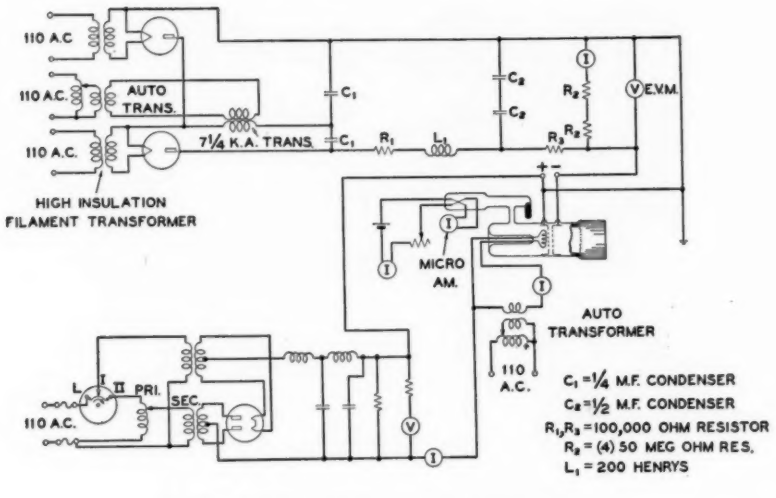

FIG. 5. Electrical circuits used with canal-ray tube.

gauge (G) which is a thermocouple gauge similar to one described by G. C. Dunlap and J. G. Trump;[4] this manometer was previously calibrated against a McLeod gauge to read hydrogen gas pressures between 0.001 mm and 0.1 mm.

The whole tube with its attached charcoal reservoir was baked out while being pumped to eliminate any foreign gases, after which the filaments were activated. Hydrogen gas to a pressure of several millimeters of mercury was admitted to the pump station and the charcoal tube was partly saturated with hydrogen by immersing it part way in liquid air. The tube was then sealed from the pump station.

Electrical power supply and measuring apparatus

The low voltage hydrogen arc was maintained between the cathode (F) Fig. 2 and the grounded accelerating electrode (A) by an a.c. rectifier capable of delivering 400 milliamperes at 100 volts. Fig. 5 shows the electrical circuit diagram and how the connections were made to the canal-ray tube. This arrangement differs from that used by H. F. Batho and Dempster[2] and others, in that the hydrogen arc was maintained in a reverse direction between the first accelerating electrode and cathode instead of between the cathode and a third electrode. Experimentally this method was found to give a more copious supply of positive ions just in front of the holes in the accelerating electrodes with a consequent brighter canal-ray beam.

The high negative potential applied to the accelerating electrode (B) was maintained by an alternating current rectifier capable of delivering up to 30,000 volts d.c. Fig. 5 shows the diagram of the electrical circuit used which is essentially a voltage multiplying circuit. The transformers and associated equipment were selected to have a much greater power rating than was necessary for the performance of this experiment thereby insuring greater steadiness of operation and decreasing fluctuations of the output voltage. The rectified voltage was smoothed by the filter network combination (R_1), (L_1) and (C_2) and fed to the canal-ray tube through the limiting resistance (R_3). The applied d.c. voltage was indicated on a high resistance voltmeter consisting of four 50 megohm resistances (R_2) in series with a zero to one hundred full scale microammeter. The resistors were especially made physically large to have very small temperature coefficient for the small current values used. The resistances were measured and the meter calibrated to read within an accuracy of one percent.

Since it was important in this experiment to hold the applied accelerating potentials very

[4] G. C. Dunlap and J. G. Trump, Rev. Sci. Inst. **8**, 37 (1937).

steady during long photographic exposures an additional voltage reading technique was employed which greatly facilitated the observation of small voltage fluctuations. This consisted of a Wülf electrostatic voltmeter whose sensitivity could be varied with the applied voltage being used. The deflected reed and illuminated scale indicating the applied voltage was projected, greatly enlarged, onto a screen across the room. The sensitivity of this arrangement could be adjusted so that 1/10 of one percent of the voltage indicated by the resistance voltmeter could be easily detected.

Voltage adjustments were made by means of a manual control in the primary circuit of the high potential transformer; this control included a variac step-down transformer and series resistance.

The spectrograph

The dispersing element of the spectrograph used was a metal on glass plane grating made by Professor R. W. Wood. This is approximately 7 inches in diameter with ruling of 15,000 lines to the inch, with grooves so controlled as to throw a very large part of the total light into the first order on one side. In conjunction with the grating were two high quality telescope objectives of approximately 5 feet focus. The grating was mounted at right angles to the axis of the telescope element, under which conditions a normal spectrum is obtained.[5] The whole spectrograph was constructed as a rigid iron box of exactly the dimensions to bring the Hβ line in the middle of the photographic plate. An accurate bilateral slit was mounted so as to be rotatable about its center point with great exactness. Behind the slit was a pivoted observing telescope and extended light source behind a transparent mirror. By observation with this microscope the orientation of the canal-ray tube and its small mirror could be made with extreme accuracy, the adjustment being complete when upon rotation of the slit its reflected image remained exactly coincident with it.

The whole spectrograph was mounted on a heavy steel framework which was arranged to be capable of rotation about a vertical axis, and the apparatus as a whole was placed on a layer of anti-vibration material in a basement room which was thermostatically controlled to hold to a temperature to within 1/10th of a degree centigrade. The arrangement of the apparatus is shown schematically in Fig. 6, and in the photograph, Fig. 7.

A number of appropriate adjusting means were provided, including screw adjustments for translation and rotation of the canal-ray tube, visible in the photograph, Fig. 8. A sighting aperture and telescope were arranged at the collimator lens, by means of which the placing of the mirror in the canal-ray tube so that it was in line with the optical axis of the spectrograph was assured by preliminary adjustment before the use of the microscope at the slit. A small slowly rotating variable sector was provided in front of the photographic plate by means of which the exposures of the various canal-ray lines could be equalized.

Measurement of the spectrograms

The dispersion of the spectrograph was 10.87 angstrom units per millimeter. The displacement due to the Doppler effect for H_2 in the neighborhood of 20,000 volts is about 2 millimeters; the expected shift of the center of gravity of the displaced lines (directly viewed and reflected in the mirror) is about 0.05A or 0.005 mm. This made it desirable to have means for measuring the spectrograms with an accuracy at least 0.001 mm. The measuring microscope used was a Carl Zeiss instrument furnished with a special large diameter reading drum, on which 0.001 mm

[5] A test for the normality of the spectrum produced by the grating-lens combination was made on three lines of the molecular spectrum of hydrogen covering a range of 250A approximately centered about the Hβ line, namely 4719.01A, 4849.32A and 4973.26A. The following figures were obtained for the quantity A/mm:

		A/mm
Interval 4719.01–4849.32A		
Plate A, measured upward	on screw	10.870
" " " downward	" "	10.875
Plate B, " upward	" "	10.876
" " " downward	" "	10.877
Mean		10.874
Interval 4849.32–4973.26A		
Plate A, measured upward	on screw	10.877
" " " downward	" "	10.874
Plate B, " upward	" "	10.872
" " " downward	" "	10.870
Mean		10.873

A hyperbolic deviation from linearity, such as would produce an apparent shift of the center of gravity of the magnitude in question in this investigation would mean a difference of 0.5 A/mm in the quantity for the two wavelength ranges measured.

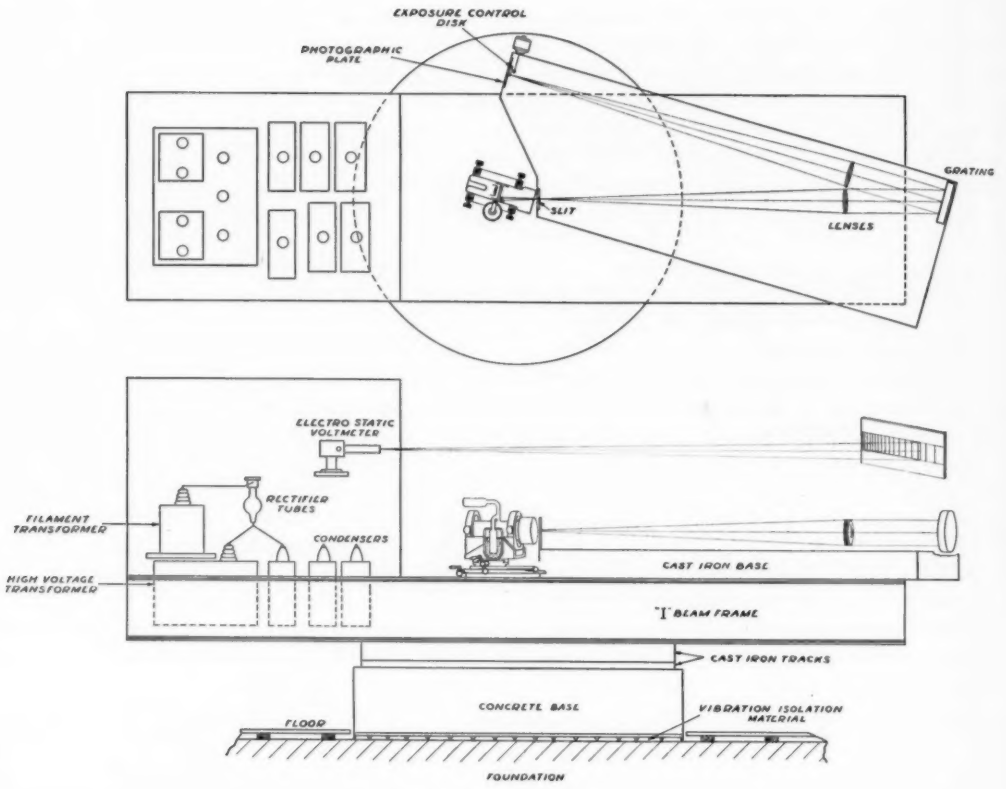

FIG. 6. Plan of apparatus.

could be read directly, and tenths of divisions estimated. The accuracy of the screw was not however to be relied upon for better than 0.001 mm, and so a special measuring procedure was employed, made possible by the approximately symmetrical character of the pattern presented by the displaced lines. A series of measurements were made of separations of the displaced lines from the center, undisplaced line, the latter being accurately located at a chosen point on the screw. The plate was then turned end for end, the center line again placed accurately on the same chosen point of the screw, and the separations remeasured. This procedure was then repeated at several points on the screw, and the mean values of the several series were used. The probable errors of the final values so obtained were found by analysis of the measurements to be about 0.0025A.

OBSERVATIONS

Characteristics of the canal rays

Typical spectrograms obtained in the investigation are shown in Fig. 9. In each the center, undisplaced line is seen, accompanied at either side by two companions, which, by their separations from the center line by distances in the ratio $\sqrt{2}/\sqrt{3}$ are identified as H_2 and H_3, or double and triple atomic hydrogen. No H_1 particles were found in this work.

A fundamental assumption in this experiment is that the light emitted by the excitation of the stationary particles in the tube, and by the excitation of the multiple mass traveling particles, is (except for the predicted second-order change), of the same frequency. Put in another way, the assumption is that in every case the emission is that of the single excited hydrogen atom, to which all the particles must be assumed

FIG. 7. Photograph of apparatus.

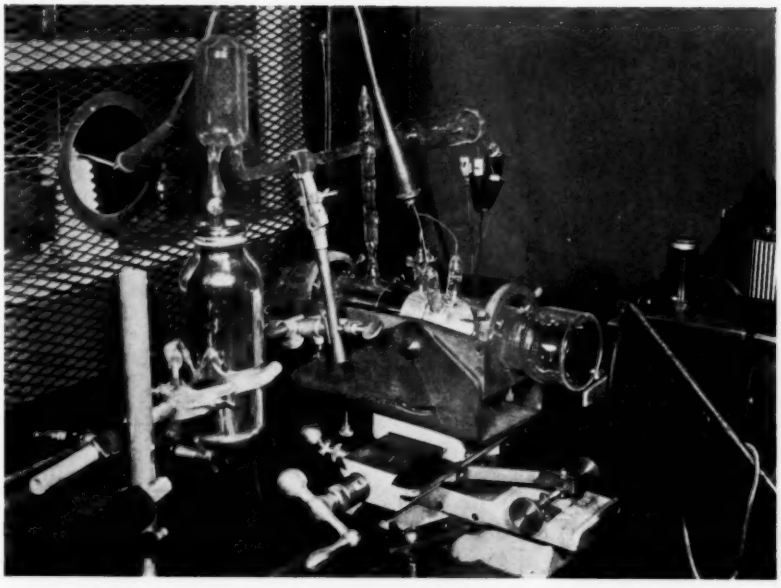

FIG. 8. Tube in place.

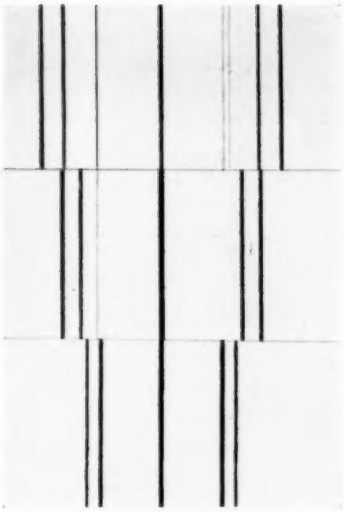

FIG. 9. Spectrograms obtained for several applied voltages.

to revert before emitting light. There is no experimental or theoretical reason for expecting this not to be the case, at least to a high order of approximation, although very considerable changes in the relative intensities and sharpnesses of the canal ray lines occur over the range of voltages and pressures used in this experiment. Thus the center, undisplaced line is very weak, relative to the displaced lines, at voltages below 3000, but is quite sharp. At voltages of 10,000 and over the center line becomes diffuse but with a sharp central core, and is much more intense than the displaced lines. (These differences in intensity do not show in the spectrograms, Fig. 9, as these were made with the variable sector adjusted to equalize the exposures.) At low gas pressures (below 0.005 mm Hg) the H_2 lines are brighter than the H_3; at higher pressures H_3 becomes relatively more intense. The Hβ line is actually a close doublet, of separation 0.09A, but always appeared single and symmetrical in our spectrograms. The possibility of a varying distribution of intensities between the components is not excluded.

In default of evidence to the contrary the assumption above stated has been taken as valid in carrying through the experiment but with recognition of the obligation to scrutinize the final results carefully for any indications that they are significantly affected by the collision and their processes active in the discharge.

Preliminary measurements and choice of conditions

The first measurements made on the spectrograms were used to check the theoretical relationship

$$eE=\tfrac{1}{2}M(V^2/c^2)$$

when E is the voltage between the electrode plates, e the charge on the hydrogen atom, and M the mass of the particle observed. V/c as obtained from the ratio $\Delta\lambda/\lambda$ should agree with the value obtained from the above formula.

In Fig. 10 are shown, by the dashed lines, the computed values of $\Delta\lambda(=\lambda_0(V/c))$, for H_2 and H_3, plotted against the square root of the voltage; and by the marked points, the observed values of $\Delta\lambda$ at seven voltages, selected as described in a later paragraph. These "observed" values are the mean measured displacements of the direct and reflected Doppler lines, increased in the ratio 1/cos 7°, where as previously described, 7° is the angular displacement of the concave mirror from the axis of the beam. This gives the displacement for observation exactly along the beam, which is the quantity directly derived from the fundamental relationship between voltage and velocity, and is the quantity with

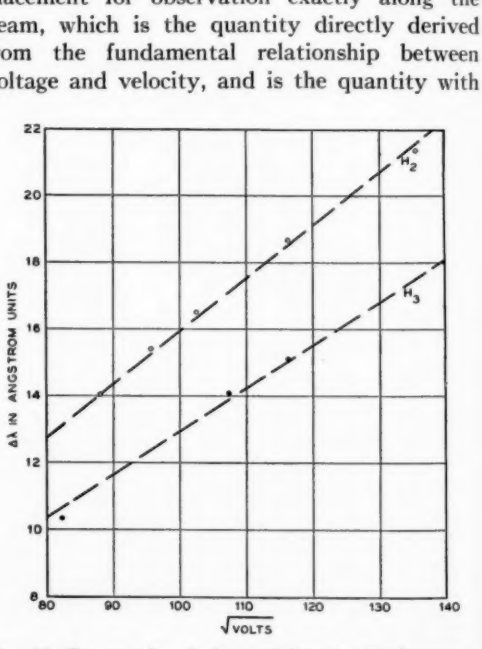

FIG. 10. Computed and observed Doppler displacements.

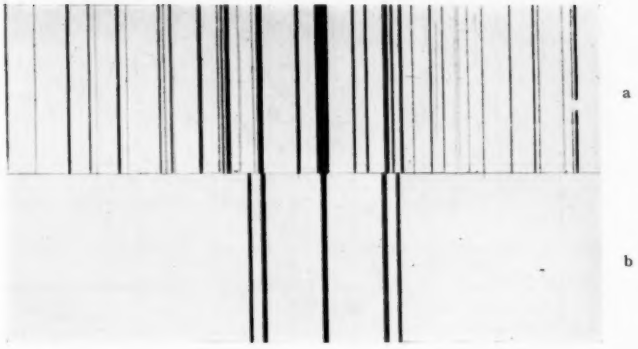

FIG. 11. (a) Molecular spectrum of hydrogen in the neighborhood of Hβ. (b) Canal-ray spectrum for voltage selected to make H_2 lines clear molecular lines.

which the second-order shift is theoretically correlated. The data used in plotting Fig. 10 are assembled in Table I. It will be seen that the observed Doppler displacements show no systematic deviations from the computed and agree with these in general to within about 1 percent.

The next measurements were those to detect and measure the shift of the center of gravity, if existent, of the directly observed and reflected lines. The first measurements revealed very erratic and confusing displacements, which showed no systematic relationship with the orientation of the apparatus or other known variables. The source of these unsystematic shifts of the center of gravity of the displaced lines was found to lie in the presence of faint lines of the second or molecular spectrum of hydrogen. A few lines of this spectrum are obviously present, at the highest voltages, at positions other than those occupied by the canal-ray lines as shown in Fig. 9. However, upon photographing the spectrum of the arc behind the electrodes (Fig. 11) or upon very long exposure of the canal-ray spectrum, a large number of these second spectrum lines appear. While very faint and under exposed in the canal-ray pictures, these lines were found, if they fell close to or partially over the canal-ray lines, to shift the position of these latter enough to vitiate the measurements.

TABLE I.

PLATE	VOLTAGE	LINE	$\lambda_0 V/c$ COMPUTED	MEAN $\Delta\lambda$ OBSERVED ($\Delta\lambda/\cos 7°$)
169	6,788	H_3	10.62A	10.35A
160	7,780	H_2	14.04	14.02
163	9,187	H_2	15.30	15.40
170	10,574	H_2	16.34	16.49
165	11,566	H_3	13.88	14.07
172	13,560	H_2	18.50	18.67
172	13,560	H_3	15.05	15.14
177	18,350	H_2	21.55	21.37

The next step was then to plot the positions of the second spectrum lines with the object of finding which voltages could be used to place the canal-ray lines in clear spaces, in Fig. 12 is shown a plot of the chief second spectrum lines in the neighborhood of the Hβ line, the lines on both red (dashed) and blue (full) sides being plotted together. On the same plot are shown the displacements of the canal-ray lines against the square root of the voltage as measured. Plotted in this way the H_1, H_2 and H_3 Doppler displacements fall on straight lines. As can be seen, the number of available voltages for securing pairs of direct and reflected lines in clear spaces is limited.

After picking voltages corresponding to satisfactorily clear spaces, the next experiments were made with sufficiently rapid plates to make possible obtaining exposures in about one hour. These plates were of too coarse grain for measurements of the highest accuracy, but the short exposure time was desired in order to investigate whether there was any effect due to the orientation of the apparatus with respect to the earth's motion. A series of plates were made, as shown in Table II, with the apparatus pointing

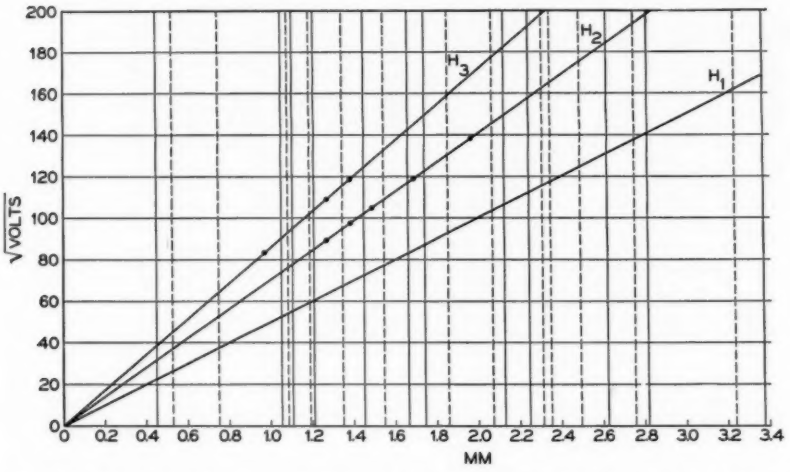

FIG. 12. Chief molecular spectrum lines of hydrogen in the neighborhood of Hβ. Lines to blue side shown full, to red side, dashed.

north, south, east and west, and using a voltage of approximately 18,000. These experiments showed at once that there is a shift of the center of the gravity of the displaced lines, that is, a change of frequency of the light emitted from the canal-ray particles. They showed that this shift was of the order of magnitude to be expected from the theory, and that it was independent of the direction of the apparatus.

An additional experiment made at this stage of the investigation was a test of the possible effect of a magnetic field. Due to the iron of the apparatus, a magnetic field existed at the tube which was fairly constant in direction with respect to the tube, and in amount. This field was neutralized by properly placed coils, and then replaced by one of approximately ten times its strength in the opposite direction. No effects of this variation of the magnetic field were found.

Final results

The final series of plates were then made with the apparatus in one position, using special Eastman type III-J plates which are of fine grain, but of a low speed, requiring all-day exposures. In this series seven different voltages were used ranging from 6788 to 18,356, adjusting as above described to locate the displaced lines in the regions of the spectrum free from molecular lines. These plates gave eight points for measurement, three due to H_3 and five to H_2.

The results are shown in Table III and Figs. 13 and 14. In the table, computations of the expected shift ($\Delta'\lambda$) are made in two ways. In column 4 the quantity $\lambda_0(\frac{1}{2}V^2/c^2)$, which should equal $\Delta'\lambda$, is computed from the values of V/c as derived from the voltage between the electrodes. From the fundamental equation connecting voltage and displacement it appears that since V^2/c^2 is proportional to voltage, $\Delta'\lambda$ so computed should be proportional to voltage, the factor of proportionality being different for the particles of different masses. In Fig. 13 the computed values for H_2 and H_3 are shown by the dashed lines, and the observed values, $\Delta'\lambda$ (6th column) by the circles and dots. These lie along the theoretical straight lines to within the probable errors of the measurements.

TABLE II.

PLATE NUMBER	DIRECTION OF DISCHARGE	OBSERVED SHIFT	$\lambda_0(\frac{1}{2}v^2/c^2)$ COMPUTED FROM OBSERVED V/c
136	N	0.036A	0.0472A
137	N	.052	"
138	S	.050	"
139	E	.045	"
140	W	.051	"
141	W	.047	"
		Mean 0.0468A	0.0472A

In column 5 values of $\Delta'\lambda$ are computed using the observed values of $\Delta\lambda(=V/c)$. This method of computation involves no knowledge of the voltages used, and so is independent of any errors of voltage measurement. The $\Delta'\lambda$'s so computed are shown, plotted against $\Delta\lambda$, by the dashed curves in Fig. 14, and the observed values are again shown by the circles and dots. The agreement is within the probable errors of the measurements, and the results are not significantly different from those plotted in Fig. 13, as should indeed be the case because of the close agreement of the Doppler shifts ($\Delta\lambda$) with the values computed from the voltages.

The conclusion drawn from these experiments is that the change of frequency of a moving light source predicted by the Larmor-Lorentz theory is verified.

Discussion

Characteristics of results

The results graphically exhibited in Figs. 13 and 14 appear to be a satisfactory confirmation of the Larmor-Lorentz theory. It is proper, however, to note features of the experiment and the results which might be improved in further work. Probably the least satisfactory feature is that the displacements of center of gravity which constitute the evidence for the change in frequency are in every case less than the known separation of the components of the Hβ line. This leaves the possibility that some of the observed shift could be due to a variation of relative intensity of these components, under the excitation conditions holding in the tubes. This variety of error could be excluded if voltages at least twice and preferably several times the highest here used could be employed. Radical changes in tube design would be necessary to permit these without a breakdown of the gap between electrodes. A possibility here is provision for continuous pumping to hold the pressures different in different parts of the tube. The same result, without the necessity for such high voltages, could be secured if the single mass particles H_1 could be produced, as these should give twice the shift of the H_2 particles. We have, following suggestions in the literature, tried the introduction of water vapor, and admixtures of helium and neon, but without success.

The lack of positive assurance that the canal-ray particles do actually emit the same frequency, despite changes of voltage and pressure conditions has already been dwelt on. Insofar as explaining the shifts of the center of gravity by a changing frequency of the *undisplaced* line, this appears very unlikely when the results are

Table III.

Plate	Voltage	Line	$\lambda_0(\frac{1}{2}V^2/c^2)$ Computed from Voltage	$\lambda_0(\frac{1}{2}V^2/c^2)$ Computed from Observed $\Delta\lambda$	$\Delta'\lambda$ Observed
169	6,788	H_2	0.0116	0.0109	0.011A
160	7,780	H_2	.0203	.0202	.0185
163	9,187	H_2	.0238	.0243	.0225
170	10,574	H_2	.0275	.0280	.027
165	11,566	H_3	.0198	.0203	.0205
172	13,560	H_2	.0352	.0360	.0345
172	13,560	H_3	.0233	.0237	.0215
177	18,350	H_2	.0478	.0469	.047

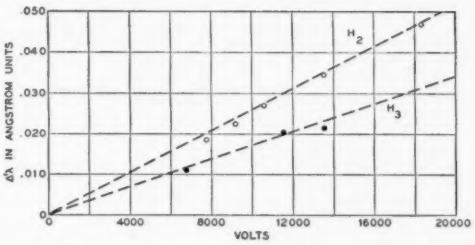

Fig. 13. Computed and observed second-order shifts, plotted against voltage.

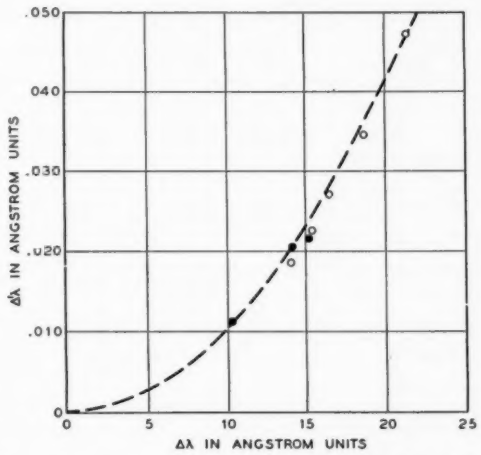

Fig. 14. Computed and observed second-order shifts, plotted against first-order (Doppler) shifts.

plotted for the two kinds of particles at the same voltages, as is done in Fig. 13. If these shifts were due wholly or in part to a change in the center line, the shifts for both kinds of particles would be expected to be the same or to fall on lines inclined otherwise than this precise way. The possibility that the stationary and traveling H_2 and H_3 particles suffer changes of frequency due to collision processes which happen to follow exactly the relation expected from the Larmor-Lorentz theory from velocity changes alone, is remote, even though conceivable. The consistency of our results with the prediction of the theory, over a considerable range of velocities, and for two kinds of particles, can itself in the absence of any other known cause for the observed effect, be taken as evidence for their correctness.

Significance of results

This experiment forms the necessary optical complement to the Michelson-Morley experiment, and the more general form of this experiment due to Kennedy and Thorndyke. The null result of the latter experiment can be explained, on the assumption of a fixed luminiferous ether, by contractions of the apparatus along and across the direction of motion which are in a definite ratio to each other, namely $(1-V^2/c^2)^{\frac{1}{2}}:1$ where V is the velocity of the apparatus and c the velocity of light. From these experiments the contractions are unfixed in absolute amount; i.e., the contractions in the two directions could be $1-V^2/c^2$ and $(1-V^2/c^2)^{\frac{1}{2}}$, etc. For each absolute contraction, there is demanded in general a change in the rate of the clock at the origin of the light signals, and an independent experiment must furnish this rate in order to completely solve the problem. The present experiment establishes this rate as according to the relation

$$\nu=\nu_0(1-V^2/c^2)^{\frac{1}{2}},$$

where ν_0 the frequency of the clock when stationary in the ether, ν its frequency when in motion. It follows then on combining this result with the results of the Kennedy-Thorndyke experiment that the dimensions of the moving apparatus are contracted by the factor $(1-V^2/c^2)^{\frac{1}{2}}$ in the direction of motion, and are unaffected at right angles to that direction.

The Michelson-Morley experiment and Kennedy-Thorndyke experiments, yielding null results, could, of themselves, be equally well explained—and more simply—by assuming an ether entrained by the earth, or a ballistic character of light emission, instead of assuming two concealed conspiring compensations—contractions of dimensions and of clock rates. The present experiment, giving a positive instead of a null result may hence be claimed to give more decisive evidence for the Larmor-Lorentz theory than is given by the experiments which have yielded null results.

The discussion of the consequences of this change in clock rate, the reality of which may be taken as established by this experiment, consists practically of the entire theory of the optics of moving bodies as developed by Larmor and Lorentz. Some of the special consequences of the use of clocks which behave in this way when in motion have been developed in earlier papers of this series.[1]

The Brightness of the Twilight Sky and the Density and Temperature of the Atmosphere

E. O. HULBURT
Naval Research Laboratory, Washington, D. C.
(Received April 4, 1938)

With a calibrated Macbeth illuminometer measurements were made of i_z the brightness of the zenith sky and of i_θ the energy flux across a vertical plane from the twilight horizon for the depression θ of the sun below the horizon from 0° to 13°. For clear sky conditions the i_z, θ and i_θ, θ curves did not change within 30 percent with the season from October, 1937, to April, 1938, and were the same for evening and morning twilight. Calculation from the Rayleigh theory of molecular scattering and the observed i_z and i_θ data showed that within ±30 percent the densities of the atmosphere from sea level to about 60 km were those of the density-height relation known to 20 km and extrapolated for a temperature of 218°K. It follows that the temperature of the twilight temperate zone atmosphere is 218°±15°K from 20 to 60 km. The influence of secondary scattering, determined from i_θ, although small for small values of θ increased rapidly with θ to such an extent that the twilight zenith sky brightness measures gave no indication of the distribution of density above about 60 km.

INTRODUCTION

IN a recent experiment[1] measurements were made of the brightness of a powerful searchlight beam directed upward from which were derived values of the density of the atmosphere to a height of about 22 km. To reach higher altitudes the illumination of sunlight, which is many times brighter than that of a searchlight, may be used. It is only necessary to measure the brightness of the zenith sky during twilight in order to derive, after proper corrections are made, information about the density of the atmosphere to considerable heights. This has been attempted by Fessenkoff[2] and by Link[3] who made sky brightness measurements for θ from about 6° to 18°, θ being the angle of the sun below the horizon.[4] They concluded that their measurements indicated atmospheric densities in the region from 50 to 150 km above sea level much greater than those obtained by simple extrapolation of the density-height relation observed from sea level to 20 km. The conclusion was based on the assumption that effects of secondary scattering were negligible, in contrast to the view expressed by others[4] that secondary scattering may play a preponderating role at the end of twilight. The conclusion appeared strange and the assumption open to question. A further investigation seemed desirable, since the method is the only one yet suggested of obtaining direct knowledge of upper air densities and since no measures were available in absolute units suitable for theoretical calculation; also there were no data from which the secondary scattering might be evaluated. As described below the brightness of the zenith sky and of the secondary scattering have been determined for θ from 0° to 13°. The results show that the densities of the atmosphere from sea level to about 60 km are approximately those of the density-height relation known to 20 km extrapolated for a temperature of 218°K. The influence of secondary scattering although small for small values of θ increases rapidly with θ to such an extent that zenith sky brightness measurements give no trustworthy indication of the distribution of density above 60 km.

The plan of the present investigation was simple. Let A and S, Fig. 1, be the positions of the observer and the sunset or sunrise point, respectively, for a depression of the sun θ. AH is the observer's horizon and Z his zenith. The region EHF is the twilight glow which the observer sees in the western sky after sunset, or in the eastern sky before sunrise. The brightness i_z of the zenith sky above the observer is the total of all the light scattered to him by the

[1] Hulburt, J. O. S. A. **27**, 377 (1937).
[2] Fessenkoff, Astrophysical Observatory, Moscow, Publications, **2**, 113 (1923) (Résumé in French, pages 113–123; complete paper in Russian, pages 7–113).
[3] Link, Comptes rendus **199**, 303 (1934); **200**, 78 (1935).
[4] Measures of twilight sky brightness are recorded by Kimball and Thiessen, Monthly Weather Review **44**, 614 (1916); by Bauer, Danjon and Langevin, Comptes rendus **172**, 2115 (1924); by Dufay, Bulletin Observatoire de Lyons, **10**, No. 9 (1928); and by Smart, Mon. Not. Roy. Ast. Soc. **93**, 441 (1932–33)

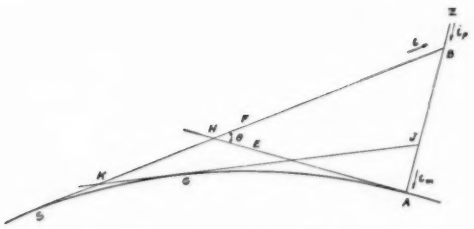

FIG. 1. Geometry of the twilight scene.

atmosphere along ABZ. In the region ZB the air is illuminated by the direct light of the sun i and in the region BA by the light of the twilight glow i_g. Measurements were made of i_z and i_g.

Denote the downward scattered light from ZB and BA by i_p and i_m, respectively. Then

$$i_z = i_p + i_m. \tag{1}$$

The molecular density n of the atmosphere to great heights was assumed. From n together with i and i_g, respectively, i_p and i_m were calculated from the Rayleigh theory of molecular scattering. Their sum was compared with the observed values of i_z to determine the correctness of the assumed values of n.

EXPERIMENTAL

Brightness measurements were made visually with a Macbeth illuminometer, Leeds and Northrup Company, equipped with a blue filter over the photometer lamp. The blue filter, selected by trial, rendered the field of the instrument approximately the same color as the sky. The color match, although satisfactory, was not perfect, the illuminometer field being a little greener than the zenith sky. In more detail, as the sun progressed below the horizon the zenith sky appeared at first a little purpler than the field, then about the same color as the field, and finally bluer than the field; this indicated that the spectral distribution of the zenith sky light changed slightly with θ during the twilight period. Curve 1, Fig. 2, is the transmission curve of the blue filter and curve 2 is the spectral energy curve of the illuminometer lamp through the blue filter. Curve 3 is the spectral energy curve of sunlight outside of the atmosphere and curve 4 the spectral energy curve of sunlight scattered by the air molecules calculated from curve 3 by means of the Rayleigh scattering equation (6.9). Curve 4 is approximately the spectral energy curve of the zenith sky during twilight, and indicates a light more blue or more purple in tint than that of curve 2. Multiplying the curves by the visibility curve of the eye yielded two curves of similar contour in accord with the observed color match.

The illuminometer was calibrated by means of a standard tungsten lamp burning at a known temperature;[5] multiplying the illuminometer readings by the calibration factor gave the energy flux from the illuminated region. It does not seem necessary to describe the details of the calibration here in spite of the fact that all of the quantitative results depended entirely on the calibration. The field of view of the illuminometer was a cone of about 4° angular diameter. By means of three neutral filters a range of intensity of 10^6 could be covered. In the case of the zenith sky the illuminometer was pointed vertically upward; the measurement gave i_z, the energy flux from the sky in ergs sec.$^{-1}$ per unit solid angle. In the case of the twilight glow measurements were made of the brightness of a white plaque of diffuse reflectivity 0.8 held in a vertical plane facing the eastern or western horizon over the sun; the measurements led to i_g erg cm^{-2} sec.$^{-1}$, the flux of energy in an approximately horizontal direction at the observer from

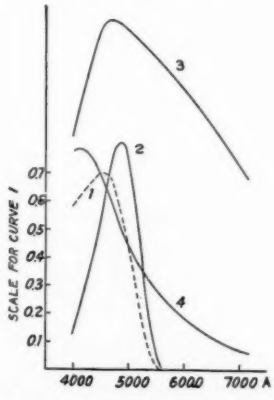

FIG. 2. 1, Transmission of filter; 2, 3 and 4, spectral energy curves of tungsten lamp through filter, sunlight outside of the atmosphere, and sunlight scattered by air, respectively.

[5] The lamp was standardized at the National Bureau of Standards by Dr. H. T. Wensell.

the twilight glow. Readings were taken at known times usually about 1 minute apart. From the time and the latitude and longitude, θ was calculated from astronomical formulae, θ being the depression of the sun, i.e., the angle between a plane tangent to the earth at the observer and a line joining the centers of the earth and sun. Neglecting atmospheric refraction the altitude h of the boundary of the earth's shadow above the observer, i.e., AB of Fig. 1, is given by

$$h = r(\sec.\ \theta - 1), \qquad (2)$$

where r is the radius of the earth.

All observations were made from a hill on the edge of the Potomac river. During many periods of clear sky from October 1937 to April 1938, i_z was observed throughout morning and evening twilight for θ from 0° to 13°, or h from 0 to 160 km. For $\theta > 13°$ i_z was too small to be readily measured with the illuminometer. Although the brighter stars were beginning to be visible at $\theta = 9°$ there was considerable daylight illumination in the zenith sky and hence the measurements were not affected by relatively faint luminous apparitions as stars, the zodiacal light and the light of the night sky. No measurements were made when the moon was brighter than the first quarter. There was no disturbing artificial illumination. A few series of values of i_z erg sec.$^{-1}$ per unit solid angle are shown by dots plotted as $\log_{10} i_z$ against θ in Fig. 3; the complete series of values were too numerous to be put in a single figure. The average of the dots is shown by the i_z curve. It is seen that individual readings departed from the average by as much as 40 percent; the curve was considered to be correct within about ±30 percent as far as instrumental readings were concerned. The values of h from (2) corresponding to θ are also marked on Fig. 3.

The i_z, θ curve was the same for evening and morning twilight and did not change with the season from October 1937 to April 1938 for clear sky conditions. The march of i_z with θ was a consistent and reproducible phenomenon and was repeated day after day with numerical precision (within ±30 percent). In accord with theory, as discussed later, it was not affected by a heavy bank of clouds rising over the sunset (or sunrise) sky nearly to the zenith as long as the zenith sky remained uncovered. It remained

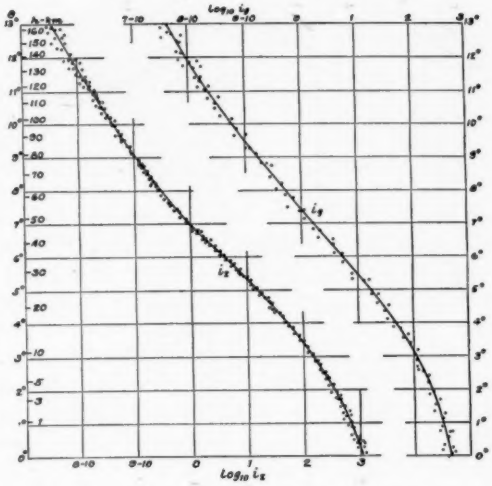

FIG. 3. Brightness of zenith sky i_z, and of twilight horizon i_θ.

the same when observed through a hole through clouds in an otherwise completely overcast sky. When the sky was noticeably hazy i_z was usually below its clear sky value. There were a few cases in which i_z seemed abnormally low and the sky normally clear, but in no case were abnormally high values of i_z encountered. On the whole when the twilight zenith sky appeared to the eye to be free from haze and clouds the i_z values were those of the curve of Fig. 3, and when the sky was visibly impure the i_z values departed from those of the curve. However, measurements of i_z accurate to a few percent would undoubtedly reveal variations due to visually imperceptible meteorological influences.

In the case of the i_θ measurement, just as for i_z, a close but not exact color match was obtained. The color of the white plaque illuminated by the twilight glow was whiter than the photometer lamp through the blue filter for $\theta < 3°$ and slightly bluer for $\theta > 5°$. This was due to the color change of i_θ with θ; i_θ at first was whiter than the blue sky because of the red, orange, green, and blue sunset (or sunrise) arcs in the west (or east) and became bluer with increasing θ.

A few of the observed values of i_θ erg cm^{-2} sec.$^{-1}$ are plotted as $\log_{10} i_\theta$ against θ in Fig. 3 for a clear and cloudless eastern or western sky; the average of all of the values of i_θ is given in the smooth curve. No differences in i_θ for sunset

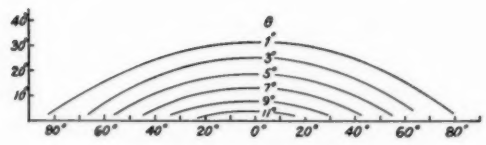

FIG. 4. Area of twilight glow.

or sunrise conditions were observed, and no change with the season from October, 1937, to April, 1938. Only values of i_g for clear sky conditions were recorded, for clouds or haze over the twilight glow *EHF*, Fig. 1, rendered the values of no meaning in the present investigation. As illustrated in Fig. 3 the i_g points for different days showed on the whole more scatter than the i_z points, possibly because of the effects of haze or clouds over the twilight glow below the horizon of the observer and hence unnoticed. The usual routine consisted in recording i_g and i_z at alternate minutes during the twilight period. Since conditions of a clear zenith sky were more frequent than those of a clear twilight glow sky more values of i_z than of i_g were obtained.

A third series of observational data, necessary to the determination of i_m, consisted in the approximate angular dimensions of the twilight glow *EHF*, Fig. 1, as viewed from *A*. The data are given in the curves of Fig. 4. The brightest region of the twilight glow was about 5° above the horizon over the sun for $\theta<9°$; each curve of Fig. 4 gives for a specified θ the contour in the sky where the brightness was about $\frac{1}{3}$ the maximum brightness. For $\theta>2°$ more than $\frac{2}{3}$ of i_g came from the region of the sky embraced by each curve. For $\theta<2°$, i.e. for the sun below and near to the horizon, the twilight glow spread over the entire sky and the curves were uncertain.

CALCULATIONS

The molecular density n of the atmosphere at high levels was obtained by extrapolation of the n, z relation observed in lower levels, z being the altitude above sea level. In Table I are given the values of n derived[6] from Humphreys'[7] tabulations based on average European observations of the temperatures and pressures to about 20 km. The values of $\log_{10} n$ are plotted as dots against z in Fig. 5. Humphreys gives two tables of atmospheric density, one for summer and one for winter; they differ by only 8 and 16 percent at $z=20$ and 40 km, respectively, and would be barely distinguishable from the average dots on the scale of Fig. 5. From about 11 to 20 km the observed temperature was about 218°K and the dots fell on a straight line. Extending the line to high levels yielded the extrapolated values of n, shown in Table I for $z>20$ km, assuming that throughout the high levels $t=218°$K and the atmospheric composition was the same as at sea level. The curve of Fig. 5 is made up approximately of two straight lines, given by

$$n=n_0e^{-pz}, \tag{3}$$

where $p=1.11\times10^{-6}$ and 1.54×10^{-6} below and above 10 km, respectively. For an isothermal atmosphere

$$p=mg/kt, \tag{3.1}$$

m being the mass of the average air particle, g the acceleration of gravity at the height z and k the Boltzmann constant.

It is assumed that (3) is approximately valid to heights which, although relatively great, are small with respect to the radius of the earth. Then the total number n_1 of molecules in a vertical column above z is from (3)

$$n_1=\int_z^\infty ndz=n/p. \tag{3.2}$$

A more rigorous extrapolation would take into account the curvature and rotation of the earth and other factors; however, it would differ but little from (3.2) for $z<300$ km.

If a beam of unpolarized light of intensity i_λ erg cm^{-2} sec.$^{-1}$ and wave-length λ passes

TABLE I. *Average temperature and molecular density of the atmosphere.*

z	t	n	z	t	n
0 km	275°K	2.61×10^{19}	80 km	218°K	1.70×10^{14}
10	219°	8.60×10^{18}	90	218°	3.59×10^{13}
20	218°	1.86×10^{18}	100	218°	7.82×10^{12}
30	218°	3.95×10^{17}	110	218°	1.66×10^{12}
40	218°	8.32×10^{16}	120	218°	3.43×10^{11}
50	218°	1.77×10^{16}	130	218°	7.28×10^{10}
60	218°	3.80×10^{15}	140	218°	1.56×10^{10}
70	218°	8.03×10^{14}	150	218°	3.42×10^{9}

[6] Reference 1, Table II.
[7] Humphreys, *Physics of the Air*, second edition (1929) p. 74.

through a gas of refractive index μ_λ and molecular density n, the intensity $i_{s\lambda}$ of the light scattered per unit solid angle at an angle ϕ to the beam is

$$i_{s\lambda}=i_\lambda 2\pi^2(\mu_\lambda-1)^2(1+\cos^2\phi)/n\lambda^4. \qquad (5)$$

Eq. (5) is derived from the Rayleigh[8] theory of scattering by particles small with respect to λ. Integrating (5) over a sphere gives the Rayleigh expression for β_λ the attenuation due to scattering,

$$\beta_\lambda=32\pi^3(\mu_\lambda-1)^2/3n\lambda^4. \qquad (6)$$

Now
$$\mu_\lambda-1=\alpha_\lambda n, \qquad (6.3)$$

where α_λ is a function of λ. α_λ has been measured[9] for air throughout the wave-length region from 2000 to 10,000A. Substituting (6.3) in (5) yields

$$i_{s\lambda}=i_\lambda 2\pi^2 n\alpha_\lambda^2(1+\cos^2\phi)/\lambda^4, \qquad (6.5)$$

which expresses the scattered intensity explicitly in terms of the molecular density n. Similarly, putting (6.3) into (6) gives

$$\beta_\lambda=32\pi^3\alpha_\lambda^2 n/3\lambda^4. \qquad (6.6)$$

In the case of scattering at right angles to the beam ϕ is 90° and (6.5) becomes

$$i_{s\lambda}=i_\lambda 2\pi^2 n\alpha_\lambda^2/\lambda^4, \qquad (6.9)$$

or $\quad i_{s\lambda}=i_\lambda s_\lambda n, \quad$ where $\quad s_\lambda=2\pi^2\alpha_\lambda^2/\lambda^4. \qquad (7)$

Curve 3, Fig. 2, is the spectral energy curve of sunlight outside of the atmosphere[10] and curve 4, calculated from curve 3 and (6.9), is the spectral energy of sunlight scattered by the atmosphere; curve 4 refers approximately to the twilight sky. If the light of total intensity i is distributed over a spectral region the total scattered light i_s is found by integrating (7) over the region. Then

$$i_s=\int i_{s\lambda}d\lambda=\int i_\lambda s_\lambda n d\lambda=n\int i_\lambda s_\lambda d\lambda,$$

which may be written

$$i_s=in\frac{\int i_\lambda s_\lambda d\lambda}{\int i_\lambda d\lambda}\equiv ins, \qquad (7.2)$$

[8] Rayleigh, Phil. Mag. **51**, 107, 274 (1871); **47**, 375 (1899).
[9] Meggers and Peters, Bul. Nat. Bur. Stand. **14**, 731 (1918).
[10] *Smithsonian Physical Tables* (1933), p. 608.

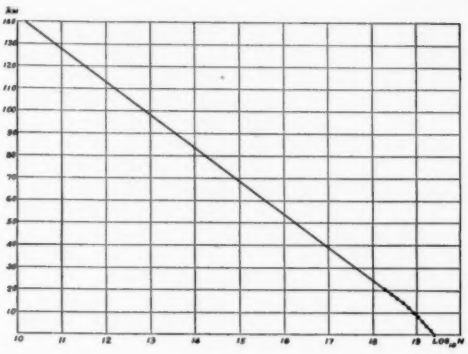

FIG. 5. Density n of the atmosphere.

where s is the ratio of the integrals. For sunlight outside of the atmosphere the solar constant, i.e., the flux in all wave-lengths, is 1.36×10^6 erg cm^{-2} $sec.^{-1}$, the flux i in the visible spectrum from 400 to 720$\mu\mu$ is 6.83×10^5, and $s=3.42\times10^{-28}$ as determined from the areas under curves 3 and 4, Fig. 2. s is the fraction of the energy in the visible wave-lengths of sunlight scattered at right angles per unit solid angle per air molecule.

A calculation of i_p requires the determination of the spectral energy distribution of the sunlight at each height z in the region BZ, Fig. 1. This in turn requires consideration of the effects of the finite angular size of the sun seen from the earth and of the refraction and attenuation by the atmosphere of solar rays passing over the sunset point S, Fig. 1, to BZ.

The radius of the solar disk subtends an angle $\delta=16$ minutes of arc at the earth. Neglecting, for the moment, atmospheric refraction and attenuation, let MS and NS, Fig. 6, be lines from the upper and lower edges of the solar disk, respectively, tangent to the earth; BS is the line from the center of the sun tangent to the earth. Since we deal with the distance AS always less than 13°, MZ is approximately vertical and perpendicular to BS. Above N the intensity is that of full sunlight i_0; below M the intensity is zero, this being the region of shadow. Let y be the angular distance measured up from M; the distance MN is 2δ. The intensity i of the sunlight in the penumbra at any point

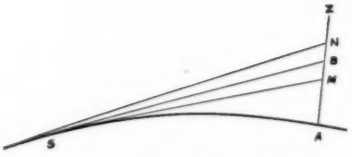

FIG. 6. Penumbra of earth's shadow.

between M and N is

$$i=i_0\{\pi\delta^2/2+(y-\delta)[\delta^2-(y-\delta)^2]^{\frac{1}{2}} + \delta^2 \sin^{-1}(y-\delta)/\delta\}/\pi\delta^2. \quad (7.3)$$

i from (7.3) is plotted in curve 1, Fig. 7.

The intensity $i_s=ins$ of the light scattered downward was calculated from (7.2) for each value of y, or corresponding level z, and is plotted in curve 2, Fig. 7. Then

$$i_p=\int_M^\infty i_s dz, \quad (7.4)$$

and is given by the area under curve 2.

Suppose that the sun were a point source concentrated at the center of the sun and giving the same i_0. There is then no penumbra; above B, Fig. 6, the intensity is i_0 and below B is zero. The intensity $i_s'=i_0ns$ of the downward scattered light at each level z was calculated from (7.2) and is plotted in curve 3, Fig. 7. In this case

$$i_p=\int_B^\infty i_s' dz, \quad (7.5)$$

and is given by the area under curve 3. Calculation shows that (7.4) is about 2 percent greater than (7.5) for $\theta=4°$ and about 6 percent greater for $\theta=11°$. In brief, (7.5) is approximately the same as (7.4). Therefore, in any calculation of i_p accurate to about 5 percent the sun may be taken as a point source at its center. The result simplifies subsequent calculations very much.

Attenuation of the rays of the sun by the atmosphere is assumed to be due only to scattering by air molecules according to the Rayleigh equation (6.6). Haze will produce an additional degradation of the rays which pass sufficiently close to the earth. The amount of haze present in any particular case was not known and its effects cannot be calculated, but as shown later they are not important as long as there is not too much haze. Referring to Fig. 1, let SB be x

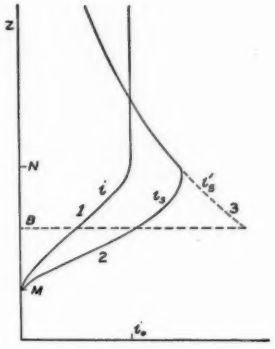

FIG. 7. Penumbra curves.

and BA be z; let r be the radius of the earth. Then $x^2=(r+z)^2-r^2$, and since z is much less than r, $x\doteq(2rz)^{\frac{1}{2}}$. Differentiating and multiplying each side of the equation by n of (3) gives

$$ndx=(r/2)^{\frac{1}{2}}n_0e^{-pz}z^{-\frac{1}{2}}dz. \quad (7.9)$$

Let n_2 be the total number of air molecules in the path of a solar ray which passes entirely through the atmosphere at a point of nearest approach to the earth where the molecular density is n_0 and the height z_0. Then r in (7.9) must be replaced by $r+z_0$, and

$$n_2=2\int_0^\infty ndx.$$

From (7.9)

$$n_2=n_0[2(r+z_0)]^{\frac{1}{2}}\int_0^\infty z^{-\frac{1}{2}}e^{-pz}dz,$$

$$=n_0[2(r+z_0)/p]^{\frac{1}{2}}\int_0^\infty (pz)^{-\frac{1}{2}}e^{-pz}dpz,$$

$$=n_0[2(r+z_0)/p]^{\frac{1}{2}}\Gamma(\tfrac{1}{2}),$$

$$=n_0[2\pi(r+z_0)/p]^{\frac{1}{2}}. \quad (8.4)$$

In some cases the integral did not extend to infinity and was evaluated by expansion in series. In most cases, however, (8.4) served as a sufficiently close approximation.

By means of (8.4), (6.6) and curve 3, Fig. 2, the spectral energy curves were calculated of solar rays after passing through the atmosphere at various distances z_0 of closest approach to the surface of the earth. The curves are given in

Fig. 8; the curve for $z_0=\infty$ is the same as curve 3, Fig. 2, for sunlight outside of the atmosphere. Because of the change in the slope of the curve of Fig. 5 at 10 km a minor numerical approximation entered into the calculation of the curves for $z_0<10$ km. The curves are the numerical representation of the reddening of the twilight sky near the horizon. Multiplying each ordinate of the curves of Fig. 8 by s_λ of (7) produced the family of curves of Fig. 9, which are the spectral energy curves of the light of the respective curves of Fig. 8 scattered by air molecules.

Solar rays passing into the atmosphere are bent downward by atmospheric refraction. The total deviation of the ray from infinity, i.e., outside of the atmosphere to closest approach z_0 is proportional to the atmospheric density at z_0, and for the ray tangent to the surface of the earth, i.e., $z_0=0$, is about 68 minutes of arc. The height of any point of a ray is determined from the ray paths.[11]

From the foregoing results i_p was calculated for various values of θ. The details are tedious and obvious and may be described by giving one example. Consider the calculation of i_p for $\theta=6°\ 25'$ corresponding to $h=40$ km from (2). The ray of original intensity 6.83×10^5 erg cm^{-2} sec.$^{-1}$ for which $z_0=10$ km is reduced by absorption to $0.14\times6.83\times10^5=9.56\times10^4$ (from Fig. 8), is bent downward 17.6′ by refraction, is spread out by dispersion, and finally passes above A, Fig. 1, with an intensity 6.20×10^4 erg cm^{-2} sec.$^{-1}$ at an altitude of 46.6 km where $n=2.98\times10^{16}$ air molecules cm^{-3}. Then from (7.2) and Fig. 9 $i_{pz}=6.28\times10^{-7}$ erg sec.$^{-1}$, where i_{pz} erg sec.$^{-1}$ denotes the downward scattered energy per unit solid angle per cm^3 of air at a height z. The value is plotted at the point marked 10 on the i_{pz}, z curve for $\theta=6°\ 25'$ of Fig. 10. Similarly, the other points of the curve were determined for the rays of various values of z_0 marked on the curve. i_p is given by the area under the curve or

$$i_p=\int_{36}^{\infty} i_{pz}dz, \tag{9}$$

which is 1.82 erg sec.$^{-1}$. The spectral energy curve of i_p being a composite of the curves of Fig. 9, is slightly more intense in the longer wave-lengths than curve 4, Fig. 2.

In like manner the other i_{pz}, z curves of Fig. 10 were determined and the values of i_p calculated from (9) as a function of θ. The i_p, θ curve is given in curve 2, Fig. 11 and the values are tabulated in column 5, Table II. For comparison the observed average i_z curve of Fig. 3 is plotted in curve 1, Fig. 11; within the error of experiment it agrees with the theoretical curve 2 for θ from 0° to about 6°, or h from 0 to about 40 km. The result establishes the correctness of the

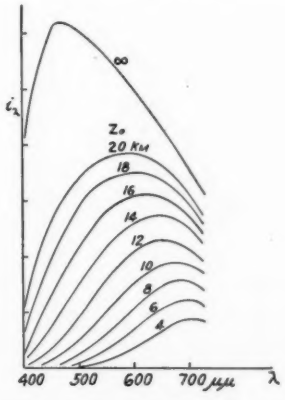

FIG. 8. Spectral energy curves of sunlight absorbed by the atmosphere.

[11] The exact paths of rays through the atmosphere have been calculated by J. Sweer of this laboratory. His work will appear in a separate paper.

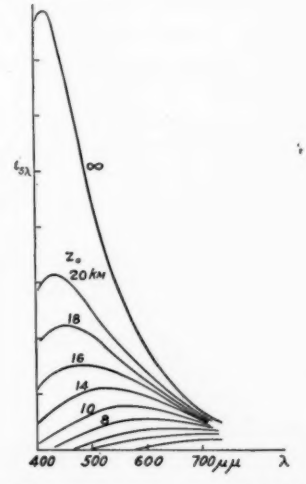

FIG. 9. Spectral energy curves of the light of the curves of Fig. 8 scattered by the atmosphere.

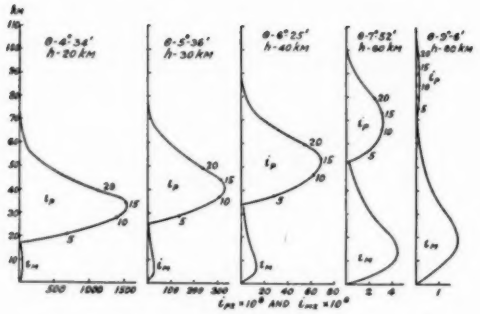

FIG. 10. Curves of zenith twilight sky light.

values of n of Table I and Fig. 5 to about 40 km for the twilight atmosphere. The small departure between curves 2 and 1 for θ from 2° to 5° is not regarded as of much significance. It is nearly within the variation of experiment; it may be real and attributable to slight haze below 20 km.

In order to calculate i_m from the observed values of i_g consider a point J on AB, Fig. 1. Let JGK be a tangent to the earth at G; the two points J and G "see" the same twilight glow region at and above K. Neglecting atmospheric absorption and refraction the flux i_j and i_g at J and G, respectively, from the twilight glow depend on the solid angles ω_j and ω_g subtended by the glow at J and K according to

$$i_j = i_g \omega_g / \omega_j. \tag{9.3}$$

ω_g and ω_j were calculated from the curves of Fig. 4 and the known values of GK and JK. i_j was then calculated for various points along AB for various values of θ. The influence of atmospheric absorption and refraction on the values of i_j is difficult to determine. An exact calculation would require, among other unavailable data, the brightness of all portions of the twilight glow regions drawn in Fig. 4. Because the light from the twilight glow on the whole traverses less atmosphere in passing to J than in passing to G, and because of downward refraction, approximate calculation indicates that i_j of (9.3) should be increased by a factor between 2 and 6 for $AJ > 20$ km. Accordingly i_j for J at 10, 20, 30 and 40 km has been multiplied by a factor $f = 1, 2, 3$ and 4, respectively. The values of i_j are not presented here.

The downward scattered light i_{mz} at J was calculated from i_j by means of (7.2) assuming, in approximate accord with observation for $\theta > 3°$, that the spectral distribution of i_j was that of curve 4, Fig. 2. On this assumption (7.2) is

$$i_{mz} = i_j n s, \tag{9.4}$$

where $s = 4.78 \times 10^{-28}$. The values of i_{mz} are plotted in the lower curves of Fig. 10. i_m is given by the area under the i_{mz}, z curve, or

$$i_m = \int i_{mz} dz, \tag{9.5}$$

the integral being taken from A to B, Fig. 1. The values of i_m are in column 6. Table II. Although the factor f which entered into the determination of i_m is fairly large and uncertain, its influence on i_m is less than a factor of 2. Hence i_m is considered to be correct with a factor of 2. No quantitative theory of i_g is offered here. The twilight glow arises from sunlight scattered in the atmosphere but no attempt is made to calculate i_g from the scattering formulae; a calculation would be complicated.[12] We have merely measured i_g and have calculated i_m from it; i_m arises from multiple scattering.

The sum of i_p and i_m should be i_z. $i_p + i_m$ is tabulated in column 7, Table II, and agrees

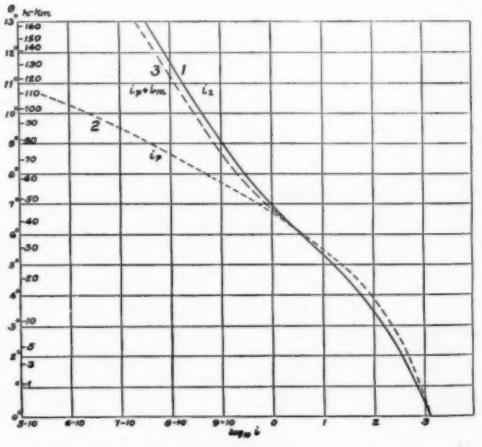

FIG. 11. Curve 1, observed, and curve 3, theoretical, zenith twilight sky brightness.

[12] Raman, *Molecular Scattering of Light* (1922), p. 39, indicated that he had attempted to formulate a quantitative theory of the intensity of twilight without, however, complete success.

within the error of experiment and calculation with the observed values of i_z in column 3; its logarithm is plotted in curve 3, Fig. 11. The values of i_p+i_m are open to two small corrections which counteract each other to some extent and hence are neglected, the one due to vertical attenuation and the other to light entering the region of i_p in addition to the direct rays of the sun. Because of atmospheric attenuation of the zenith sky light as seen by the observer, the values of i_p+i_m should be decreased by about 10 percent, for from (6.6) wave-lengths 6500A and 4500A are decreased 4 and 21 percent, respectively, in passing vertically through the atmosphere. Light other than the direct rays of the sun, such as light of the twilight glow i_g, passing into the region of i_p will increase i_p+i_m by an amount considerably less than 20 percent, since the brightness of the illumination from the sky on a sunny day is only about $\frac{1}{5}$ that from the sun. For this reason there is no entry for i_m at $\theta=0°$ in Table II. It is much smaller than i_p, but its exact value cannot be derived simply from the present measurements; it could of course be determined from an easily arranged experiment.

Conclusions

It is seen from Table II, or Fig. 10, that i_p is larger than i_m for $h<60$ km, or, in other words, that the zenith sky light is mainly due to light scattered from the atmosphere lighted by the direct rays of the sun. i_p is calculated from the molecular density n above h. Therefore the agreement of i_p+i_m with i_z indicates that n of Table I for temperate latitudes during twilight is correct within ± 30 percent for altitudes up to about 60 km. For $\theta>8°$, or h above 60 km, i_m is much greater than i_p; i_m is due to scattered sunlight rescattered mainly from levels below 30 km as shown by the i_m curves of Fig. 10. Therefore the twilight sky measurements lead to no information about n in levels above 60 km.

A repetition of the present investigation might be profitable, preferably with higher precision and from a mountain or other locality where a clear atmosphere prevails; possibly approximately monochromatic light could be used although this might be difficult. Polarization observations and data of the sky brightness at other points than the zenith would contribute further details of twilight phenomena. Data obtained during the long twilight of high latitudes, or during a solar eclipse might be of exceptional interest. However, in view of the rapidity of the decrease of i_p and the increase of i_m with increasing θ, it is doubtful whether twilight sky brightness measurements can yield any exact values of atmospheric densities much above 60 km. The conclusions of various writers[2, 3, 13] that twilight phenomena offer information about the atmosphere in reaches above 80 or 100 km appear to need correction, for the results of the present investigation indicate that phenomena which were thought to arise from primary scattering in relatively high levels probably arise from secondary scattering in relatively low levels.

The explanation of the small or negligible effect on the brightness of the zenith twilight sky occasioned by clouds over the sunset or sunrise horizon emerges from the curves of Fig. 10. Clouds are usually confined to heights below 8 km, and it is seen from the curves of i_p and i_m that the contribution from light which has passed within 8 km of the earth's surface is relatively small. In other words, the attenuation in even a clear atmosphere of rays of light which traverse levels below 8 km is so great that an additional opacity due to clouds is of little consequence. Similarly, haze in the lower atmosphere causes little change in the sunlight illumination of the zenith twilight sky and reduces the zenith brightness in so far as it obstructs the observer's upward view.

The experimental result that the molecular density of the atmosphere up to about 60 km is that of Table I within about ± 30 percent leads

Table II. *Twilight sky data.*

(1) θ	(2) h	(3) i_z	(4) i_g	(5) i_p	(6) i_m	(7) i_p+i_m
0°	0 km	1140	436	1170	—	1170
4° 34′	20	27.5	31	36.3	0.50	36.8
5° 36′	30	7.41	8.7	7.9	0.43	8.3
6° 25′	40	2.19	3.3	1.8	0.21	2.0
7° 52′	60	0.339	0.64	8.8×10^{-2}	0.12	0.21
9° 36′	80	0.0676	0.090	3.4×10^{-2}	0.063	0.066
10° 9′	100	0.0398	0.051	1.4×10^{-4}	0.026	0.026
11° 8′	120	0.0158	0.020	5.0×10^{-6}	0.0071	0.0071
12° 2′	140	0.0076	0.010	2.1×10^{-7}	0.0049	0.0049
12° 52′	160	0.0040	0.005	8.3×10^{-9}	0.0024	0.0024

[13] For example, Wegener, *Lehrbuch der Physik*, Vol. 5 (Müller-Pouillets, 1938), p. 228.

to knowledge of the temperature. From (3) and (3.1) t is 218°±15°K from about 12 to 60 km for the twilight atmosphere of a temperate latitude. The conclusion is in agreement with the theoretical deductions of Maris[14] concerning the thermal state of the night atmosphere in high levels; it does not support contentions[15] of high night temperatures below 60 km.

The accuracy of the determination of n is not sufficient to throw light on the question at what altitude complete mixing of the atmospheric gases ceases and isothermal separation begins. It is known from high altitude balloon flights[16] that the proportions of nitrogen and helium at 20 km and of oxygen at 29 km are the same as at sea level within a few percent, and hence that complete mixing exists at least up to 20 km. Maris[14] has given a convincing calculation that complete mixing should prevail up to 100 km. If isothermal separation should set in at 20 km n at 40 and 60 km would be 1.5 and 6.2 percent greater than the values of Table I which were based on the assumption of complete mixing. The difference is too small to be revealed by the present measurements.

The observed constancy within ±15° or ±6 percent of the temperature t of the twilight atmosphere for z from about 12 to 60 km deserves further comment. It has been shown that if the atmosphere is in thermal equilibrium with outgoing terrestrial radiation[17] t should decrease with increasing z about 4° per km, and if an adiabatic condition prevails[7] due to wind mixing t should decrease with increasing z about 10° per km. The approximate constancy of t with z therefore requires explanation. This is found in the hypothesis that sunlight is absorbed in levels above 20 km at such a rate that, together with the absorbed outgoing terrestrial radiation, t is approximately constant with z during twilight. The hypothesis necessitates the conclusion that the atmosphere above 30 km is warmer during the day than during the night, and warmer during evening than morning twilight. However, the diurnal temperature change may be only a few degrees for z below 50 km but may increase with z.

The conclusions which have been derived from the present experimental data have depended on the correctness of the Rayleigh scattering formula (5). The agreement between the observed i_z and theoretical i_p curves of Fig. 11 in levels below 20 km where n is known constitutes perhaps the most direct verification of the formula which has been made, and precludes disposition to question its validity. The establishment of the attenuation formula (6) for a clear atmosphere by Fowle[18] is an important but indirect confirmation of (5). The conclusions would be disturbed if there were appreciable fluorescence of the high atmosphere under the stimulation of sunlight. Although Slipher's[19] observations of the nitrogen "flashes" in the predawn sky indicate that some fluorescence occurs, it seems probable that for $\theta < 13°$ no fluorescence exists of intensity comparable with that of the scattered solar radiation in the zenith twilight sky.

[14] Maris, Terr. Mag. **33**, 233 (1928); **34**, 45 (1929).

[15] Martyn and Pulley, Proc. Roy. Soc. **154**, 455 (1936), argued that the temperature increased from about 220°K at 40 km to above 400° at 70 km. See also Godfrey and Price, Proc. Roy. Soc. **163**, 228 (1937), and Kidson, Roy. Met. Soc., Quart. Jr., **63**, 477 (1937).

[16] Shepherd, National Geographic Society—U. S. Army Air Corps Stratosphere Flight of 1935. Technical Papers, p. 117 (1936); Regner, Nature **138**, 544 (1936); Lepape and Colange, Nature **137**, 459 (1936); Paneth and Gluckauf, Nature **136**, 717 (1935); Prokofiew and Glotzman, Nature **133**, 918 (1934).

[17] Hulburt, Phys. Rev. **38**, 1876 (1931).

[18] Fowle, Smithsonian Miscellaneous Collections **69**, 3 (1918).

[19] Slipher, Lowell Observatory Circular, February 20, 1931; Mon. Not. Roy. Ast. Soc. **93**, 657 (1932–1933).

Tungsten, Mercury and Sodium Illuminants at Low Brightness Levels

MATTHEW LUCKIESH AND A. H. TAYLOR
Lighting Research Laboratory, General Electric Company, Nela Park, Cleveland, Ohio
(Received April 5, 1938)

IT is well known that the spectral sensitivity of the visual sense shifts somewhat toward shorter wave-lengths at relatively low brightness levels. This Purkinje effect is generally confined to brightness levels lower than 0.1 footlambert and becomes marked for brightnesses less than 0.01 footlambert. Its magnitude depends upon the color and brightness of the object and its background and upon the spectral character of the illuminant. Some confusion has arisen in researches dealing with vision at low brightness levels by considering the stimulus to be brightness instead of radiant energy. In addition to theoretical or academic interest in vision and seeing at low brightnesses, the advent of new illuminants and the development of low level illumination outdoors, on the highways for example, have created a practical interest in seeing under these conditions.

It is seen in Fig. 1 that the maximum sensitivity of the visual sense to the production of luminosity by means of radiant energy is at about λ5550 for cone vision or ordinary brightness levels. For very low brightnesses this "luminosity curve" shifts to somewhat shorter wave-lengths. For these reasons tungsten-filament, sodium vapor and mercury vapor illuminants, obtained from commercial lamps, were studied.[1] They differ widely in spectral character and cover a considerable range in this respect. The sodium doublet is on the long wave side of the maximum of the luminosity curve of the eye. Therefore, a pronounced Purkinje effect is to be expected with sodium light. Mercury lines *M* are found on both sides of the maximum which indicates a lesser effect. The distribution of energy of the various wave-lengths differs with pressure, etc. In this work an H-3 mercury vapor lamp was used, the energy distribution in the various lines being as shown in Fig. 1.

APPARATUS AND PROCEDURE

In our study of the Purkinje effect the two light sources being compared were enclosed in light-tight boxes having opal glass windows in one end. These were placed at opposite ends of a photometer bar. A wedge photometer, movable on the bar between the two boxes, provided the photometer field which was of the form of a circle divided in half vertically. Circular diaphragms placed in front of the wedge limited the size of the photometric field to 2, 5, and 10 degrees, respectively.

The brightness of the photometer field was reduced in definite steps by means of circular diaphragms of various sizes placed over the opal glass windows of the boxes containing the light sources. Duplicate diaphragms were provided for the two boxes, and the quantitative reduction of luminous energy by each diaphragm was measured by a phototube and amplifier. Thus it was possible to reduce illumination of the photometer field by the same amount on each side, and measure the Purkinje effect by rebalancing the photometer. The position of the photometer when balanced was automatically recorded on paper beneath the photometer by closing an electrical circuit. The room was dark excepting for the light from the two opal glass windows in the light boxes, so that the photometer field was very much

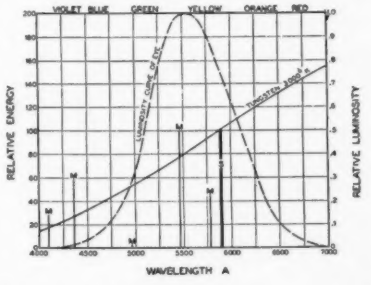

FIG. 1. Spectral distribution of energy emitted by tungsten filament, sodium vapor and mercury vapor (H-3) lamps. The luminosity curve of the eye is for brightness levels greater than one footlambert.

[1] M. Luckiesh and Frank K. Moss, "Seeing in Tungsten, Mercury and Sodium Lights," Trans. I. E. S. **31**, 655 (1936).

brighter than any other object visible to the observer.

With sodium vapor and tungsten filament lamps seven observers made complete sets of comparisons throughout a wide range of photometer field brightnesses with the three field sizes. Observations were also made with the 5-degree field with the addition of a glare source to determine whether or not the Purkinje effect was suppressed or eliminated by maintaining the eyes at a higher level of adaptation. Six observers compared the light from a tungsten filament lamp with that from a mercury vapor lamp at various brightness levels, using a 10-degree photometer field.

It is customary to assume that the unit of brightness has a fixed value in terms of energy-density of the stimulus, regardless of the spectral distribution of the radiant energy from the light source. This assumption is a safe one for brightnesses above 0.1 footlambert, but for brightnesses below this value the relationship between the stimulus (energy) and the brightness sensation produced is no longer constant owing to the Purkinje effect. Consequently it has been necessary for the authors to measure the brightness produced by two of the illuminants in terms of the third. For example, if the density of radiant energy from a tungsten filament lamp falling on a white surface is sufficient to produce a brightness of 1 footlambert, it has been necessary to assume that the brightness will be 0.001 footlambert when the energy-density is reduced to 0.001 of its former value. This provides a base for the determination of relative brightnesses produced by the other illuminants. Brightness values presented in this paper are relative to this arbitrary basis.

When making a set of observations the observer adapted for five minutes at the highest brightness level measured, approximately 0.5 to 1.0 footlambert. He then made measurements at successively lower brightness levels, the two opal glass windows being reduced in area by equal diaphragms to obtain the lower brightnesses of the photometer field. This reduced by known amounts the stimulus or energy reflected by each half of the photometer field. Adaptation tests made prior to these measurements showed that very little change due to adaptation took place at the higher brightness levels and that adaptation was sufficiently complete for the purpose at the lowest brightness level in 10 to 15 minutes. Since the total time required for one set of measurements by an observer was about 30 minutes, a longer period of adaptation than was used could not influence the practicability of the results.

TABLE I. *Showing the influence of the Purkinje effect upon the luminous efficiency (lumens per watt) of sodium and mercury lamps relative to that of the tungsten filament lamp for various brightness levels expressed in footlamberts.*

FOOTLAMBERT*	1	0.1	0.01	0.001	0.0005
Tungsten filament	20	20	20	20	20
Sodium vapor	50	41	29	15	13
Mercury vapor	30	29	30	33	34

* Apparent footlamberts for tungsten-filament light.

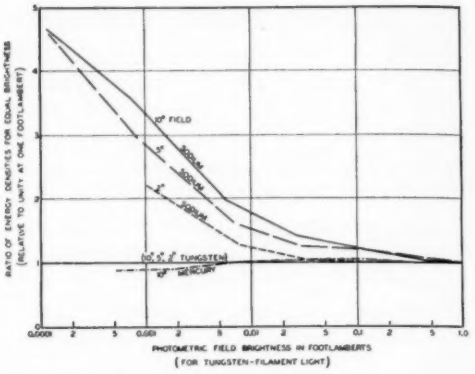

FIG. 2. Showing the relative magnitude of the Purkinje effect for sodium and mercury illuminants in terms of a tungsten filament illuminant.

In Fig. 2 are plotted the average results obtained by seven observers, with three sizes of photometric field for the sodium vapor illuminant, and for one field size for the high pressure mercury (type H-3) illuminant, in terms of the tungsten filament illuminant. From these curves it is seen that the Purkinje effect has a much greater influence on the light from the sodium lamp than on that from the tungsten filament or mercury lamp.

Owing to the Purkinje effect the luminous efficiency (lumens per watt) of a light source is generally different at low brightness levels from that at high ones where cone vision is operative. Table I shows the relative over-all luminous

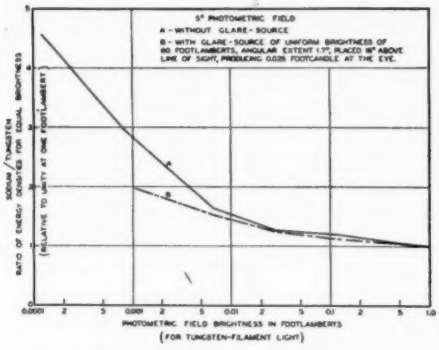
5° PHOTOMETRIC FIELD
A - WITHOUT GLARE - SOURCE
B - WITH GLARE - SOURCE OF UNIFORM BRIGHTNESS OF 60 FOOTLAMBERTS, ANGULAR EXTENT 1.7°, PLACED 18° ABOVE LINE OF SIGHT, PRODUCING 0.025 FOOTCANDLE AT THE EYE.
RATIO OF ENERGY DENSITIES FOR EQUAL BRIGHTNESS SODIUM / TUNGSTEN (RELATIVE TO UNITY AT ONE FOOTLAMBERT)
PHOTOMETRIC FIELD BRIGHTNESS IN FOOTLAMBERTS (FOR TUNGSTEN-FILAMENT LIGHT)

FIG. 3. Showing the effect of a given glare source in reducing the Purkinje effect for sodium light compared with tungsten filament light.

efficiencies of the three sources at low brightness levels, as derived from the data in Fig. 2.

Figure 3 shows the result of a glare source in reducing the Purkinje effect at brightness levels between 0.01 and 0.001 footlambert. The presence of the glare source made it impossible to make photometric measurements at brightness levels below 0.001 footlambert.

MINIMUM PERCEPTIBLE STIMULUS DIFFERENCE

Because of the fact that the light from the sodium lamp is essentially monochromatic, visual acuity is greater at a given brightness level with this illuminant than with the other illuminants. However, visual acuity is of much less importance than brightness contrast in seeing[2] large objects and this is particularly true at low brightness levels. Consequently some studies of minimum perceptible stimulus difference were made. With brightness at low levels depending upon the spectral character of the illuminant, it is necessary to deal with the true stimulus (energy-density) in order to avoid ambiguity. Besides brightness is the sensation and not the stimulus. Therefore, we determined minimum perceptible stimulus difference instead of the usual minimum perceptible brightness difference as is common at ordinary brightness levels involving cone vision.

The test objects used were photographic prints of our black parallel bar test object,[2] having different degrees of contrast with the white background. This test object consisted of two vertical black rectangles, each 2 inches high and $\frac{2}{3}$ inch wide, separated by a white space $\frac{2}{3}$ inch wide. A series of these test objects of progressively increasing contrast was placed behind a large white screen through which one object at a time could be viewed. The series was moved back and forth until the observer, seated eight feet in front of the screen, selected the object having the lowest contrast which he could distinguish. When making these measurements the observer adapted for five minutes at the highest screen brightness (0.35 footlambert) and then began his observations. After a series of observations was made the energy density on the test-object was reduced to about $\frac{1}{4}$ of its former value, and after a further adaptation of about two minutes a series of observations was made at the lower screen brightness. This procedure was repeated for still lower brightness levels.

In Table II are shown the results obtained by

TABLE II. *Minimum perceptible stimulus differences (in percent) obtained by six observers at various brightness levels for three illuminants. The latter were adjusted to produce the same field brightness at 0.35 footlambert. Each lower brightness level was obtained by identical physical reductions applied to the three illuminants.*

FOOTLAMBERTS*	0.35	0.090	0.023	0.0062	0.00135
Sodium Vapor					
AAE	3.2	6.0	11.5	30	82
AHT	3.2	6.1	9.8	19	59
GPK	3.2	6.1	9.0	27	56
TB	4.2	6.1	11.2	25	69
SPG	1.3	3.8	6.5	13	40
JD	1.3	4.2	9.8	19	46
Average	2.7	5.4	9.6	22	59
Tungsten-Filament					
AAE	3.2	6.7	10.8	27	63
AHT	1.5	3.6	7.0	16	36
GPK	3.2	5.7	12.3	27	59
TB	3.2	6.1	10.8	23	57
SPG	1.3	3.2	7.3	15	36
JD	2.8	5.6	10.2	19	58
Average	2.5	5.1	9.7	21	51
Mercury Vapor					
AAE	4.2	5.2	14.5	32	79
AHT	4.0	5.6	8.4	22	36
GPK	4.2	6.1	10.8	20	50
TB	4.2	6.1	10.8	21	51
SPG	1.3	4.0	7.7	14	30
JD	1.3	4.0	7.4	12	32
Average	3.2	5.2	10.0	20	46

* Apparent footlamberts for tungsten light.

[2] Matthew Luckiesh and Frank K. Moss, *The Science of Seeing* (D. Van Nostrand Company, New York, 1937).

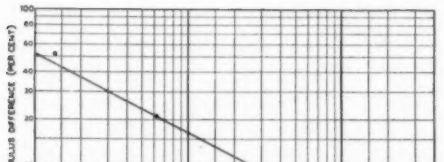

FIG. 4. The minimum perceptible stimulus difference is the same for tungsten, mercury and sodium illuminants at various low energy-density levels.

six observers for the three illuminants. An apparently new fact, established within the errors of measurement, is that the minimum perceptible stimulus difference is the same for all three illuminants when the energy density is reduced by the same amount from a common base. This apparently indicates that the greater loss in field brightness with sodium vapor light at low brightness levels is fully compensated for by an increased sensitivity to threshold stimulus (energy density) difference. The large variations in threshold difference or contrast among the observers reveals the desirability of testing persons for this aspect of vision and seeing, particularly for driving on highways at night.

The average results for the six observers plotted in Fig. 4 indicate that if measurements begin at about 0.35 footlambert as measured photometrically with the three sources, a reduction in stimulus or energy density on the screen to $\frac{1}{4}$ doubles the minimum perceptible stimulus difference or threshold energy density difference. Successive similar reductions for three more steps show that this relationship continues to hold. Obviously if the three light sources were of equal candlepower in a given direction the brightness of a given object at a distance, sufficient to reduce the brightness levels below 0.1 footlambert, would be lower for sodium light than for the tungsten and mercury lights. However, contrast sensitivity would not differ materially under the three illuminants.

When comparing the sodium vapor and tungsten filament illuminants in the wedge photometer with 10-degree field, all observers could detect a color difference between the two fields when the field brightness was as low as 0.0008 footlambert. When comparing the mercury vapor and tungsten filament illuminants, a color-difference was perceptible when the field brightness was as low as 0.002 footlambert. These brightnesses are much lower than those at which color is usually assumed to disappear.

Photometry of Colored Light Sources

W. E. Forsythe, B. T. Barnes and Ann L. Shrider
Lamp Development Laboratory, General Electric Company, Nela Park, Cleveland, Ohio
(Received March 30, 1938)

HETEROCHROMATIC photometry — the measurement of the luminous output of sources that emit colored light—has become very important in the last few years on account of the necessity of measuring the output of several new sources that emit colored light. Among these new sources are: high intensity mercury lamps, sodium lamps, neon lamps, and fluorescent lamps of various colors.

Photometrists have agreed[1] upon a definite method of calibrating tungsten lamp standards at various color temperatures in terms of the intensities of carbon lamp standards. The plan chosen was: first, to adopt as standard the best experimental values of the luminosity factors for the average eye; then, to measure the light output of sources of higher color temperature, in terms of that of carbon standards, by using selected blue glass filters to overcome the color difference between the carbon standards and the secondary tungsten standards. The blue filter is used between the carbon lamp and the photometer; its transmission, for the light from the carbon lamp, is given by the following formula:

$$T=\int_0^\infty J(\lambda T)T_\lambda K_\lambda d\lambda \Big/ \int_0^\infty J(\lambda T)K_\lambda d\lambda.$$

Where $J(\lambda T)$ is the spectral intensity of the radiation from the comparison lamp source, T_λ the spectral transmission of the filter, and K_λ the spectral luminosity factor. The Lummer-Brodhun contrast photometer with a field of 8 to 10° is to be used in this work.

When the problem of measuring the light output of the new highly colored light sources came up, it was decided to use this same method, that is, to use the direct comparison photometer with a colored filter between the comparison source and the photometer. This filter was so selected as to overcome, as nearly as possible, the color difference between the tungsten comparison lamp and the source being studied. Photometrists, in general, decided to make these measurements with a 2° photometric field as recommended by Ives.[2] The transmission of the filter was calculated by the formula already given. When measuring the light output of the high intensity mercury arc, a blue filter generally is used on the comparison lamp side of the photometer; some photometrists, however, use two filters, one on each side of the photometer.

It was shown by Little and Estey[3] that it usually is possible to select a filter which, when used with the tungsten comparison lamp, gives a very good color match for each of these highly colored light sources. These experimenters showed the color agreement for the standard observer by the use of a color mixture diagram. However, even if the filter is right for the average observer, different observers may find marked color difference and may obtain readings of light output which differ by several percent. Since exact color match is seldom obtained, even with the best possible filters, and since the spectral distribution of the radiation from the tungsten comparison lamp, after passing through the filter is almost never the same as that from the lamp being measured, some care[2] should be exercised in the selection of the observers for this work.

As a test of some of the photometric methods, six different kinds of lamp—400-watt high intensity mercury arcs, 10,000 lumen sodium lamps, neon lamps and three kinds of fluorescent lamp, a pink, a green, and a blue, were selected and a number of measurements made of their light output by seventeen experienced observers. These observers were selected from the laboratories at Nela Park, i.e., six from the Testing Section, two from the Lighting Research Laboratory, two from the Engineering Department,

[1] E. C. Crittenden and J. Franklin Meyer, Proc. International Congress on Illumination, p. 1138, 1928. H. Buckley, Phil. Mag. **24**, 1059 (1937).

[2] H. E. Ives, E. F. Kingsbury, Trans. I. E. S. **10**, 203 (1915).

[3] W. F. Little and R. S. Estey, Trans. I. E. S. **32**, 628 (1937).

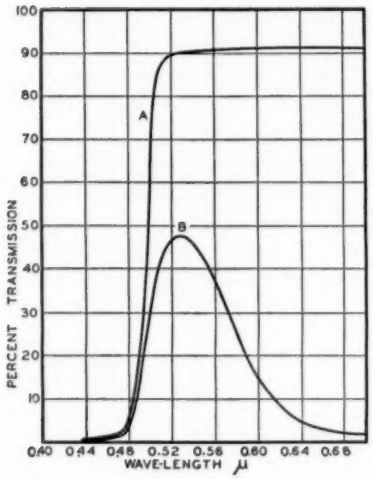

FIG. 1. Transmissions of the yellow and green filters that were obtained from the Osram Company for use in measuring the luminous output of mercury lamps.

and seven from the Lamp Development Laboratory. The characteristics of the observers' eyes were determined by having each measure, using the Ives-Brady flicker photometer, the relative transmission of the Ives[2] yellow and blue solutions; from these measurements the so-called Y/B ratio was computed for each observer. These ratios are given in the second column of Tables IV and VII. This work was done with the solutions at a temperature of about 25°C. Thus, according to Crittenden and Richtmyer,[4] our values of the Y/B ratios are all too high by about 0.5 percent.

The first test was measurements of the average luminous output of three 400-watt high intensity mercury lamps using the regular Lummer-Brodhun contrast photometer with an 8–10° field and with filters selected to eliminate, as nearly as possible, the color difference. These measurements were repeated using the same photometer with a small diaphragm which gave a two part field 2° in size. Two of the lamps were measured in a sphere by eight of the sixteen observers; the third lamp was measured on the horizontal bar photometer by the same observers. The horizontal candlepower was changed to lumens by use of a reduction factor.

[4] E. C. Crittenden and F. K. Richtmyer, Bull. Nat. Bur. Stand. **14**, 93 (1918).

The relation between results with the large and those with the small field was determined four different times, using each time a different glass filter to overcome the color difference between the tungsten comparison lamp and the mercury lamp. The first set of filters was obtained from the Osram Lamp Company in Berlin and consisted of a light yellow filter which was placed between the mercury lamp and the photometer and a green filter between the

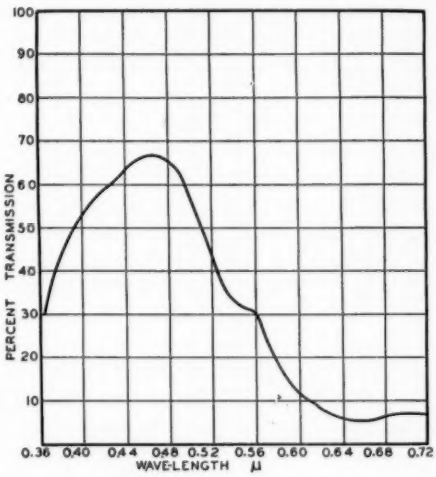

FIG. 2. Transmission of the blue glass filter similar to the one selected by the N.B.S. for use in measuring the high intensity mercury lamps.

tungsten comparison lamp and the photometer. The yellow filter removed the blue light from the mercury lamp, thus making it easier to color match the mercury light with the screened tungsten light. The transmissions of these two filters are given in Fig. 1. The second filter was similar to the one used at the National Bureau of Standards for the same kind of work; its transmission is shown in Fig. 2. The third filter, whose transmission is shown in Fig. 3, was of the type used at the Electrical Testing Laboratories. The fourth was selected by the engineers at the G. E. Vapor Lamp Company; its transmission is shown in Fig. 4.

The voltage of the comparison lamp was set in each case at the average value selected by the different observers for the best color match. The diaphragm used in the eyepiece of the photometer to give the 2° field could be easily removed so

that the observers could take alternate sets of readings with the large and small field. In nearly all of the work two observers worked together and took alternate sets of readings, one observer resting while the other took his set of readings. The results of this test are shown in Table I. It will be noted that some of the observers obtained about the same value for the average light output of the mercury lamps with the small and with the large field, and that the average difference depended upon the particular filter used. When a color difference existed, some of the observers, in making photometric settings with the large field, selected a small portion of the field near the center and neglected, as far as possible, the rest of the field. Thus they were, in part, using a small field. Certain other observers, when using the large field, attempted to use the contrast

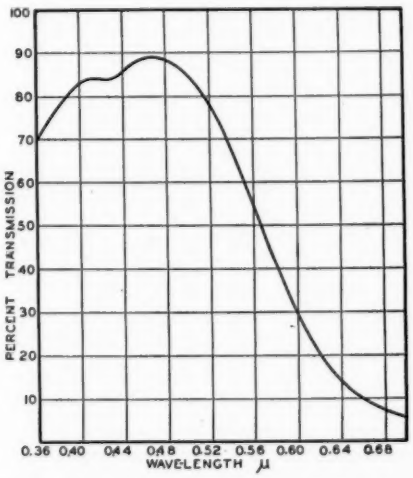

FIG. 3. Transmission of the blue glass filter similar to the one selected by the E.T.L. for use in measuring the output of the high intensity mercury lamps.

method of setting and thus made use of the entire field. Most of the observers who took part in this test thought that the filters obtained from the Osram Company and the one similar to the E.T.L. filter were the most satisfactory. It is to be noted that the mean value obtained with each of the filters for one field size agrees very well with the exception of the value obtained with the small field for the G.E.V.L. filter. Each observer made at least two sets of ten readings in measuring these lamps and the two sets agreed for the most part to better than 1 percent.

The next comparison was between measurements made respectively with the equality of brightness photometer, with a 2° field and a filter to equalize the color difference, and with a flicker photometer. In this test, measurements were made of the high intensity mercury lamp, the 10,000 lumen sodium lamp and a 1200-lumen, green fluorescent lamp. In order to obtain higher intensities with the fluorescent lamps, four lamps were mounted side by side and used as source. The E.T.L. filter (Fig. 3) was used with the mercury lamps; the filters used for the sodium lamp and for the green fluorescent lamp are the ones whose transmissions are shown in Figs. 5 and 6. The flicker photometer was of the Ives-Brady[5] type and was used at about 10–12 alternations per second. A cross section of the eyepiece of this flicker photometer and the field used is shown in Fig. 7. The surrounding field of the flicker photometer was illuminated so that its brightness was about 20 to 50 percent of that of the field studied. This work was done on the horizontal bar photometer and the two photometers were so mounted that one could be removed and be replaced by the other in order that the observer could make alternate sets of readings

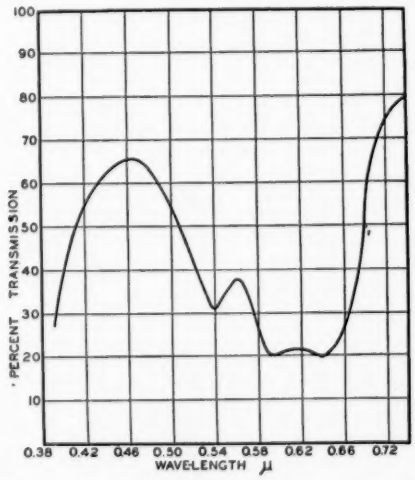

FIG. 4. Transmission of the blue glass filter similar to the one selected by the G.E.V.L. for use in measuring the output of the high intensity mercury lamps.

[5] H. E. Ives, E. J. Brady, Phys. Rev. **4**, 222 (1914).

with the two photometers. Two observers worked together as above. The results obtained, together with some of the conditions of operation are shown in Table II. The values obtained, using the two photometers, check very well considering the small number of observers and the range of their Y/B ratios.

The third test was a measure, with the flicker photometer, of the horizontal candlepower of six different types of lamp each giving a different color of light. The lamps measured were: 400-watt high intensity mercury lamps, 10,000 lumen sodium lamps, neon lamps (two together), green fluorescent lamps (four together), blue florescent lamps (eight together), and pink fluorescent lamps (eight together). At the same time the ratio of the intensity of the light output of the 400-watt high intensity mercury lamp and the 10,000 lumen sodium lamp was measured by having the two lamps so mounted that first one and then the other could be moved into the field of view. In a like manner, the ratio of the light output of eight pink fluorescent lamps to eight blue fluorescent lamps was measured. The results of this test are shown in Table III.

A number of observers who took part in these tests measured the output of one of the high intensity mercury lamps using a flicker photometer and the E.T.L. blue glass filter to reduce the color difference encountered. It was thought that, if the color difference was reduced to a minimum, the different observers would obtain values that were in better agreement. At the same time that the lamp was measured with the flicker photometer and color filter, it was measured with the flicker photometer alone, for comparison. The results are shown in Table IV. This test showed that, when the color filter was used, the results were, in general, in better agreement; it also showed that the final averages by both methods agree very well, particularly after neglecting the values obtained by the very blue sensitive observer (C.F.K.).

The spectral radiant intensity of the different lamps used in this test are shown in Table V. From these values and the standard I.C.I. luminosity factors, the luminous intensities of the different lamps were calculated and are shown in Table VI, together with the mean measured value for the luminous intensity for comparison.

The colors of the lamps used in this test are shown on the color mixture diagram (Fig. 8). The points were obtained by using the coefficients for the standard observer, as given by Judd.[6] Also the colors of the light from the tungsten comparison lamp, after passing through the filters, used with the sodium, the mercury and the green fluorescent lamps, are shown. These points show how well the colors of the different lamps were matched by the use of tungsten lamps and colored filters.

If the luminous output of the various lamps obtained by the different observers are plotted against the observers' Y/B ratio, interesting relations are shown.[7] The values for the mercury

[6] D. B. Judd, J. O. S. A. **23**, 359 (1933).

[7] E. C. Crittenden and F. K. Richtmyer, Bull. Nat. Bur. Stand. **14**, 98 (1918). C. C. Patterson, Proc. Phys. Soc. London, **50**, 119 (1938).

TABLE I. *Measurement of mercury lamp* by a number of observers with a large (L) and a small (S) field.*

Observer	Eye Constant Y/B	Screen							
		Osram		N.B.S.		E.T.L.		G.E.V.L.	
		L	*S*	*L*	*S*	*L*	*S*	*L*	*S*
W.E.F.	1.004	14020	14380	15030	15340	14500	14560	14860	14940
A.L.S.	0.964	13870	13990	13860	14110	13590	13960	14070	14330
E.M.W.	1.032	13910	14100	14300	14080	13940	13560	14120	14140
E.Q.A.	0.967	13560	13940	13390	13530	13530	13670	13800	14240
M.G.	0.998	13930	14030	12830	13640	13230	13790	13480	15290
J.F.R.	1.001	13980	14290	13410	13940	13470	14460	13790	16490
C.F.K.	0.677	14000	15120	12860	14810	12910	14730	14110	16150
N.F.	1.079	13780	13920	14450	14770	13780	14020	13670	13420
Means	0.965	13860	14220	13770	14280	13620	14120	13980	14880
Percent gain			2.3%		3.7%		3.7%		6.5%

* Average of three lamps. Results in lumens. *L*, 8–10° field. *S*, 2° field.

lamp show no very definite trend. The sodium lamp values are apparently linear, but the value found by the very blue observer (CFK) is too high to fit the curve. The values obtained for the neon lamps and for the three types of fluorescent lamps when plotted against the observers' Y/B ratio indicate a straight line relation. However, for some of these lamps, the values obtained by certain observers are further from the average straight line then can be accounted for by any

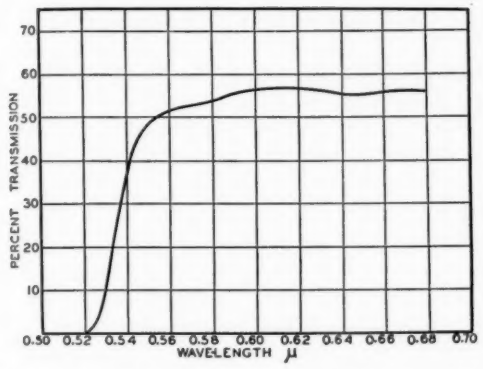

FIG. 5. Transmission of the glass screen used in measuring the output of the sodium lamp.

errors that may have been made in making these measurements. It did not seem that an average from such a relation would be any more accurate than the mean given. Such results indicate that the Y/B relation is not a sufficient criterion when measuring the output of highly colored light sources. This might well be, since two observers might have the same Y/B ratio but one might have a wide luminosity curve and the other a narrow one. Thus they would react quite differently to highly colored light, such as that of a sodium or a neon lamp. Nevertheless, the results given in Tables I to VII show that the Y/B ratio is a very valuable criterion as to the character of results one may expect from different observers even when measuring the output of some of the newer highly colored light sources.

When this work was started, only three or four of the observers had had any experience with the flicker photometer, and only one (A.H.T.) any very extended experience with this type of photometer. Some objections were made at first such as, "This is very tiresome work on the

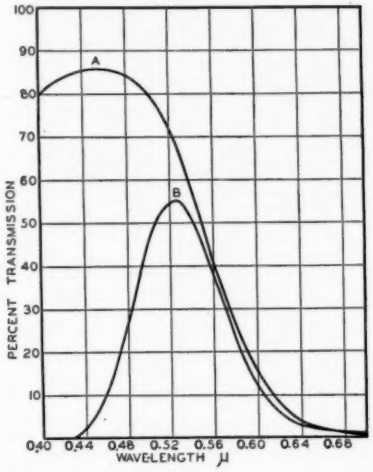

FIG. 6. Transmission of the screen used between the comparison lamp and the photometer when measuring the green fluorescent lamps.

eye," "One cannot be sure that he is repeating results," etc. However, before the end of the tests, all observers were convinced that they would rather use a flicker photometer than a direct comparison photometer when measuring light of a color different from that of the comparison lamp. Most of the observers became quite skillful in making settings with the flicker photometer. Indeed in general they were able to make and repeat settings that were better than was warranted by the constancy, over a long period of time, of lamps of these types.

Some objections were advanced that the flickering of the light (all lamps were operated on a.c.) would introduce an error in the results with the flicker photometer. Such was not found to be the case. The results show that, with the use of a flicker photometer of the Ives-Brady type, results on luminous intensity measurements are obtained, even for some of the more highly colored light sources, that agree with like values obtained with a direct comparison photometer and a filter to eliminate the color difference. This is true, even with a small number of observers, providing some care is taken in selecting observers who have a Y/B ratio not too far from unity.

With the flicker photometer, observers obtain results that depend markedly upon the charac-

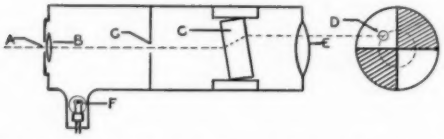

FIG. 7. Cross section of the eyepiece and field of the Ives-Brady flicker photometer. *C*, rotating prism; *D*, appearance of field; *G*, limiting diaphragm; *F*, lamp for illuminating field.

teristics of their eyes; with the direct comparison photometer and a screen to equalize the color difference, at least in part, observers make readings that more nearly agree. Furthermore, the standard luminosity factors are used in the calculation of the transmission of the screen, on which, of course, the final results depend. The use of such screens with the flicker photometer should give better agreement among observers.

When the measurements reported above were about half finished, the paper by Dresler[8] on the same subject appeared in *Das Licht*. Since our results did not agree with his, it was decided to make another test which he had made. This was a comparison of the measured with the calculated ratio of the luminous intensities of two strong mercury lines (λ's 5461 and 5780A). Therefore

[8] A. Dresler, Das Licht **7**, 81, 107 (1937).

TABLE II. *Comparison of direct comparison and flicker methods of measuring candlepower.*

Observer	*Y/B* Eye Constant	Green Fluores. 4 lps.			Sodium			Mercury		
		Direct	Flicker	Direct Flicker	Direct	Flicker	Direct Flicker	Direct	Flicker	Direct Flicker
Field Brightness		7 mL			8 mL			10 mL		
W.E.F.	1.008	466	447	1.042	927	967	0.957	1436	1416	1.014
A.L.S.	0.964	461	468	0.985	899	912	0.985	1330	1402	0.949
G.K.	1.047	500	451	1.108	967	989	0.979	1520	1425	1.067
A.H.T.	1.055	484	441	1.097	930	971	0.958	1467	1421	1.032
B.T.B.	1.004	480	463	1.037	972	977	0.995	1476	1470	1.005
C.F.K.	0.677	488	625	0.781	955	838	1.140	1446	1656	0.873
J.F.R.	1.001	472	453	1.042	968	1019	0.950	1559	1554	1.003
E.M.W.	1.032	463	447	1.036	918	965	0.952	1556	1469	1.060
E.Q.A.	0.967	477	482	0.990	982	930	1.056	1374	1410	0.974
N.F.	1.072	480	409	1.173	950	1003	0.947	1440	1303	1.105
M.G.	0.998	483	463	1.043	902	925	0.975	1424	1417	1.005
Average	0.984	478	468	1.033	943	954	0.991	1457	1449	1.008

TABLE III. *Candlepowers of a number of different colored lamps as measured with a flicker photometer.*

Observer	*Y/B* Eye Constant	Fluorescent Lamps					Hg Av. 3 lps.	Na Av. 3 lps.	Hg/Na
		Neon 2 lps.	Green 4 lps.	Blue 8 lps.	Pink 8 lps.	Pink Blue			
Field Brightness	3 mL	3	7	2.8	3.2		10	8	
W.E.F.	1.008	700	475	323	407	1.260	1480	1025	1.443
A.L.S.	0.964	674	498	370	394	1.065	1456	978	1.490
G.K.	1.047	719	479	314	399	1.270	1490	1078	1.382
A.H.T.	1.055	736	469	299	407	1.361	1471	1051	1.400
B.T.B.	1.004	690	492	325	398	1.225	1522	1029	1.479
P.D.C.	0.908	616	534	389	380	0.977	1522	952	1.599
C.F.K.	0.677	377	664	468	316	0.675	1733	926	1.871
J.F.R.	1.001	676	482	316	407	1.287	1480	1090	1.358
E.M.W.	1.032	706	475	348	413	1.186	1441	1027	1.403
E.Q.A.	0.967	654	512	379	391	1.031	1448	966	1.500
N.F.	1.072	838	435	330	444	1.345	1485	1131	1.314
M.G.	0.998	694	492	359	393	1.094	1484	1004	1.476
Average	0.989	674	501	352	396	1.128	1501	1021	1.476

TABLE IV. *Candlepower of H-1 lamp using flicker photometer with and without color screen (E.T.L.).*

OBSERVER	EYE CONSTANT Y/B	USING COLOR SCREEN	WITHOUT SCREEN
W.E.F.	1.008	1491	1430
A.L.S.	0.964	1396	1410
P.D.C.	0.908	1394	1446
E.Q.A.	0.967	1353	1388
C.F.K.	0.677	1475	1715
E.M.W.	1.032	1368	1391
A.H.T.	1.055	1397	1370
G.K.	1.047	1391	1370
Mean	0.957	1408	1441
Mean (without C.F.K.)	0.997	1399	1401

TABLE VI. *Measured and calculated values of the candlepowers of a number of lamps.*

LAMP	CANDLEPOWER MEASURED	CANDLEPOWER CALCULATED
Tungsten standard*	1415	1408
Mercury H-1	1501	1470
Sodium	1021	967
Neon	337	335
Fluorescent		
green	125.2	135.0
pink	49.5	46.9
blue	44.0	45.0

* Mean from standard lamp (color temp. 2850°K) calibrated at N.B.S.

filters suitable for isolating each line (No. 5.1 and No. 4.1) were obtained from Corning Glass Works. The ratio of the luminous intensities from a particular mercury lamp transmitted by these two filters was determined by sixteen observers, using the Ives-Brady flicker photometer with a 2° field (Dresler used a 1.1° field). Table VII shows the results, together with the Y/B ratios of the observers. The ratio of the luminous intensities transmitted by the two filters was calculated from the spectral intensities of the radiation from the lamp, the spectral transmissions of the filters (both measured with our double monochromator[9] and the standard I.C.I. luminosity factors.[10] The result was 1.33, which is in good agreement with the measured ratios, (1.06 to 1.52) average for sixteen observers, 1.36.

These last results, as well as the other results given, show that measurements made with a flicker photometer of the type used here agree

[9] W. E. Forsythe and B. T. Barnes, Rev. Sci. Inst. **4**, 289 (1933).
[10] Trans. I. E. S. **28**, 268 (1933).

TABLE V. *Spectral intensity, milliwatts per steradian, perpendicular to axis of lamp for the lamps used in these tests.*

WAVE-LENGTH BAND	FLUORESCENT LAMPS: GREEN LAMPS	FLUORESCENT LAMPS: PINK LAMPS	FLUORESCENT LAMPS: BLUE LAMPS	MERCURY H-1 LAMP	WAVE-LENGTH BAND	NEON LAMP
3960–4019	1	.6	71	6	5650–5731	1.5
4019–4079	42	61	149	464	5731–5816	11
4079–4142	3	3.1	97	46.5	5816–5905	93
4142–4209	2	1.4	106	8	5905–5998	83
4209–4280	2	1.1	117	10	5998–6094	142
4280–4431	83	126	403	945	6094–6194	243
4431–4516	1	1.3	138	13.6	6194–6300	138
4516–4605	2	1.4	141	10.3	6300–6412	509
4605–4696	2	1.7	141	10.4	6412–6528	297
4696–4789	4	1.4	135	11.7	6528–6647	138
4789–4892	11	1.5	127	16.4	6647–6772	151
4892–5002	46	1.6	119	25.6	6772–6900	35
5002–5123	132	1.3	108	13.8	6900–7035	189
5123–5252	252	1.9	95	14.2	7035–7182	81
5252–5388	262	3.7	80	24.5	Candlepower*	335
5388–5536	223	86	150	1210		
5536–5691	93	36	55	35.0		
5691–5863	58	132	67	1160		Sodium Lamp
5863–6043	20	224	33	31.2		
6043–6245	9	306	23	26.9	5409–5589	.7
6245–6470	5	300	16	27.6	5589–5786	31
6470–6705	2.5	224	11	30.5	5786–6001	1965
6705–6960	1.7	136	8	47.7	6001–6244	34.5
6960–7250	.9	69	5	46.0	6244–6515	40
Candlepower*	540	375	360	1470	6515–6816	16.0
					6816–7151	14.6
					Candlepower*	967

* Calculated from intensity and standard luminosity factors and certain corrections for variations of lamp during successive tests.

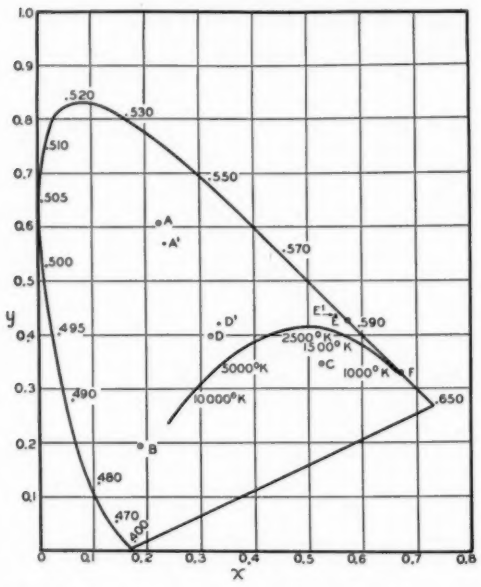

FIG. 8. I.C.I. color coordinates of the lamps used in this test. *A*, green fluorescent lamp; *A'*, comparison lamp as seen through screen whose transmission is shown in Fig. 6; *B*, blue fluorescent lamp; *C*, pink fluorescent lamp; *D*, high intensity mercury lamp; *D'*, comparison lamp as seen through E.T.L. screen; *E*, sodium lamp; *E'*, comparison lamp as seen through screen whose transmission is shown in Fig. 5; *F*, neon lamp.

well with the results obtained by calculation, using spectral intensities and the standard I.C.I. luminosity factors. All of these measurements were made with a flicker photometer having a 2° field with the surrounding field illuminated to an intensity comparable with that of the field observed. Also, in every instance the brightness of the field as observed was kept above 2.5 millilamberts. There might be a difference if a field of about half this size were used, as was done by Dresler. It must be remembered, however, that the standard luminosity factors were obtained with a field of about the size and a field brightness of the same order as that used here.

TABLE VII. *Relative luminous intensity of the yellow and the green mercury lines as measured by a number of observers using a flicker photometer.*

OBSERVER	EYE CONSTANT *Y/B*	OBSERVED LUMINOUS OUTPUT THROUGH THE SCREEN		
		YELLOW	GREEN	*Y/G*
W.E.F.	1.008	447	324	1.379
A.L.S.	.964	427	319	1.340
A.H.T.	1.055	443	312	1.420
G.K.	1.047	446	314	1.423
C.F.K.	.677	451	425	1.061
N.F.	1.072	454	316	1.438
J.F.R.	1.001	472	334	1.410
M.G.	.998	431	321	1.340
O.U.	1.004	450	331	1.360
W.J.M.	.997	435	316	1.377
G.R.B.	1.113	426	280	1.521
V.J.	.951	439	348	1.263
P.D.C.	.908	428	326	1.310
E.Q.A.	.967	421	310	1.356
B.T.B.	1.004	449	337	1.357
R.W.U.	1.058	420	301	1.393
W.E.F.	1.009	440	316	1.393
A.L.S.	.964	420	313	1.341
Mean	.989			1.360

Since such satisfactory results were found with the flicker photometer in this investigation, the Testing Section at Nela Park has decided to install a flicker photometer of this type on their large sphere and try this method for the routine measurements of the luminous output of the different types of lamps giving colored light.

This investigation was made possible by the cooperation of the different observers who helped in making these measurements. The authors take this opportunity to thank them for taking the time to help with this work.

An Experimental Study of Latent-Image Formation by Means of Interrupted and Herschel Exposures at Low Temperature

Measurements of Reciprocity Law Failure at Low Temperature*

J. H. Webb and C. H. Evans
Eastman Kodak Research Laboratories, Rochester, New York

(Received May 11, 1938)

The present paper contains results of experiments carried out to test the theory of latent-image formation recently proposed by Gurney and Mott. In their theory, these authors have introduced the concept of electrolytic transport of Ag+ ions to account for the nucleation of latent image Ag about the sensitivity specks preexistent on the surface of the grains. The Ag+ ions are supposed to diffuse to the specks under the attraction of electrons trapped there during the exposure to light. The first experiment consisted of a series of intermittent exposures made at liquid air temperature with warm-up periods between flashes. The results indicate that something vital to the photographic process takes place during the warm-up period between exposures. The second experiment consisted of a series of Herschel exposures made under the following temperature conditions: (a) White-light exposure 20°C, Herschel exposure 20°C; (b) white-light exposure 20°C, Herschel exposure −186°C; (c) white-light exposure −186°C, Herschel exposure 20°C; (d) white-light and Herschel exposures both at −186°C; (e) case (d) repeated with warm-up period between the exposures. The results obtained are radically different under the different conditions. Finally, results are presented on reciprocity measurements at temperatures 20°C, −78°C, and −186°C. These results show that the low-intensity reciprocity law failure has disappeared at −78°C and that the high intensity failure has practically disappeared at −186°C. All of the foregoing results are shown to have ready interpretation on the Gurney-Mott picture of latent-image formation.

Introduction

In a former paper[1] one of the authors outlined a theory of latent-image formation based on the new quantum mechanics model of crystals. In a recent paper,[2] Gurney and Mott working along similar lines have extended the theory of this subject considerably and through the introduction of new concepts have arrived at a picture of latent-image formation which appears very promising in the light of experimental evidence. The introduction by these workers of the concept of electrolytic transport of Ag+ ions as an accessory process of latent-image formation is thought to be a most important contribution to the solution of this problem. This single idea appears to afford at once an explanation of the effect of temperature on sensitivity, an explanation of the reciprocity law failure at high intensity, and a mechanism by which Ag atoms can coagulate about sensitivity nuclei preexistent on the surface of the grain to form the latent image.

The purpose of the present paper is to give the results of some experiments at low temperature, which strongly point to the correctness of the picture of latent-image formation proposed by Gurney and Mott.

Before giving the experimental results, a brief outline of the theoretical model of latent-image formation will be presented with the thought that it will furnish a logical introduction to the experimental results which are to follow, and at the same time will give a theoretical framework in which these experimental results find ready interpretation.

Theoretical Description of Latent-Image Formation

In the theoretical discussion of the latent-image formation to be given here we shall take as starting point the energy diagram of a AgBr crystal derived from quantum mechanics. An idealized energy diagram of this type is illustrated in Fig. 1. As is known, the electronic energy spectrum of an insulating crystal like AgBr includes bands of allowed levels separated by disallowed zones. For purposes of discussion of the latent-image problem, only two of the

* Communication No. 674 from the Kodak Research Laboratories.

[1] J. H. Webb, J. Opt. Soc. Am. **26**, 367 (1936).

[2] R. W. Gurney and N. F. Mott, Proc. Roy. Soc. **164**, 151 (1938).

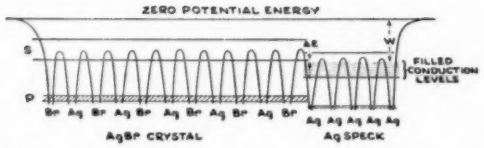

FIG. 1. Energy level diagram of Ag speck in contact with AgBr.

allowed bands need be considered. One of these is an upper S band which is normally empty and which is referred to as the conduction band, and the other is a lower P band which is normally completely filled with electrons. Upon exposure of a AgBr crystal to light absorbed in the long-wave-length end of the characteristic absorption band, the crystal becomes conducting. This property is known as photoconductance and on the basis of the quantum mechanics treatment, results from the removal of electrons from the lower P band of levels to the upper S conduction band. Electrons in this upper conduction band behave exactly like free electrons in a metal and give rise to conductivity.

Primary process

In common with a number of previous workers, Gurney and Mott assume in their theory that the initial process of latent-image formation is to be identified with the photoconductance effect. There is good experimental evidence to show that these two processes are the same, chief of which is their agreement in spectral sensitivity.[3] As a result of this initial action of light, there is assumed to be created within the single crystal of the photographic grain a sort of atmosphere of free electrons. These electrons may be expected to move about readily in the crystal, being reflected at the boundaries of the lattice. However, there is always a certain probability that the electrons may become stuck in localized levels existing around irregularities in the crystal,[4] or return to their original empty levels (parent bromine atoms). This gas of electrons may therefore not be expected to persist indefinitely in the crystal. The state of affairs in a single grain resulting from the initial act of exposure is represented schematically in Fig. 2a.

[3] F. C. Toy, VIIth Internat. Cong. Phot. London, p. 14, 1928. See also W. Lehfeldt, Nachr. Ges. Wiss. Göttingen Math. Phys. Kl. **1**, 171 (1935).
[4] I. Tamm, Physik. Zeits. Sowjetunion **1**, 722 (1932).

To explain the second step in the latent-image process, the so-called sensitivity specks are brought into account. Work by Svedberg,[5] Sheppard, Trivelli, Loveland, and Wightman,[6] Clark,[7] Toy,[8] and others has shown that foreign specks exist on the grains prior to exposure and that these specks play an important role in latent-image formation. Work by Sheppard,[9] Clark,[10] and others has shown that these specks of foreign material consist of Ag_2S and there is also evidence to show that there may be colloidal silver[10] in combination with the Ag_2S. The most generally accepted theories of latent-image formation today identify the latent image itself with metallic silver and assume that the function of the sensitivity specks is to act as centers for the nucleation of the latent-image silver during exposure to light. Gurney and Mott retain this feature in their theory and have proposed the following mechanism whereby the sensitivity specks act to accomplish this.

Secondary process

During exposure to light we have seen that there is created within the photographic grain a sort of gas of free electrons. Gurney and Mott

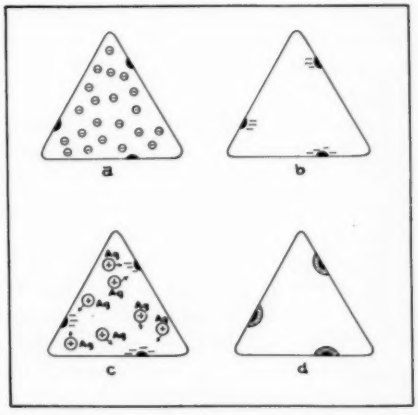

FIG. 2. Schematic representation of electronic and electrolytic processes in photographic grain in formation of latent image.

[5] T. Svedberg, Phot. J. **62**, 183 (1922).
[6] S. E. Sheppard, A. P. H. Trivelli, and R. P. Loveland, J. Frank. Inst. **200**, 51 (1925). S. E. Sheppard, A. P. H. Trivelli, and E. P. Wightman, Phot. J. **67**, 281 (1927).
[7] W. Clark, Phot. J. **48**, 1 (1924).
[8] W. Clark and F. C. Toy, Phil. Mag. **44**, 352 (1922).
[9] S. E. Sheppard, Phot. J. **65**, 1 (1925).
[10] W. Clark, Brit. J. Phot. **74**, 227 (1927).

assume that some of these electrons, in their excursions through the crystal, will come in contact with the sensitivity specks located on the surface of the grain and become trapped there (Fig. 2b). The negative charge thus acquired by the sensitivity specks is then supposed to act through electrostatic attraction to coagulate about the specks, interstitial Ag+ ions, which have been dislodged by heat motion from their regular lattice positions at random points in the crystal (Fig. 2c). These ions will begin to diffuse toward the specks and, when they reach the negatively charged specks, will neutralize the excess electrons there and form silver atoms which remain bound together in metallic clumps. These metallic clumps are then supposed to act as nuclei for inducing development. The final condition in the grain may be schematically illustrated as shown in Fig. 2d.

The way in which the sensitivity specks are assumed to trap electrons may be best understood by reference to Fig. 1, in which the energy diagram of a silver speck is shown adjacent to the energy diagram of AgBr. The energy of a free conduction electron in AgBr lies in the upper conduction band. Gurney and Mott point out that, if the bottom of this band lies above the filled conduction levels of the metallic silver speck, then electrons coming in contact with the Ag speck may be expected to drop down the energy step ΔE, and become trapped. Good evidence that electrons in the conduction level of crystals can be trapped in this way by colloidal metal specks has been given by Glaser and Lehfeldt[11] who worked with KCl crystals containing colloidal specks of K. Lehfeldt[12] has also obtained similar results using large single crystals of AgBr containing colloidal particles of Ag embedded in the crystal. The mechanism of electron trapping outlined here will account for the growth of a Ag particle if there is a Ag nucleus present to start with. Thus, the formation of the latent image can be explained in this way if it is assumed that there is initially present in the sensitivity speck a small amount of metallic silver. Gurney and Mott point out that if there is no Ag present initially, and Ag_2S alone is the active component of the sensitivity specks, then the same mechanism of electron trapping is to be supposed operative for the Ag_2S. The only condition that need be fulfilled is that the conduction band in Ag_2S lie below that of AgBr as shown in Fig. 3.

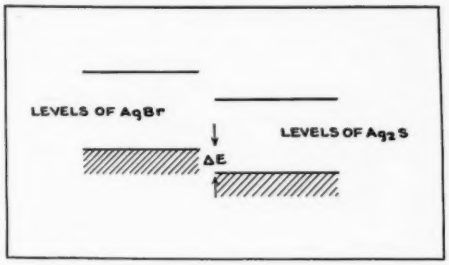

FIG. 3. Conduction levels of AgBr and Ag_2S.

As stated above, the negative charge acquired by the sensitivity specks by trapped electrons will attract interlattice Ag+ ions to the specks. In this way it is supposed that a silver clump will be built up to a size capable of inducing development. The source of Ag+ ions for this purpose is considered to be identical with that which gives rise to ionic conductivity in AgBr. Tubandt and Eggert[13] have shown that the ionic conductivity in Ag halides is to be attributed to the movement of Ag+ ions, and Frenkel[14] has given a very satisfactory theoretical model to explain the manner in which this electrolytic conductivity takes place. Recent theoretical work by Jost[15] has shown from energy considerations that the Frenkel model is very probably correct for the Ag halides. According to the Frenkel-Jost picture, at any temperature, T, there will be a certain number of Ag+ ions dislodged by heat motion from their regular lattice positions and removed to interlattice positions as illustrated in Fig. 4. It can be shown that under conditions of equilibrium the number of ions that are displaced from the regular lattice position in this way will be given by an expression of the type

$$N_T = Ce^{-Q/2kT},$$

[11] G. Glaser and W. Lehfeldt, Nachr. Ges. Wiss. Göttingen, Math. Phys. Kl. **2**, 91 (1936).
[12] W. Lehfeldt, Nachr. Ges. Wiss. Göttingen, Math. Phys. Kl. **1**, 171 (1935).
[13] C. Tubandt and S. Eggert, Zeits. f. anorg. allgem. Chemie **110**, 196 (1920).
[14] I. Frenkel, Zeits. f. Physik **35**, 652 (1926).
[15] W. Jost, J. Chem. Phys. **1**, 466 (1933).

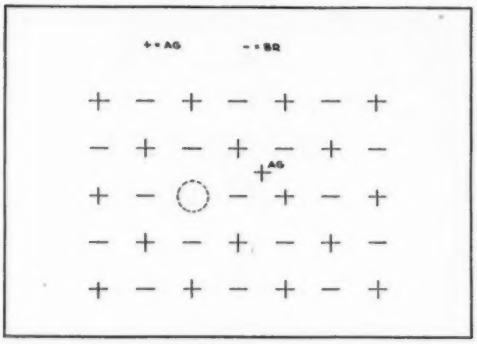

FIG. 4. Model to illustrate electrolytic conductivity in AgBr.

in which Q is the energy required to remove an ion from its regular lattice position to an interlattice position. Electrolytic conductivity is ascribed to the movement of these interlattice Ag+ ions and also to movement of the vacant places in the lattice left by these ions. The vacant places diffuse by replacement conduction. That is, an ion next to a vacant place will jump into the vacant place, leaving, in turn, its own place vacant. Then another ion will jump into this vacant place, etc., thus resulting in the movement of the vacant place through the crystal. The diffusion of the vacant places is not assumed to contribute to the latent-image process, but only the diffusion of the Ag+ ions. According to the Frenkel model illustrated in Fig. 4, it is to be noted that the average number of ions per elementary cube of the crystal does not change with the number of displaced ions and therefore with temperature. Wagner and Beyer[16] have carried out experiments to test this by measuring the macroscopic density and interlattice spacing (by x-ray analysis) at different temperatures. Their measurements on AgBr at 20°C and 395°C gave results that are completely compatible with the Frenkel model.

Thus, the assumption made by Gurney and Mott to explain the secondary process of latent-image formation appears to be in good accord with the facts known about electrolytic conductivity.

[16] C. Wagner and J. Beyer, Zeits. f. physik. Chemie **32B**, 113 (1936).

Reciprocity law failure

Gurney and Mott have shown that their theory of latent-image formation can account for the well-known phenomenon of reciprocity law failure. The low intensity reciprocity law failure is attributed to the tendency of electrons to be ejected from the sensitivity specks by temperature motion. The dependence of this effect on intensity level is explained as follows: At any given temperature, a metallic silver speck in contact with AgBr (see Fig. 1) may be expected to give off a few electrons by virtue of the temperature motion of its conduction electrons. Thus, a metallic speck originally neutral would acquire a slight positive charge. From this it may be concluded that, conversely, in order to place an excess of electrons on the speck, it will first be necessary to build up a certain minimum concentration of free electrons in the grains so as to overcome the negative space charge around the metallic speck. At low intensities of exposing light, the electron concentration in certain grains will never reach this minimum value required for the specks to start to charge up negatively, and these grains will not acquire a latent image. This will result in a diminished number of developable grains and the effect will increase with lowered intensity. Since the tendency for electrons to be ejected from the sensitivity speck is decreased by lowering the temperature, it is to be expected that the low-intensity reciprocity law failure should decrease with lowered temperature.

The high intensity reciprocity law failure is considered to be connected with the secondary process of latent-image formation consisting of Ag+ ion diffusion. At high light-intensities it is supposed that the electrolytic movement of Ag+ ions cannot keep pace with the movement of electrons to the sensitivity specks. This prevents immediate neutralization of the negative electronic charges as they collect at the specks. The unneutralized negative charge resulting on the specks will thus build up a repelling force for further electrons and hold down the subsequent rate of trapping of electrons to the rate at which Ag+ ions can reach the specks. As a consequence, many internally re-

leased electrons will be lost* in this way for the latent-image process, resulting in a decrease of sensitivity of the emulsion. This effect will obviously become more pronounced as the intensity increases and will therefore manifest itself as a loss of sensitivity with increased intensity level.

Effect of temperature

On the basis of the foregoing theory of latent-image formation, it is possible to make certain qualitative predictions about the effect of low temperature on the photographic process. Experiments in this direction therefore suggest themselves immediately as a means for testing the validity of the theory.

The primary process of latent-image formation, consisting of internal release of electrons by light absorption and the subsequent movement of these electrons, is believed to be little affected by low temperature down to −186°C. This belief is based on experiments on photoconductivity carried out by Lehfeldt[17] in which no drop in photoelectron yield was found down to the temperature of liquid air. The secondary process of latent-image formation consisting of electrolytic transport of Ag+ ions is, however, expected to be critically dependent upon temperature and should give rise to observable photographic effects. In accordance with the Frenkel-Jost model of electrolytic conductivity in AgBr, the number of Ag+ ions available for conductivity and also their mobility are dependent entirely upon temperature motion of the lattice. At the temperature of liquid air, mobility of the ions, if not completely eliminated, should at least be very materially decreased. What will be the effect of this on the latent-image process? It has been pointed out that for efficient utilization of the light action, the intensity level of the exposing light should be such that the movement of the Ag+ ions to the sensitivity specks can keep pace with the electrons being trapped there. If, by a drop in temperature, the mobility of these ions is materially reduced, this condition of efficient utilization will be upset and the Ag+ ions will then not be able to keep the sensitivity specks completely neutralized. The effect of this will be to slow down the rate of trapping of further electrons. Electrons repelled away from the sensitivity specks in this way will become lost for the latent-image process by recombination with the parent bromine atom or by trapping at irregular points inside the crystal. Thus a smaller amount of accessible latent-image silver, and therefore a drop in sensitivity, should result at lower temperature. It is to be noted here that (for high intensities) a decrease in temperature should act in the same way as an increase in light intensity. This is so because both act in such a way as to effectively slow up the ionic diffusion rate relative to the rate of charging up of the speck.

Experiments carried out at low temperature to test some of the above features of the theory will now be presented and it is believed that in all cases the experimental results are adequately explained by the theory.

Experimental Part

The first experiment to be described illustrates the effect of low temperature (−186°C) on the sensitivity of the emulsion used in the following tests. The exposures in this experiment were made through a neutral density step wedge placed in front of the emulsion. For temperature control the emulsion was inserted in a metal guide placed vertically against the inner wall of a Dewar flask as shown in Fig. 5. The exposing light was obtained from a tungsten lamp in a metal lamphouse having a double ground-glass diffusing window. The source intensity of the illuminated window was 157 cp and the color temperature 2920°K. The lamp was placed at a distance of 4 m from the film, and the total time of exposure was 160 seconds. The characteristic curves made at room temperature (20°C) and liquid air temperature (−186°C) are shown in Fig. 6. The curve *A* was made with the Dewar flask empty and the curve *B* with the Dewar flask filled with liquid air. The great

* Electrons thus rejected by the speck will either return to their parent bromine atoms or be trapped at irregularities in the crystal lattice. It is also possible that they may be trapped by sensitivity specks on the interior of the grain and build up latent-image specks inaccessible to the developer. Lüppo-Cramer has recently given evidence that the reciprocity law failure and Clayden effects are to be attributed to formation of the latent image in the interior of the grain.

[17] W. Lehfeldt, Nachr. Ges. Wiss. Gött., Math. Phys. Kl. 1, 171 (1935).

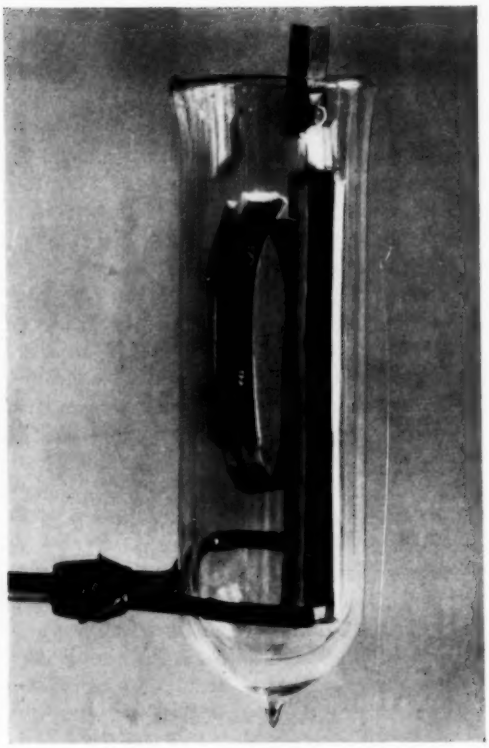

FIG. 5. Apparatus for maintaining film at liquid-air temperature during exposure.

fall in sensitivity noted here is to be attributed, according to the theory of Gurney-Mott, to the effect of low temperature on the mobility of Ag+ ions. The primary process of release and movement of electrons is supposed to proceed at low temperature exactly as at high temperature. On account of the sluggish movement of the Ag+ ions at low temperature, however, the Ag+ ions cannot move up to the speck and neutralize the charge of the negative electrons as they become trapped. The charge on the speck therefore soon reaches a value so large that further electrons are repelled. Sensitivity specks are thus limited at liquid air temperature to acquiring only a few electrons, which in turn will be neutralized by correspondingly few Ag+ ions when the crystal is warmed up. Consequently, it is believed that only those grains which can be brought to a developable state by the nucleation of an additional small number of atoms of Ag will become developable at all under these extreme conditions of temperature. It is thought therefore that the densities represented by the curve *B* are due to the more sensitive grains of the emulsion and that the great majority of grains which account for the upper part of the curve *A* never acquire sufficiently large development nuclei to become developable at the low temperature.

The following experiments are thought to afford very direct evidence that the loss in emulsion sensitivity with lowered temperature is due to the drop in ionic conductivity as described by Gurney and Mott. These experiments consist of two series of intermittent exposures (A) and (B) made at liquid-air temperature (−186°C). The results may be seen in Fig. 7. In both series (A) and (B), the emulsion was exposed in the same way. The only difference between the series (A) and (B) was the treatment received by the emulsion between flashes. In the (A) series the emulsion was warmed up to 20°C for a brief time during the dark period between flashes and then lowered again to −186°C before the succeeding flash, while in the (B) series the emulsion was maintained at −186°C throughout the intervening dark period.

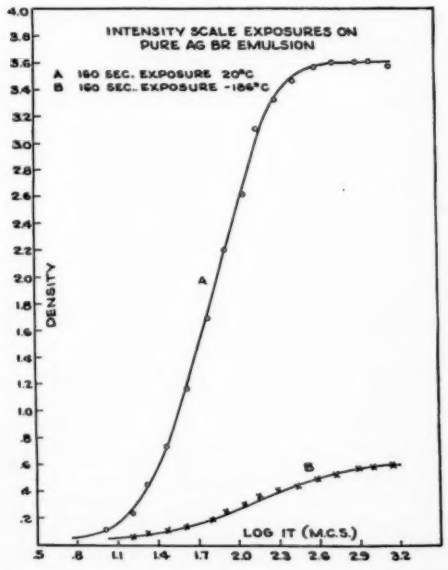

FIG. 6. Curves illustrating effect of low temperature on emulsion sensitivity.

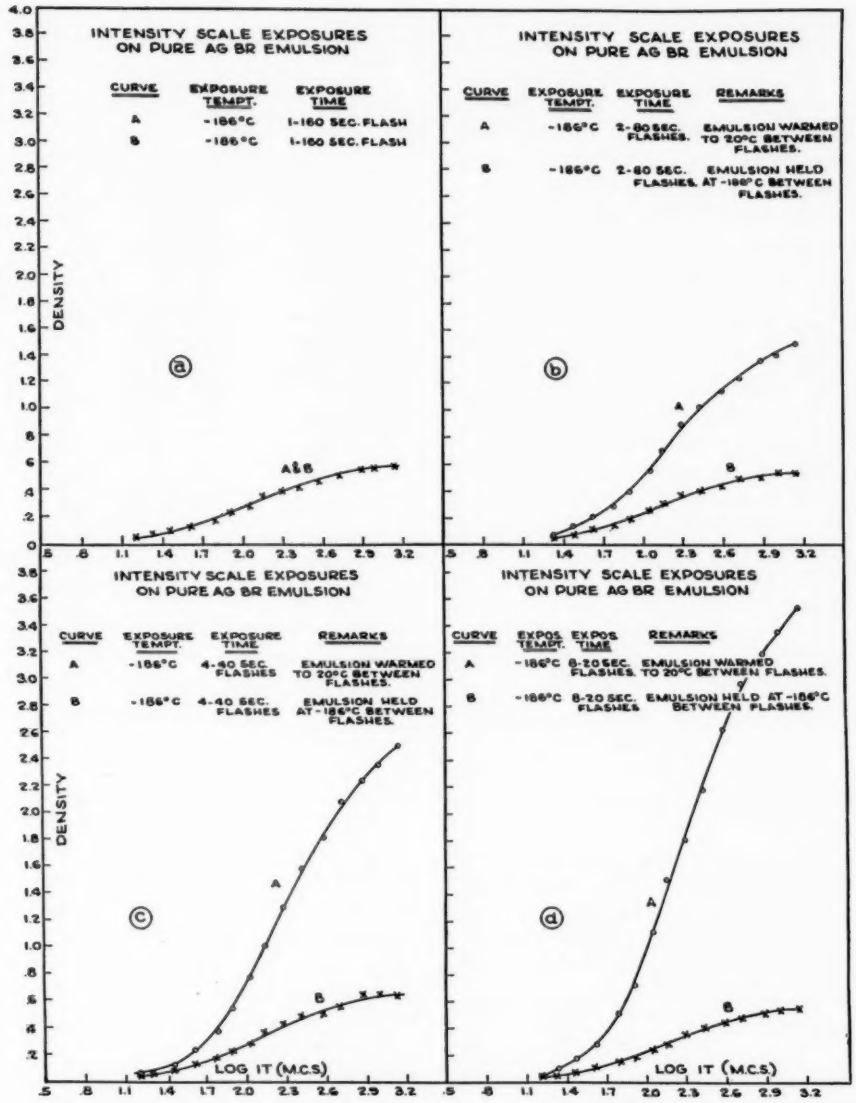

FIG. 7. Curves illustrating effect of making an interrupted exposure at liquid-air temperature and warming up the emulsion between exposure periods.

The length of the dark period between flashes was the same for series (A) and (B) and amounted to 2 minutes. To warm up the emulsion between flashes in series (A), the film was withdrawn from the liquid air immediately upon completion of a flash and was waved several times through the air. This procedure brought the film quickly to room temperature. After holding the film at room temperature for 45 seconds, it was replaced in the liquid-air bath. The film then had the remaining part of the 2-minute period, which always amounted to a full minute, to come to liquid air temperature before the succeeding exposure was started.

The (B) curves of Fig. 7 show that there is no noticeable effect from interrupting the exposures made at liquid air temperature, providing the low temperature is maintained during the intervening dark periods. The (A) curves, on the other hand, show that the same procedure produces a marked effect if the emulsion is warmed up between flashes. Breaking the exposure into two 80-second flashes and giving one warm-up period (Fig. 7b) materially increased the resulting photographic effect. Breaking the exposure into four 40-second flashes (Fig. 7c) and warming up between flashes still further enhanced the photographic effect, and breaking the exposure into eight 20-second flashes (Fig. 7d) with a warm-up period between flashes brought the sensitivity up to a value comparable with the sensitivity at 20°C. The effect of increasing the number of flashes with intervening warm-up periods is shown to better advantage in Fig. 8 in which the entire series of intermittent exposures made at −186°C have been placed on the same graph along with the exposure curve made at 20°C. The curves of Fig. 8 are replots of the (A) curves of Fig. 7. It may be seen that, providing the emulsion is warmed up between flashes, the greater the number of flashes, the greater is the photographic effect obtained. These experiments show definitely that some action vital to the latent-image process takes place during the warm-up periods between flashes. According to the Gurney-Mott picture, this action consists of the movement of Ag+ ions to the charged sensitivity specks. The manner in which the warm-up period acts to increase the sensitivity of an emulsion is thought to be interpretable in the following manner: If it is supposed that the first flash leads to the trapping of several electrons on a sensitivity speck, then upon warming up, Ag+ ions can move up to the speck and neutralize these electrons. A further flash exposure at low temperature will now add several more electrons to the speck and upon warming up again, further Ag+ ions will diffuse to the speck. As a given exposure is broken into more and more flashes, this process is repeated more and more times, and since the greater the number of flashes, the smaller the negative charge that need be added to the speck at each flash, the less is the unneutralized charge placed on the speck at each flash. Since, for smaller unneutralized charges, fewer electrons are lost for the latent-image process, the photographic effect should increase in proportion to the number of flashes into which the total exposure is broken.

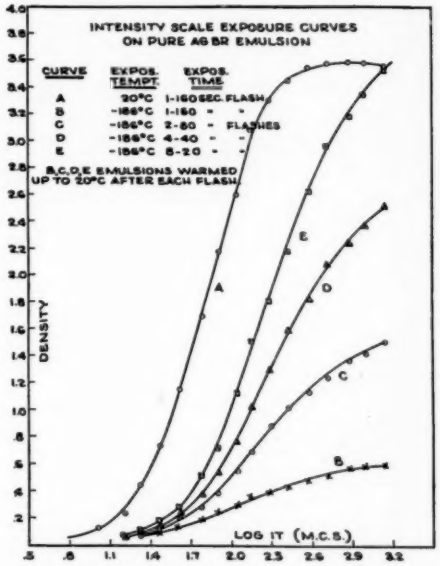

FIG. 8. Curves illustrating the effect on emulsion sensitivity of increased number of interruptions with warm-up periods between exposures.

The above experiments are thought to give positive evidence on the question as to whether for single exposures made at sufficiently low temperature, a part of the latent-image process takes place upon warming the emulsion up after exposure and before development. The fact that all the (B) curves of Fig. 7 are identical within experimental error may be taken as evidence that no electrolytic conductivity takes place during the dark periods, providing the emulsion is held down to −186°C. This is thought to be true since if such conductivity did take place the photographic effect would necessarily increase with increased number of dark periods. The marked increase of photographic effect with increased number of dark periods when warming up was carried out, however, indicates that the ionic conductivity does take place in the warm-up period following the exposure periods. Thus, if an exposure at

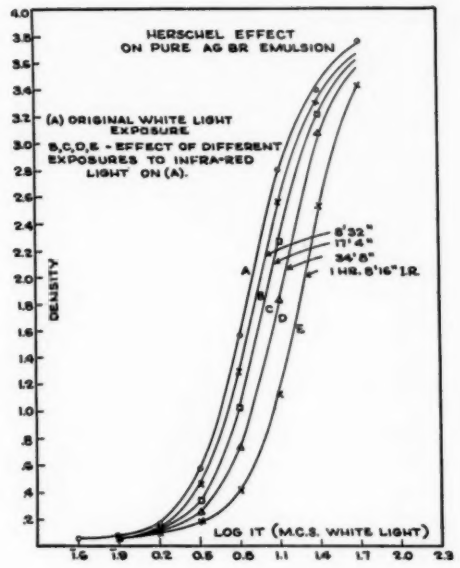

FIG. 9. Curves illustrating the normal Herschel effect on a pure AgBr emulsion.

liquid-air temperature is given in a single instalment, it must be concluded that the entire secondary process of latent-image formation occurs during the warm-up period following exposure and prior to development.

All of the foregoing experiments are considered as affording strong evidence in favor of the Gurney-Mott postulate of electrolytic transport of Ag+ ions as the secondary process of latent-image formation.

HERSCHEL EFFECT

The results to be reported now are thought to give added evidence that there is a secondary process of latent-image formation consisting of electrolytic transport of Ag+ ions and at the same time are thought to give some information on the primary electronic process of latent-image formation. These experiments pertain to the Herschel effect, which consists of the erasure by infra-red light of the forward action of a previous exposure to white light. These experi-

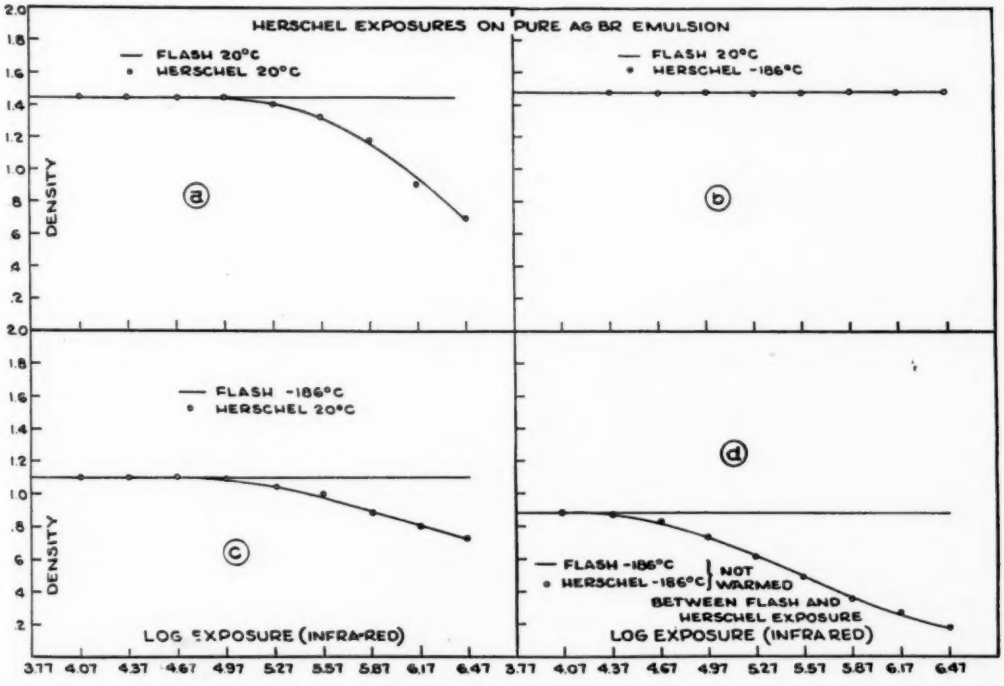

FIG. 10. Curves illustrating the Herschel effect under varied temperature conditions.

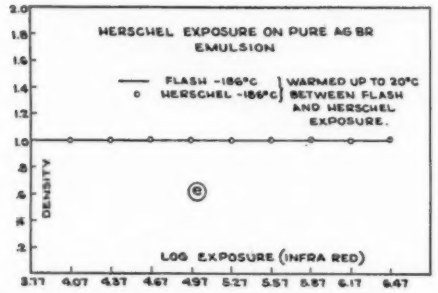

FIG. 11. Curves illustrating the Herschel effect at liquid-air temperature with warm-up period between white and infra-red exposure.

ments were also made under conditions of varied temperature.

The same emulsion (pure AgBr) was used in these experiments on the Herschel effect as was used for the preceding intermittent exposures. In this connection, it has been shown[18] that pure AgBr emulsions exhibit a larger Herschel effect than do bromo-iodide emulsions, so it was expedient in this case to use a pure AgBr emulsion. The simplicity of this emulsion, however, is considered to give an added attractiveness to its use for these experiments. In order to show the extent to which this emulsion is capable of exhibiting the Herschel effect at normal temperature, the curves of Fig. 9 are presented.

The curve *A* represents a time scale *II* and *D* curve made to white light. The other lower curves show the decrease in density obtained when the original exposure strip was subjected to infra-red exposures of different lengths of time. The source of infra-red illumination used in these experiments was a 500-watt tungsten projection lamp burning at 110 volts and filtered by two pieces of Wratten No. 87 filter and one piece of Wratten No. 25 filter. As may be seen from Fig. 9, there is no indication here of an equilibrium density below which the red light has a forward action. The red light is seen to have a reversing action at all density levels. This would seem to indicate that the forward action at low densities, reported by other workers, is to be ascribed to the action of a certain amount of spurious blue light. It was difficult to eliminate an effect due to this cause in the present experiments. Only after considerable experimentation with different filter combinations was this effect entirely removed.

The results of the experiments carried out on the Herschel effect at different temperatures are shown in Figs. 10 and 11. In these diagrams the straight horizontal line represents the density obtained by a primary flash exposure to white light. The points with circles represent the diminished density values obtained upon subsequent exposure to infra-red light superposed on the white-light exposure. In these experiments the primary exposures to white light were adjusted so as to give approximately the same density at 20°C and −186°C. The infra-red exposures were identical at the two temperatures. The infra-red exposures were made to a tungsten 500-watt projection lamp burning at 110 volts, placed at a distance of 0.6 meter from the film. The light from this source passed through two layers of Wratten No. 87 and one layer of Wratten No. 25 filter film. The exposures were made through a power-of-two step wedge giving intensity scale modulation, and had a duration of 900 seconds. The complete data on the exposures to white light and to infra-red light are given in Tables I and II. By reference to the relative energy distribution curve for tungsten at 3000°K, shown in Fig. 12, it is possible to compute approximately the relative energy values of the infra-red and white-light exposures. This has been done in Table III, assuming that the maximum wave-length radiation capable of giving the Herschel effect is 1200 mμ.

The curves of Fig. 10a show the normal Herschel effect in which both the flash white

TABLE I. *White-light exposure (tungsten 2920° K).*

TEMP.	SOURCE INTENSITY	DISTANCE	EXPOSURE INTENSITY	EXPOSURE TIME	EXPOSURE IN M.C.S.	FILTER
20°C	157 cp	5.64 m	4.95 M.C.	3 sec.	14.85	None
−186°C	157 cp	5.64 m	4.95 M.C.	120 sec.	594.0	None

TABLE II. *Infra-red exposure (tungsten 3100° K).*

TEMP.	SOURCE INTENSITY (UNFILTERED)	DISTANCE	EXPOSING INTENSITY (MAX. STEP)	EXPOSURE TIME	EXPOSURE IN M.C.S. (UNFILTERED)	FILTER
20°C	1100 cp	.6 m	3300 M.C.	900 sec.	2.97×10^6	2-No. 87, 1-No. 25
−186°C	1100 cp	.6 m	3300 M.C.	900 sec.	2.97×10^6	"

[18] A. P. H. Trivelli, J. Frank. Inst. **207**, 765 (1929).

exposure and the subsequent infra-red exposure were made at room temperature (20°C). The curves of Fig. 10b show the results for the case in which the flash white exposure was made at 20°C and the infra-red Herschel exposure applied after the emulsion had been taken down to −186°C in temperature. As may be seen, no Herschel effect was obtained in this case. The results of the next experiment tried are shown in Fig. 10c in which the flash white exposure was made at −186°C and the Herschel exposure put on after the emulsion was warmed up to 20°C. It is seen that a considerable Herschel effect was obtained in this case. Identical results with those of Fig. 10a are not to be expected here since the original densities from the white-light exposures probably result from entirely different grain-size classes. The last experiment of the series is that shown in the Fig. 10d in which the flash white exposure and the subsequent infra-red exposure were both made at −186°C and the emulsion maintained at this low temperature between exposures. In this case it is seen that a large Herschel effect was again obtained and, toward the low exposure end, only about one-fourth as much infra-red exposure was required to give the same density decrease as was required in the 20°C case.

In order to interpret the foregoing experiments, it is necessary to consider briefly the explanation of the Herschel effect according to the present theory. Consider for this purpose a single grain which has received an exposure to white light. Electrons are released internally by light and then become trapped on the sensitivity specks. If the crystal is at room temperature it is supposed that Ag+ ions diffuse to the negatively charged specks and form specks of metallic Ag around these sensitivity specks. The Herschel exposure to infra-red light presumably destroys this speck of metallic Ag, or at least reduces its size. This is thought to come about as a result of the ejection of electrons from filled levels of

TABLE III.

TEMP.	RATIO INFRA-RED EXPOSURE / WHITE-LIGHT EXPOSURE
20°C	5.42×10^6
−186°C	0.135×10^6

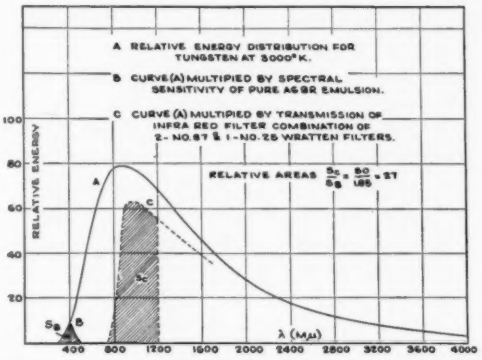

FIG. 12. Curve showing relative energies in white-light and infra-red exposures.

the metallic speck, into the conduction level of the AgBr (see Fig. 1). Disintegration of the metallic speck follows by the diffusion away of the Ag+ ions of the speck. This analysis is considered as explaining the normal Herschel effect obtained at room temperature as shown in Fig. 10a. Consider now the case in which the flash white exposure is given at 20°C and the emulsion then lowered to −186°C for the Herschel exposure. On exposure to the infra-red light at the low temperature, it is supposed that the electrons are ejected from the levels of the metallic speck just as in the former case, but now the Ag+ ions cannot diffuse away at the low temperature. Thus, the electrons ejected will be attracted back again to the latent-image specks and the latent-image nuclei will remain intact after the infra-red light stimulus is withdrawn. This analysis appears to be in good accord with the results shown in Fig. 10b in which the flash white exposure was made at 20°C and the Herschel exposure at −186°C. No Herschel effect was observed under these conditions.

The next case to be considered is that for which the flash white exposure was made at −186°C and the Herschel exposure was made after the emulsion had been warmed up to 20°C. On the basis of the above analysis, this case should correspond very closely to the one in which both exposures were made at 20°C, since warming up the emulsion for the Herschel exposure permits the completion of the formation of the latent image, which then is subject

to destruction in the same way as described for the normal case. It may be seen from Fig. 10c that a normal Herschel effect was obtained in this case.

The last experiment of the series is that in which both the flash white exposure and the Herschel exposure were applied at −186°C with the emulsion maintained at the low temperature between exposures. In this case it is assumed that, on making the white-light exposure, electrons are released in the grain and become trapped on the preexistent sensitivity specks as usual. The Ag+ ions not being able to diffuse to the specks and neutralize these electrons, the specks soon acquire such high negative charges that they begin to repel further electrons which become lost for the latent-image process. Thus, the potential latent image that can be built up in this way is limited. If, now, the sensitivity specks, while charged in this manner, are subjected to infra-red illumination, the question arises: will it be possible to eject electrons from the speck and thus erase this so-called potential latent image? The experimental results of Fig. 10d appear to answer this question in the affirmative. Here a strong Herschel effect was obtained with somewhat less infra-red exposure than was required at room temperature. This indicates, in fact, that the electrons are more easily liberated from the speck in this case because of the negative charge.* [19, 20]

An experiment which is thought to give added support to the foregoing interpretation is that shown in Fig. 11. This experiment consisted of making a flash white exposure at −186°C and a Herschel exposure also at −186°C, but warming the emulsion up to 20°C between exposures. This warming-up period allows complete formation of the latent image, which should then react to a subsequent infra-red exposure in precisely the same way as was found in the experiment shown in Fig. 10b, in which the white exposure was made at 20°C and the infra-red exposure at −186°C. That this is the case is confirmed by the data in Fig. 11. This result appears the more striking when a direct comparison is made between the curves of Figs. 10d and 11. The exposures in the two cases were in every way identical and both were made at −186°C. The only difference between the two experiments was that in the experiment of Fig. 11, the emulsion was warmed up to 20°C for a brief interval during the period between the white and infra-red exposures.

It was stated earlier that the experiments on the Herschel effect also throw some light on the primary electronic process of latent-image formation. It is thought that this is brought out in the experiment of Fig. 10d, in which the Herschel effect is obtained, presumably, before the secondary process of latent-image formation has occurred. It appears that the electrons trapped on the original sensitivity specks (consisting of Ag_2S, or Ag, or perhaps a combination of both) can be ejected by the infra-red light as well before the Ag+ ions have coagulated as after. The fact that the Herschel effect seemed even stronger in this case (reversal was obtained with less exposure and a greater percentage decrease in density was obtained throughout) than in the case where the latent image was already completely formed, indicates that the electrons are ejected more readily from the sensitivity specks before the coagulation of Ag+ ions than after.

Reciprocity Law Failure

The remaining experimental results to be reported have to do with the reciprocity law failure at low temperature. The theory of latent-image formation outlined by Gurney and Mott has been seen to account for the reciprocity law failure at both high and low intensity and the manner in which it is expected to change with temperature. The following experiments were carried out to test this aspect of the theory.

The experiments on reciprocity law failure were not made on the same emulsions used in the previous experiments. The emulsions chosen for these tests were the same as those used by one of the authors in some former low-tempera-

* An alternative view put forward by Mott[19] here is that in exposures made at low temperature, the electrons mainly become stuck at irregular levels in the crystal and go to the sensitivity specks after the crystal is warmed up. If this is the case, then the infra-red exposure must be supposed to eject electrons from these irregular levels in producing the Herschel effect at low temperature. Berg[20] has recently carried out experiments on the Herschel effect to test Mott's hypothesis and these results will be published in the near future.

[19] N. F. Mott, Phot. J. Special Number **77**, 286 (1938).

[20] W. F. Berg (private communication).

ture experiments[21] on this same subject. The experiments to be described here confirm this former work insofar as the results overlap and, in addition, show up a new effect which sets in only at extremely low temperature.

Experimental Procedure

The exposures were made on two commercial emulsions, one a high speed blue-sensitive emulsion and the other a high speed panchromatic emulsion. These will be referred to subsequently by the numerals I and II, respectively.

Exposures were made on the regular reciprocity sensitometer,[22] the exposures consisting of time-scale curves. The exposing light was a tungsten lamp burning at 2500°K and the intensity was varied over the desired range by moving the lamp and thus varying the intensity in accordance with the inverse square law. Exposures were made at intervals of powers-of-four in intensity, the time of rotation of the sector being quadrupled each time the intensity was lowered by a power-of-four step.

The temperature of the emulsion was maintained during the exposures by means of a specially built low temperature apparatus described in the former work carried out on this subject.[21] It consisted of a double outer-walled, brass cylindrical container, with a rotatable inner drum on which to place the film. The drum could be rotated by a handle extending to the outside so that a series of exposure curves could be made on a single piece of film wrapped on the drum. The exposing light was admitted through an evacuated, double-walled glass window.

Results

The experimental results may be seen from Figs. 13 and 14. The curves are plotted in the usual manner for constant density values, the ordinates of the curves representing the log of the exposure value required to produce unit density as a function of the log of intensity at which the exposure was made. The normal reciprocity curves at room temperature (20°C) are included on the diagrams. At this temperature the curve exhibits a minimum at some intermediate intensity level known as optimal intensity. The rise in the curve at intensities above and below optimal shows that more exposure is required to produce a given density at these intensity levels. This rise of the curve at high and low intensity is termed the high-intensity and low-intensity reciprocity law failure, respectively. If the reciprocity law were valid, the lines of constant density would be straight horizontal lines on this diagram.

The present results show that the low intensity reciprocity law failure diminishes rapidly with lowered temperature. At −78°C there is no indication of the upturn of the reciprocity curve down to the lowest intensities reached in these exposures. This is true for both emulsions as may be verified from Figs. 13 and 14. At the still lower temperature of −186°C, the curves have become flatter throughout the intensity range covered, and there appears to be an increased tendency to flatness at the high-intensity end. It thus appears that the high intensity reciprocity law failure is also disappearing with sufficiently low temperature. It should perhaps be remarked here that the vertical shift upwards of the entire curves with lowered temperature is in accord with the general drop in sensitivity with lowered temperature discussed earlier. The difference in the amount of this shift for the two emulsions used is not understood at present. Whereas the No. I emulsion seems to show a continuous drop of sensitivity with temperature down to −186°C, the No. II emulsion appears to drop to a certain low value and then not change with further change of temperature. Only a study of this effect at smaller temperature steps can clear up this point. For the present only the shapes of the curves are of importance and it is evident that the curves at −186°C for both emulsions are very much flatter than the curves at −78°C.

These results on reciprocity law failure are thought to be further evidence in favor of the theoretical picture of latent-image formation proposed by Gurney and Mott. According to their theory the low intensity reciprocity law failure is attributed to a tendency for the sensitivity speck to lose electrons by heat motion. As a result of this tendency, it is assumed that at any temperature a certain minimum concen-

[21] J. H. Webb, J. Opt. Soc. Am. **25**, 4 (1935).
[22] L. A. Jones, J. Opt. Soc. Am. **7**, 305 (1923).

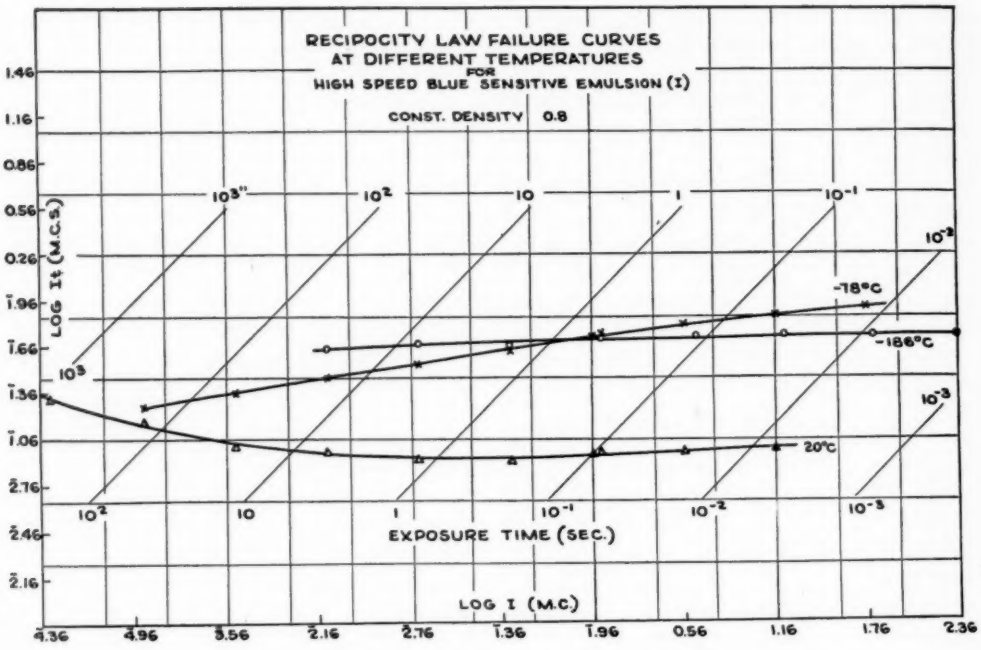

FIG. 13. Reciprocity law failure curves at different temperatures.

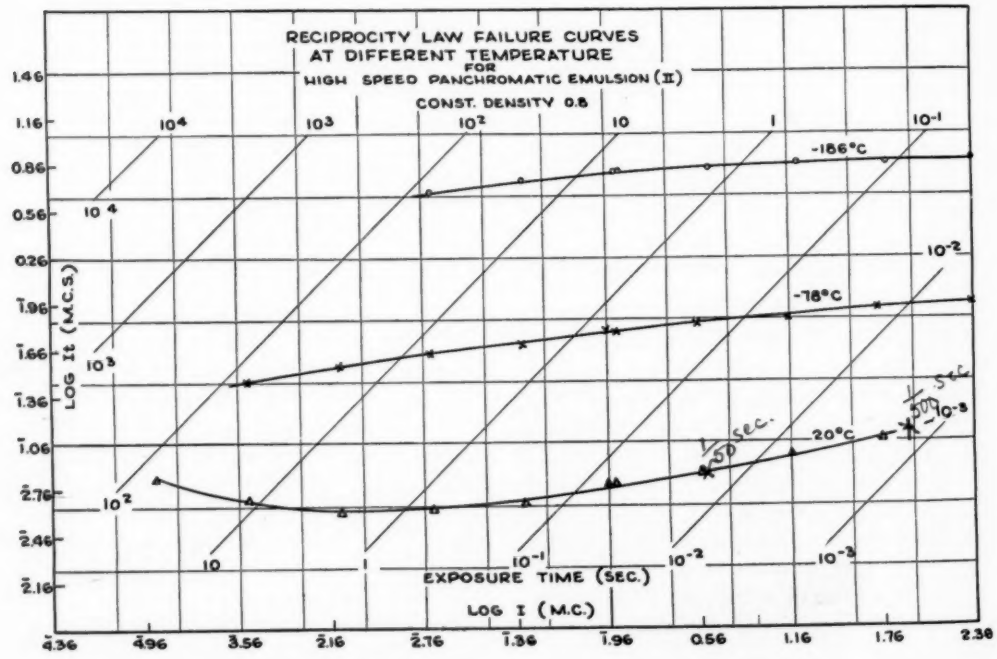

FIG. 14. Reciprocity law failure curves at different temperatures.

tration of electrons must first be built up in the crystal before electrons will begin to be trapped by the sensitivity speck. In some grains, at low intensities, the requisite concentration will not be attained and so these grains will not become developable. However, at low temperature, the electrons would not be ejected to the same extent from the speck and consequently the minimum concentration required for placing electrons on the speck should be lowered. Thus, the intensity level at which lowered efficiency sets in should be pushed to lower values by lowering the temperature. In other words, there should be less reciprocity law failure at low temperature. The experimental results in Figs. 13 and 14 show that the upturn of the curves at low intensities does die out with lowered temperature and are in direct accord with this explanation of the reciprocity law failure given by the theory.

An alternative, though similar, explanation of the low intensity reciprocity law failure which is thought to fit in equally well with the experimental results is the following: The reciprocity law failure at low intensity simply signifies that the efficiency of production of the latent image is low at weak intensities. It seems possible that this may be attributable to a dissociation of the Ag speck, when it begins to form, by thermal excitation of the electrons of the metallic speck. If an electron were ejected by heat motion, a Ag+ ion would diffuse away after it. If the stability of the Ag nucleus increases with size, then the effect of intensity may be readily accounted for. At low light intensity where single or double atoms of Ag may have to exist for long periods, the probability of thermal annihilation may be very large. This appears reasonable as it is easy to believe that the mutual binding of a large number of Ag atoms in a clump would give added stability. Whereas the Gurney-Mott explanation assumes that, at low intensities, electrons will not become trapped on the speck below a certain minimum concentration, the present explanation assumes that they become trapped and neutralized, but that there is a strong probability of the electron being ejected again when the speck is still small. Which explanation is in accord with fact can only be decided by further experiments.

The results on the high intensity reciprocity law failure are considered to be very simply and directly explained on the Gurney-Mott theory. The loss of efficiency at high intensities is attributed to the sluggishness with which the Ag+ ions can diffuse to the charged sensitivity specks. At high intensities the diffusion of Ag+ ions cannot keep pace with the rate of charging up of the sensitivity specks by the electrons. Consequently, the specks become too highly charged and electrons are temporarily repelled. This results, as was described earlier, in a reduced amount of latent-image silver being formed at extremely high intensities and thereby a falling off in the efficiency. This dependence of efficiency on intensity level is to be expected to persist at all temperatures down to the point at which ionic mobility ceases. The curves of Figs. 13 and 14 show that the reciprocity law failure curve has become nearly horizontal at −186°C. It is to be noted further that it is horizontal at the high intensity end and this is as it should be.* [23] When the combined effect of temperature and intensity is such that the Ag+ ions cannot reach the speck during the entire period of exposure to light, then further increase of intensity should not make any difference. It is obvious that either decreased temperature or increased intensity can act to produce this same effect. From the appearances of the curves at low temperature this seems to be experimentally confirmed.

* Work by Berg and Mendelssohn soon to be published shows that, for emulsions tested by them, the curves are flat throughout at −186°C. It may be that the temperature in the present experiment was not completely down to −186°C in the long exposures due to heating of the emulsion by radiation through the exposing window. It is rather obvious, however, what the trend is in these experiments and they are considered to be in direct accord with Berg's and Mendelssohn's results.

[23] W. F. Berg and K. Mendelssohn (private communication).

Apparatus for the Study of the Raman Effect

A. H. PFUND
Rowland Hall, Johns Hopkins University, Baltimore, Maryland
(Received April 19, 1938)

AS the result of an attempt to devise apparatus for the routine study of the Raman effect, an apparently novel design has been evolved. The new apparatus is relatively inexpensive yet very efficient in its utilization of the radiant output of the source. In spite of the fact that but a glass mercury lamp is used, photographs of the stronger Raman lines of benzol may be obtained after an exposure of less than five minutes.

The essential parts of the apparatus are shown in Fig. 1 where A_1 is a (Ford) automobile headlight reflector (silvered). After having filed out the crimped collar intended for the insertion of the small headlight lamp, a Pyrex mercury lamp L is introduced. This lamp, which is to be discussed later, rests on strips of asbestos (not shown) glued to the outside of the reflector. Three small wooden blocks (not shown) are glued to the lower edge reflector for purposes of ventilation; these blocks rest on a sheet of Pyrex glass G_1 under which is a second sheet of ordinary glass G_2 separated by wooden blocks from G_1. The cooling attained through the use of these pieces of glass is sufficient to prevent the liquid in the Raman tube from boiling. If it be desired to excite Raman spectra with the 4358 line only, an Eastman A-2[1] filter, which renders the 4047 line innocuous is introduced between the pieces of glass. In case a quartz-mercury lamp is used, it will be desirable to make an absorption cell out of these sheets of glass. By adjusting their separation to about 15 mm and, filling the cell with a saturated solution of $NaNO_2$,[2] the Raman tube is kept cool and the 4047 line is likewise greatly reduced in intensity. All of this apparatus rests on a second reflector A_2, glued to an ordinary tripod T. Fitting snugly into the crimped collar at the base of this reflector is the Raman tube R (about 10 cm long and 1.4 cm internal diameter) blackened at the upper end and provided with a side-tube S for purposes of filling. Since organic liquids are to be studied, the plate of glass, closing the lower end of the tube, is attached with a cement made of dry cane sugar, melted down to form a yellowish-brown mass. A totally-reflecting prism P allows the light to proceed in a horizontal direction. Upon looking into the prism one sees (if the tube be filled with benzol) a circular disk of bluish light with a bright central "core." This core is focused on the slit of a spectrograph by means of a glass lens. The reading of the very complete directions given by Wood[3] for the "pointing" of the spectroscope is recommended. Unmodified light of the mercury arc, for purposes of comparison spectra, is obtained by removing the Raman tube and, inserting the metal collar C (shown in Fig. 1) into the crimped collar of the reflector. The concave side of the tongue F is fumed with MgO from burning magnesium ribbon.

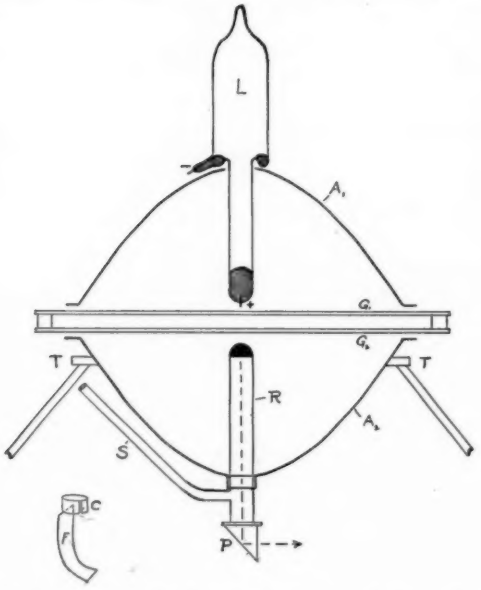

FIG. 1. Elevation showing the disposition of the various parts of the Raman apparatus.

Without attempting to prove the point by means of an elaborate system of ray-tracings it

[1] P. L. Bayley, J. O. S. A. **27**, 303 (1937).
[2] A. H. Pfund, Phys. Rev. **42**, 581 (1932).
[3] R. W. Wood, Phil. Mag. **6**, 729 (1928).

is evident that a large fraction of the total angular emission of the mercury lamp ultimately passes through the axial portion of the lower reflector—a position occupied by the Raman tube. The mercury lamp is of a type previously described.[4] Connected to 110-volt d.c. terminals through series resistance, it operates on a current of 2 amperes. The lamp is started by heating with a Bunsen burner and by tipping so that the mercury flows toward the upper (negative) electrode. It has been found that the life of such a lamp is materially lengthened by using only mercury which has been distilled into the lamp and by employing rugged tungsten wire (1 mm in diameter) as electrodes.

Raman spectra of benzol and carbon tetrachloride obtained with this apparatus, after an exposure of 20 minutes, are shown in Fig. 2. These liquids were taken directly from bottles, i.e., they were neither filtered nor redistilled. It is evident that all three spectra are convincingly different. Of particular interest are the anti-Stokes lines of CCl_4 shown on the short wave-length side of the 4358 line. The quartz spectrograph used was the small Hilger E-31. In spite of the fact that the linear separation of the 4358 and 4915 lines on the negative was but 3.5 mm the wave-lengths of infra-red absorption bands, calculated from the data presented by Raman spectra, were found to be in excellent accord with observed values.

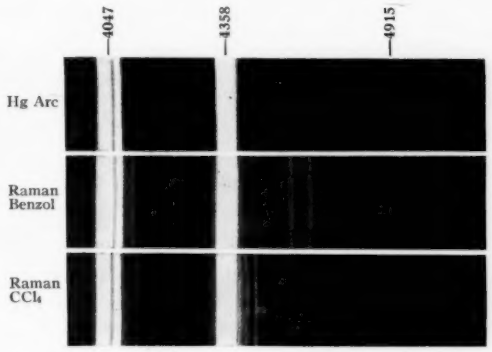

FIG. 2. Photographs showing the Raman effect. Upper photograph, bare mercury arc. Middle photograph, Raman spectrum of benzol. Lower photograph, showing Raman effect of carbon tetrachloride.

After this work had been completed it was found possible to double the light intensity from the Raman tube by gluing a flat silvered mirror of circular outline, to the inner surface of the upper, closed end of the Raman tube. Such a mirror, when so adjusted that its normal lies parallel to the axis of the tube, will double the effective length of the tube and hence increase the light intensity markedly. In place of the silvered mirror an aluminized one is recommended because of its greater freedom from tarnish.

[4] A. H. Pfund, Phys. Rev. **3**, 314 (1914).

A Spring Suspended and Thermostated Littrow Spectrograph

NORTON A. KENT AND REGINALD G. LACOUNT
Boston University, Boston, Massachusetts
(Received March 10, 1938)

A system is described for mounting a Littrow spectrograph so as to overcome both mechanical vibration and temperature variation.

THE 30-foot Littrow spectrograph of our basement research laboratory—the purchase of parts of which, some years ago, was made possible by grants from the Rumford Committee of the American Academy of Arts and Sciences—was formerly[1] used only visually owing to extremely bad conditions, the "Boston Elevated" subway being but 50 feet distant and steam pipes running through the room. Both these difficulties have been eliminated to a satisfactory degree.

The vibration problem has been solved as follows: The frame of the instrument is made of two 10″ I beams I and II in Fig. 1a), 34.5′ and 31.5′ long, respectively. These are joined by iron plates $\frac{1}{2}$″ thick and 3″ wide, as shown in Figs. 1a and 1b, the "*a*" plates being flat and bolted to the tops or bottoms of the I beams and the "*b*" plates being bent so as to join the top of one I beam to the bottom of the other or *vice versa*. Massive plates, bolted to the beams, hold the grating, G, with lens, L, and the slit, S, with camera box, C, and plane mirror, M_p. The end of beam I supports a framework upon which is mounted the concave mirror, M_c. When the instrument is "crossed" with an etalon the latter is set at E. The optical arrangement is similar to that previously used.[2]

This system, quite a rigid entity, weighing over a ton, is supported as shown in Fig. 2. Eight four-inch U beams, U, bored at each end, have laid upon them strips of "Keldur," K, 4″ wide and nearly as long as the U beams, above which strips are plates, p, 4″ wide and $\frac{1}{2}$″ thick; above which are felt pads, f, where the plates contact the beams.

Bolts, B_1 and B_2, join the U beams through turnbuckles, T, to 16 helical steel springs designed for us by Professor Arthur E. Norton of Harvard University, so that when under load they are extended to about double their non-load length. The characteristics of these springs are shown in Table I.

Bolts B_3 run through holes in plates, P_1, of different sizes—approximately 11″ square to 17″ square. These plates are separated by heavy felt pads, F_1. The lowest plate in each set rests upon felt and spans two 3″ I beams, I_1 and I_2, of Fig. 2a, lying north and south; these rest upon a set of plates, P_2, separated by felt pads, F_2, and supported below by a plate, P_3, through which four $\frac{5}{8}$″ bolts, B_4, one at each corner, pass up to the ends of strips, S_1, $\frac{1}{4}$″ thick and 2″ wide which in turn span 3″ I beams, I_3, lying east and west; these latter rest at their ends upon L plates bolted to the walls and piers of the building. Almost all of the contacts are through felt.

Thus between trussed frame and wall "Keldur" enters once, a spring once, and felt seven times. A mercury surface shows that most of the vibration is eliminated by the springs.

To discourage lengthwise and sidewise motion the rod systems are inclined from the vertical in both N–S and E–W planes, as indicated in Fig. 2b. To damp out quickly any horizontal or vertical motion which might distort the trussed beams we at first used dashpots filled with water, oil-covered to prevent evaporation. These transmitted vibration from the floor. We therefore rejected this method and mounted—on adjustable wooden plates supported from the floor—twelve red rubber sponges (10¢ each!), three near the ends of each of the big I beams—one sponge at the extreme end, outside and below—all barely touching the beams. This system is proving entirely satisfactory.

Drs. L. D. Leet and H. G. Taylor of Harvard

[1] Proc. Am. Acad. **57**, 3–18 (1921).
[2] Phys. Rev. **51**, 241 (1937).

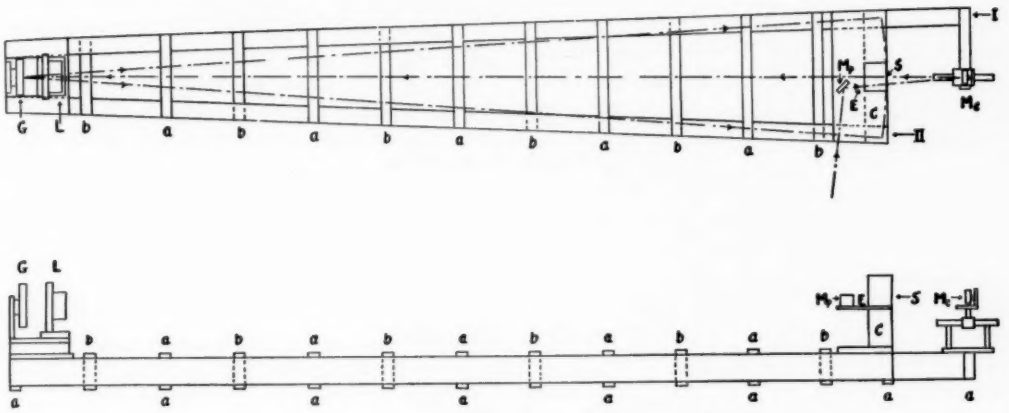

FIG. 1. (a) Top; (b) bottom.

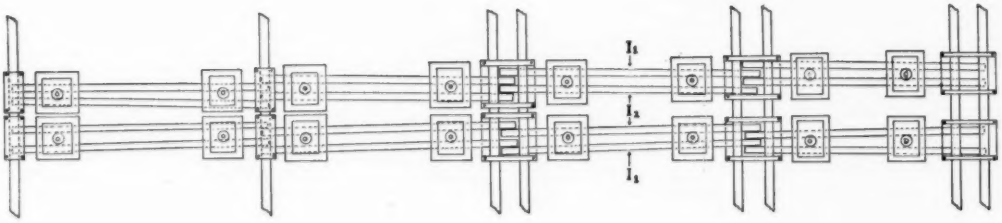

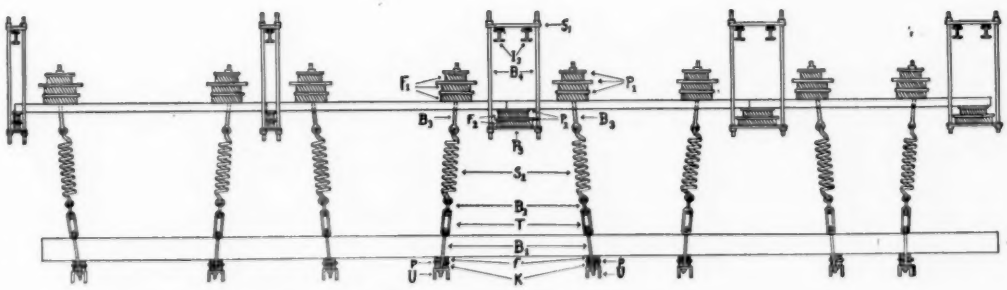

FIG. 2. (a) Top; (b) bottom.

very kindly made two sets of seismograph tests for us. The average amplitude of vibration is 0.0001 inch. In the process of construction, when the mount was supported by wooden trusses resting on the floor, the spectrum lines when viewed by means of an ocular showed a vibration which was extremely violent at times. With the springs in use perfect steadiness of the images exists.

To control the temperature the entire mount, except the ends of the upper E–W I beams, I_3, is enclosed in an inner room built of a framework of 2×3 lumber covered with "Celotex" below and two thicknesses of heavy 6-ply building paper above. The ends of these I beams are wound with layers of felt and building paper and the openings through which they enter the inner room are stuffed with felt. The floor of the inner room is made of 2″×3″ beams covered with building paper and overlaid with tongued and grooved wood. This inner room has no thermostat. The outer is equipped with fans—one at an opening in a basement window near the slit end of the inner room and another near the grating end. An "Aminco" regulator starts the fans when cold air is desired and closes a damper in the opening when the temperature has fallen sufficiently. "Sunbowl" electric heaters are left on at night to compensate for the lack of steam heat. The temperature variation in the inner room is less than 0.05°C during a nine-hour exposure; that in the outer room is about 1°C. During the past summer when the heat in the building was "off," no thermostating was necessary, the temperature in the inner room rising but 3°C in four weeks.

Light sources and electrical apparatus lie outside the inner room, the light entering through a lens which fits snugly in a tube joined to the wall.

The work of measuring the wave-lengths of certain suitable lines in the spectra of H_2, HD, and D_2 by crossed interferometer and grating as well as the wave-lengths of a great number of lines in these spectra by grating alone is proceeding with considerable speed.

The expense of this installation and research are being met from grants made to the senior writer by the Committee of the Permanent Science Fund of the American Academy of Arts and Sciences. This aid is most gratefully acknowledged. We wish also to mention the valuable assistance of our graduate students—especially Professor Lewis S. Combes and Mr. Charles S. Tarr.

TABLE I. *Data concerning sixteen tension springs.*

Number of Springs	Load in Lbs. Carried by Each Spring	Load in Lbs. Carried by All Springs in Each Group	Wire Diam. in Inches	No. of Coils	Solid Height in Inches	Free Height in Inches	Outside Diam. in Inches
1	300	300	$\frac{9}{32}$	32	9″	19″	$2\frac{3}{8}$
1	230	230	$\frac{1}{4}$	36	9″	19″	$2\frac{1}{8}$
2	171	342	$\frac{1}{4}$	36	9″	19″	$2\frac{3}{8}$
12	124	1488	$\frac{3}{16}$	48	9″	19″	$1\frac{5}{8}$

An Adaptometer for Measuring Human Dark Adaptation*

SELIG HECHT AND SIMON SHLAER†
Laboratory of Biophysics, Columbia University, New York, N. Y.
(Received March 25, 1938)

An instrument is described with which one can measure the course of human visual dark adaptation under specified but flexible conditions useful for physiological and clinical investigation. The preadapting light adaptation is controlled in brightness, retinal location, and duration, and the subsequent dark adaptation of a specific retinal area is measured with light flashes whose spectral composition and duration are controlled.

I. PURPOSE

IT has long been known that the incidence of night blindness is in some way related to the state of nutrition of the body, and this has recently become understandable in terms of the connection of vitamin A with the composition of visual purple, the photosensitive substance of the retinal rods.[22] Since dark adaptation is mainly a phenomenon of rod function and is associated with the regeneration of visual purple,[4, 21] efforts have been made to use the behavior of dark adaptation as a means of diagnosing vitamin A deficiencies.[11, 12, 16]

Dark adaptation has been studied in our laboratory for several years.[6, 8, 9] As a result, many requests have come to us for assistance and advice, and we have frequently been asked for an apparatus which could be used in physiological and clinical investigations. It is for this purpose that we have devised the apparatus to be described. The instrument was designed and built in the spring of 1937, and has been in constant use in our laboratory since; moreover, several duplicates have been made and are in use in other laboratories.‡ We publish a description of it now, as a preliminary to the publication of results achieved with it, and with the hope that it may be useful to others.

II. NATURE AND COURSE OF DARK ADAPTATION

To understand the reasons for the design of the apparatus, it is necessary to know what dark adaptation is, and what conditions determine its magnitude and course. Dark adaptation is the change in light sensitivity which the eye undergoes in the dark following a stay in the light. The change in sensitivity is recorded by the amount of light necessary for a minimal stimulation of the eye at different times in the dark; the way in which this minimal intensity varies with time represents the course of dark adaptation.

The retina possesses two kinds of receptor elements, (*a*) the cones which function at the higher light intensities and are concerned with color vision, and (*b*) the rods which are especially active at the lower light intensities and are concerned with vision without color. For many years after its discovery by Aubert[1] and its first measurement by Piper,[19] dark adaptation was supposed to take place only in rod vision; however, since 1921 it has become well established[6] that dark adaptation occurs in cone vision as well, and both processes easily become apparent under proper conditions of measurement.

Reversing the usual procedure, we shall present some results with the apparatus before describing it in detail. Fig. 1 shows a typical course of human dark adaptation as measured with the present apparatus. The points are single measurements and record the light intensity which the eye can just barely see as the observer stays in the dark. Because the range of intensities is so large, it is necessary to plot the data on a logarithmic or power scale; this has the additional advantage that at all intensities, a given percentage of the intensity occupies a constant vertical scale distance.

The measurements show that dark adaptation proceeds in two steps. The first is rapid and is over in a few minutes; the second is late in start-

* Publication assisted by Ernest Kempton Adams Fund for Physical Research of Columbia University.
† Aided by a grant from the Rockefeller Foundation.
‡ These instruments, as well as our own original model, were constructed by Mr. O. C. Rudolph, 55 Van Dam Street, New York City.

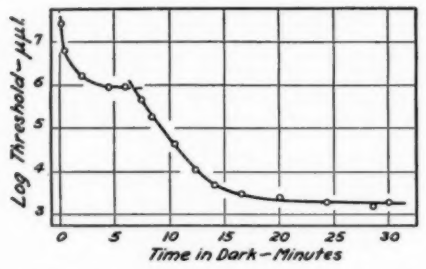

FIG. 1. The course of human dark adaptation following light adaptation to a brightness of 1550 millilamberts. The points are single measurements and record the threshold of a retinal field 3° in diameter and situated 7° nasally. The measuring light is from the violet end of the spectrum below 460 mμ. The first section of the data records cone function, while the second section records rod function. This is evidenced, among other things, by the fact that even at the threshold for the first five points the light appears definitely blue, whereas for the remaining points the threshold is without color. The ordinates are in micro-microlamberts (μμl).

ing and goes on for a half-hour or more. The work of the last fifteen years has shown conclusively that the rapid first adaptation records the behavior of the cones, while the delayed and slower second adaptation records the function of the rods. This division of dark adaptation into two sections is in complete harmony with the findings for many other visual functions such as intensity discrimination, visual acuity, and flicker recognition[7] and expresses the duality of visual function first recognized by Schultze[20] and incorporated in the well-known duplicity theory by von Kries.[14]

The measurements in Fig. 1 represent the course of dark adaptation under certain specific circumstances. The conditions have to be specified because the relative extent, the duration, and even the shape of the two parts of the dark adaptation curve depend on a variety of factors concerned with the light adaptation which precedes the dark adaptation, and with the means used for measurement during dark adaptation. For example, if the brightness of the adapting light has been high, then during the subsequent dark adaptation the cone section will be extensive and the rod section will be delayed to such an extent that the rod-cone transition may not appear until 15 minutes stay in the dark.[8] As the preadaptation brightness decreases, the cone section decreases in range and duration, and the rod section appears sooner. In fact, if the light adaptation is below a certain brightness, the cone section does not appear at all, and only rod adaptation shows up.[24] Its extent continues to decrease as the preadaptation intensity is decreased; even its shape changes somewhat. The duration of the light adaptation affects the subsequent dark adaptation in much the same way as the intensity, in that the shorter the preexposure, the less extensive is the cone portion, and the sooner does the rod section appear;[15] moreover, in the dark adaptation which follows very short exposures even to high intensities, only rod function is evident.[23]

The precise specifications of the light used for measuring dark adaptation influence the data just as profoundly as the preadaptation conditions. The rods are relatively much more sensitive to blue and violet light than the cones, due to the position and shape of their luminosity curves.[7] The two systems have about the same thresholds for red light. Thus, when the measurements are made with extreme red light, only one continuous and shallow dark adaptation is apparent, corresponding to cone function.[6, 8, 13] With orange light, a small rod component appears quite late; and with yellow, green and blue lights respectively this rod section becomes increasingly prominent and appears earlier and earlier in the course of dark adaptation.[13]

Similarly extensive differences in dark adaptation appear depending on the size and location of the retinal area used for making the measurements.[9] A central visual area, 2° in diameter, shows only cone adaptation because there are practically no rods in this region. With increasingly larger centrally-fixated areas, dark adaptation shows more and more rod adaptation, the maximum amount of rod function being evidenced by a central area occupying 20° or 30° visual angle in diameter. Practically the same changes are produced if dark adaptation is measured with a small area located in different parts of the retina. A 2° field located centrally, shows only cone adaptation. Placed excentrically, it shows an increasing amount of rod adaptation the farther it is from the fovea.

Finally, the duration of the light used for making the measurements influences the appearance of the data, because the intensity

necessary for a threshold effect varies inversely with the duration.[2, 3, 5] Moreover, since the relation between duration and intensity is different for the cones and for the rods,[17, 18] the two sections of the dark adaptation curve will be affected differently by the measuring exposure to light, and as a result their relative extent and the rod-cone transition point will be altered.

III. Construction of the Apparatus

It is apparent from the preceding section that there are at least six specifications which must be made in recording dark adaptation. These are the intensity and the duration of the preadaptation light, and the area, the retinal location, the color, and the duration of the measuring light. The adaptometer which we have designed not only incorporates these specifications, but is so arranged that the specifications can be varied in order that any aspect of dark adaptation may be studied under different but controlled conditions.

For convenience in presentation we may consider first the light adapting arrangements, and then the measuring arrangements. They are shown separately in top view in Fig. 2; actually they are together in the adaptometer. The eye remains in a fixed position, and the change from light adaptation to dark adaptation is accomplished in a fraction of a second by the simple shift of a lever.

The optical system for light adaptation is shown in the upper part of Fig. 2. The source is a circular ground glass window G, 20 mm in diameter, in a lamp housing which contains a 40-watt Mazda frosted lamp M running on a fixed amount of current. The lens L_1 is 60 mm in diameter and has a focal length of 12 cm. It is placed at its focal distance from the source G. The beam of approximately parallel light is then picked up by the lens L_3 which has a focal length of 6 cm, and a diameter of 48 mm. This lens system thus produces an image of the source G in the plane of the exit pupil EP which is situated at the principal focus of L_3. The result is that when the eye is placed at the pupil, the lens L_3 appears uniformly illuminated and covers an area whose diameter is about 35° visual angle. Between the source G and the lens L_1 there is place for two filters N and C so that both the intensity and the color of the adapting light may be varied with neutral and colored filters. About 5 cm behind the lens L_3 there is a clear glass plate P in the center of which is scratched a mark X to serve as a fixation point. This plate can be slid horizontally by means of a convenient lever so that the light-adapting field may fall on any desired part of the retina, comparable to the part later to be tested for its dark adaptation by the measuring light.

The optical arrangements for threshold testing during dark adaptation are shown in the middle of Fig. 2. The lamp M, the ground glass source G, and the lens L_1 are the same as in the previous system. However, the lens L_3 and the glass plate P have been replaced by the lens L_2 of about 36 cm focal length and 60 mm diameter. The present lens combination again images the source in the plane of the exit pupil, EP, and the eye which is there sees the lens L_2 as a uniformly illuminated circular field.

The exit pupil EP is an opening in a proper eyepiece into which may be put a lens for correcting the vision of the observer; this is neces-

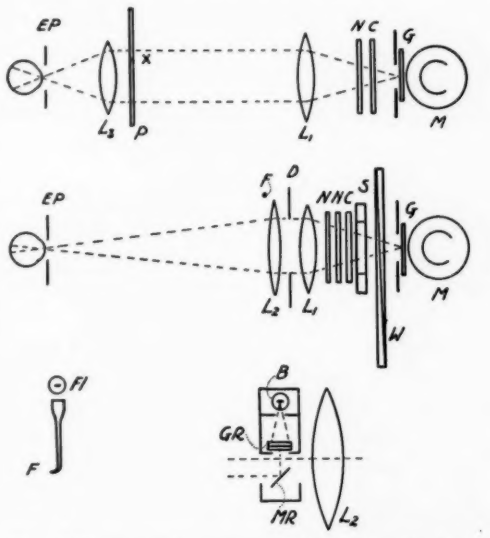

Fig. 2. Diagrammatic representation of the optical parts of the apparatus. The upper portion of the figure is the optical system for light adaptation, and below it is the system for measuring dark adaptation. At the bottom to the left is the arrangement for the luminous fixation point, while to the right is the standard for calibration. The different parts are explained in the text.

sary only under special conditions. If it is desired to keep the observer's pupil constant, this may be done by making the exit pupil small. This is necessary only for the most precise physiological work, because the change of the pupil from the light adapted condition to dark adapted condition happens so quickly that it hardly enters into the measurements.

The mount for the lens L_2 carries a groove for holding the metal diaphragm D which controls the field size. The maximum diameter of the test field is about 9.5°, but it can be any size below that. Just above the lens L_2 on the same mount is a rack carrying a luminous fixation point F, which may be placed in any position corresponding to that of the fixation mark X on the plate P used during light adaptation.

The fixation point assembly is shown separately in the lower left of Fig. 2. It consists of a small lamp-housing containing a flashlight-lamp Fl, the light from which is led down to the level of the center of the lens L_2 through a thin silvered and blackened glass rod, whose final open point F is thus small and brightly luminous. The brightness of the fixation point can be varied with either of two rheostats in series with the lamp. One of these may be operated from the observer's end, and the other from the recorder's. The entire fixation point assembly may be moved along its graduated rack and set to any position within 20° from the center to either side in the horizontal meridian.

Between the lens L_1 and the source G there is now an intensity control assembly consisting of a neutral tint gelatin-between-glass wedge, W, with its compensator, a shutter S, and a rack for two neutral filters, NN, and one color filter C. The wedge W is moved by a rack and pinion, and may be driven by either one of two knobs: one at the front of the instrument for the observer, and the other at the rear for the recorder. The wedge covers an intensity range of 1 to 1000; it is 15 cm long, and its position may be read on a millimeter scale attached to it. By the addition of neutral filters at NN, the intensity of the illumination may thus be continuously varied to any required extent.

Even though it has these two optical systems, the adaptometer is a unit, and is properly housed in a blackened metal case, which contains screens and diaphragms wherever necessary. Some idea of the actual instrument may be gained from the photographs in Fig. 3, which show it arranged for light adaptation and for dark adaptation. The instrument is used in a dark room, and is set in the wall of a cubicle which is open at the back, and in which the observer sits. This arrangement is shown in Fig. 4, and is for the purpose of shielding the observer from stray light emitted by the ground glass G, or from the small lamp used for illuminating the scale of the wedge.

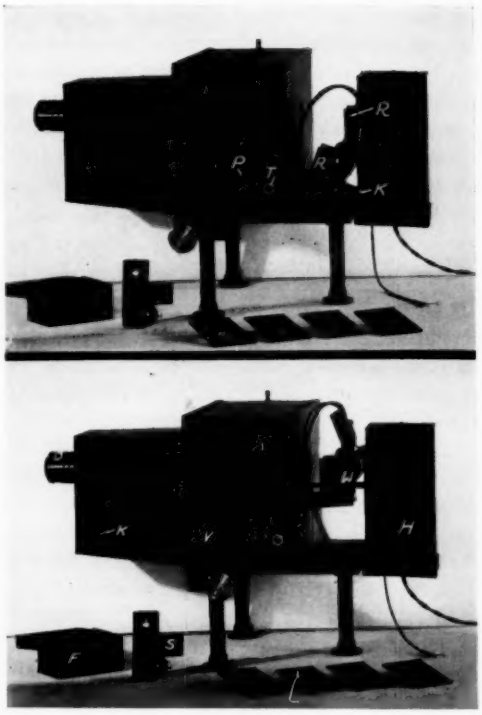

FIG. 3. The assembled adaptometer. In the upper picture it is arranged for light adaptation; in the lower for dark adaptation. The change from the one optical system to the other is made by shifting the lever V. Note the different position of the wedge-shutter-filter-rack assembly in the two conditions. The wedge is marked W, and the two filter racks R. The wedge is moved by either of two knobs K. The lamp housing is H; the switch is T. The rheostat knob for the fixation point is P; a similar rheostat and knob is on the side of the instrument not visible in the figure, and enables the subject himself to control the brightness of the fixation point. The ocular is O; the box containing the neutral and color filters is F; and the standard lamp and photometric device for calibrating the absolute brightness is S.

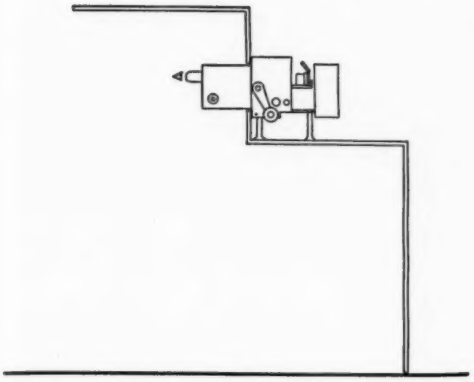

FIG. 4. The arrangement of the adaptometer in actual use. Its front end is inserted in the wall of a cubicle open at the back in which the subject sits comfortably. The subject's chin is in a chin-rest so that his eye always comes to the correct position in front of the eyepiece as indicated.

IV. CALIBRATIONS

We used five neutral filters transmitting respectively 1/4, 1/10, 1/100, 1/1000, and 1/10,000. These were calibrated with a Martens polarization photometer according to the method of Hecht, Shlaer, and Verrijp.[10] We also used two color filters, Wratten 88 which transmits only the extreme red of the spectrum beyond 680 mμ, and Corning 511 which transmits only the extreme violet of the spectrum below 460 mμ. These were calibrated for total transmission against white light with the Martens photometer. The wedge and its balancer were calibrated with white light and with each of the two color filters; similarly the neutral filters were calibrated not only for white light but for the two color filters as well.

With the wedge in place, it was necessary to determine the absolute value of the brightness visible to the eye at some one position of the wedge. This we accomplished by means of a calibrated standard specially arranged for this purpose, and shown in the lower right of Fig. 2. A small battery lamp *B* running on a controlled current illuminates three layers of ground glass *GR*. This is viewed through the circular opening by means of the mirror *MR* (a thin silvered cover slip). The current through the lamp is so regulated that the apparent brightness is 10 millilamberts as measured with a Macbeth illuminometer. The whole standard is properly encased and can be suspended in front of lens L_2 in the apparatus. Thus the eye at the exit pupil *EP* sees a circular photometric field, the left half of which is formed by the light from the lens L_2 and the right half of which is the mirror reflecting the light from the ground glass. By moving the wedge *W*, the position is then found at which the two are equal, and this sets a given position of the wedge as yielding an apparent brightness of 10 millilamberts. From this value and the calibrations of the wedge and of the filters we constructed a table showing the value of the brightness at any position of the wedge in conjunction with the necessary filters so as to give a continuously variable intensity for threshold measurements over a range of 1 to 10^{10} units.

Most measurements of dark adaptation made with reasonably sized test areas reach a final threshold of about one-millionth of a millilambert, which is nearly the same as one-millionth of a footcandle. Since the threshold intensities are to be plotted in logarithms, which would have to be negative for these intensities, we have found it convenient to use a unit which is much smaller than the millilambert. This is the micromicrolambert ($\mu\mu$l) and is the equivalent of one million millonth of a lambert, or lambert $\times 10^{-12}$. It is very nearly equal to one thousand millionth of a footcandle. With this unit, all possible values of the threshold yield positive logarithms.

V. PROCEDURE

Since the course of dark adaptation depends on so many conditions, it required many preliminary tests to ascertain the best conditions for routine determinations of dark adaptation.** Because the precise effects of nutritional states and pathological conditions on the course of dark adaptation are not known, it seemed advisable to choose such a light adaptation that both cone adaptation and rod adaptation will be separately and adequately represented in the results. This is achieved when the brightness of the light-adapting field is about 1500 ml, and is accomplished by putting a $\frac{1}{4}$ transmitting filter in the path of the light adapting system. Without the

** Most of these exploratory tests were made by Dr. Charles Haig, and we wish here to acknowledge his help and kindness.

filter, the light adapting system produces a brightness of about 6000 ml.

We chose a test field 3° in diameter as a compromise between a smaller field which would report the behavior of a reasonably uniform portion of the retina, and a larger field which can be more easily seen by untrained observers. The test field and the light-adapting field are viewed 7° nasally, using the right eye. At 7° nasally, the retinal populations of rods and cones are more nearly equal than in the center or farther in the periphery. In addition, the luminous fixation point is sufficiently removed from the measuring region of the retina so that it does not interfere with the observations. The fixation point is always maintained at a brightness that is just comfortably visible; this can be controlled either by the observer or by the recorder.

Generally the Corning filter 511 is placed in the beam of the measuring system to isolate the extreme violet of the spectrum. Two things result from this choice. First, the rod section of the dark adaptation curve is maximal in range, and second, there is a sharp and easily noticeable color difference between those threshold measurements which are made with the cones, and those made with the rods. Even the most inexperienced observer will record the fact that at the threshold the lights corresponding to the first section in Fig. 1 are all colored blue or violet, while those corresponding to the second part of the curve in Fig. 1 show no color at the threshold.

The measuring light is exposed in flashes of one-fifth of a second. This is long enough to produce a good perception of the test field during dark adaptation and short enough to be near the physiological limits of the retinal action time.

The subject enters the cubicle in the dark room and sits on a chair whose height is adjusted for comfortable observation. The chin rest is arranged so that the subject's eye fits into the eyepiece and he can easily see the fixation point through the exit pupil. A few flashes of the test light are shown for illustration, and the procedure is explained to the subject. Then he is exposed to the light-adapting system. The diameter of the light-adapting field is nearly twelve times that of the test field; its area is therefore more than 100 times as great. This assures a good light adaptation for a large area surrounding the one used later for testing.

Some seconds before making the change from light to darkness, the subject is warned, and precisely after 3 minutes of light adaptation, the lever is moved and the measuring system brought into place. From previous experience we know the approximate intensity which will be visible after a few seconds of darkness, and the wedge is set at this position before the change to darkness. This intensity is flashed on every second or so, and the observer is asked whether he has seen the circle of light. He usually reports its appearance between 6 and 8 seconds after dark adaptation has begun. He then relaxes for a minute and then resumes his observing position. The wedge has been changed so as to produce a lower brightness; the light is flashed on and the subject is asked to report its presence. He usually cannot see it, whereupon the wedge is changed so as to increase the intensity. The light is again flashed and the subject says whether he saw it or not. Depending on his answer, the wedge is changed and the light flashed every 15 seconds until a point on the wedge is found above which the subject reports that he can see the flash, and below which he reports that he cannot. The subject rests for a minute, and the procedure is repeated to determine the threshold. This is done four or five times in the next 7 or 8 minutes, thus establishing the course of the cone adaptation. The subject always reports these flashes as blue or violet. When the rod portion is reached, measurements are made once every two minutes on the rapid down portion, and then once every three or four minutes until the end of thirty or thirty-five minutes in the dark. These lights are always reported as colorless. Between test flashes, at least ten or fifteen seconds are allowed, and between the separate threshold determinations the subject always takes his eye away and relaxes. Either the subject or the recorder varies the brightness of the fixation point so that it is only just visible.

It is unnecessary to give any preliminary dark adaptation before the light adaptation. The subject always spends a few minutes in the dark room before entering the cubicle and beginning the run, and this is adequate. Moreover, the light-adapting brightness is high enough to out-

weigh any residual light-adapting effects that may remain from the time before the subject has entered the dark room.

At the end of the measurements, the subject has been dark adapted for at least thirty minutes and perhaps longer. It is often useful to make a rapid dark adaptation run at this point. For this purpose the light adaptation intensity is 3 millilamberts, and also lasts three minutes. Because the light adaptation is so low, the resulting dark adaptation is purely rod adaptation and is very rapid indeed. It is usually over in four or five minutes; it is best, however, to continue the measurements for ten or twelve minutes. In most cases the threshold which is achieved this way corresponds almost precisely to the one achieved at the close of the previous dark adaptation.

If one should wish to determine only the final threshold, this short dark adaptation would be adequate. However, this cannot be done without first dark adapting the eye completely for at least 20 minutes. Therefore one may as well avoid this inactive period by first making the controlled dark adaptation measurements following a high light adaptation.

The data already shown in Fig. 1 were made according to the procedure here given. With an inexperienced subject no great stress is to be laid on the accuracy of the first few points, because the subject is really learning how to make the measurements. The subsequent points, however, are usually very reliable. A good deal depends on the skill and experience of the experimenter. These he can acquire by practice on willing subjects. In addition it is well for the experimenter to serve as subject several times so as to realize what confronts the inexperienced person whose dark adaptation is to be measured. It deserves to be pointed out that the data given in Fig. 1 were secured on an intelligent subject who made the run for the first time, and who was completely inexperienced in making measurements of any kind.

Bibliography

1. H. Aubert, *Physiologie der Netzhaut* (Breslau, E. Morgenstern, 1865), 394 pp.
2. A. M. Bloch, "Expériences sur la vision," Compt. rendus Soc. Biol., **2**, 493 (1885).
3. A. Blondel, and J. Rey, "Sur la perception des lumières brèves à la limite de leur portée," J. de phys. et rad. **1**, 530 (1911).
4. L. S. Fridericia, and E. Holm, "Experimental Contribution to the study of the Relation Between Night Blindness and Malnutrition. Influence of Deficiency of Fat-Soluble A-Vitamin in the Diet on the Visual Purple in the Eyes of Rats," Am. J. Physiol. **73**, 63 (1925).
5. C. H. Graham, and R. Margaria, "Area and the Intensity-Time Relation in the Peripheral Retina," Am. J. Physiol. **113**, 299 (1935).
6. S. Hecht, "The Nature of Foveal Dark Adaptation," J. Gen. Physiol. **4**, 113 (1921).
7. S. Hecht, "Rods, Cones, and the Chemical Basis of Vision," Physiol. Rev. **17**, 239 (1937).
8. S. Hecht, C. Haig and A. M. Chase, "The Influence of Light Adaptation on Subsequent Dark Adaptation of the Eye," J. Gen. Physiol. **20**, 831 (1937).
9. S. Hecht, C. Haig and G. Wald, "The Dark Adaptation of Retinal Fields of Different Size and Location," J. Gen. Physiol. **19**, 321 (1935).
10. S. Hecht, S. Shlaer and C. D. Verrijp, "Intermittent Stimulation by Light. II. The Measurement of Critical Fusion Frequency for the Human Eye," J. Gen. Physiol. **17**, 237 (1933).
11. P. C. Jeans, E. Blanchard and Z. Zentmire, "Dark Adaptation and Vitamin A," J. Am. Med. Ass. **108**, 451 (1937).
12. H. Jeghers, "Night Blindness as a Criterion of Vitamin A Deficiency," Annals of Internal Medicine **10**, 1304 (1937).
13. A. Kohlrausch, "Tagessehen, Dämmersehen, Adaptation," *Handbuch der normalen und pathologischen Physiologie*, Vol. 12 (1931), p. 1499.
14. J. von Kries, "Zur Theorie des Tages- und Dämmerungssehens," *Handbuch der normalen und pathologischen Physiologie*, Vol. 13 (1929), p. 678.
15. H. K. Müller, "Über den Einfluss verschieden langer Vorbelichtung auf die Dunkeladaptation und auf die Fehlergrösse der Schwellenreiz-bestimmung während der Dunkelanpassung," Arch. Ophth. **125**, 624 (1931).
16. C. E. Palmer and H. Blumberg, "The Use of a Dark Adaptation Technique (Biophotometer) in the Measurement of Vitamin A Deficiency in Children," U. S. Public Health Report **52**, 1403 (1937).
17. H. Piéron, "De la variation de l'energie liminaire en function de la durée d'excitation pour la vision fovéale," Compt. rendus Acad. Sci. **170**, 525 (1920).
18. H. Piéron, "De la variation de l'energie liminaire en fonction de la durée d'excitation pour la vision périphérique," Compt. rendus Acad. Sci. **170**, 1203 (1920).
19. H. Piper, "Über Dunkeladaptation," Zeits. f. Psychol. u. Physiol. Sinnesorg. **31**, 161 (1903).
20. M. Schultze, "Zur Anatomie und Physiologie der Retina," Arch. mikr. Anat. **2**, 175 (1866).
21. K. Tansley, "The Regeneration of Visual Purple: Its Relation to Dark Adaptation and Night Blindness," J. Physiol. **71**, 442 (1931).
22. G. Wald, "Carotenoids and the Visual Cycle," J. Gen. Physiol. **19**, 351 (1935).
23. G. Wald and A. B. Clark, "Visual Adaptation and Chemistry of the Rods," J. Gen. Physiol. **21**, 93 (1937).
24. C. P. Winsor and A. B. Clark, "Dark Adaptation after Varying Degrees of Light Adaptation," Proc. Nat. Acad. Sci. **22**, 400 (1936).

Note on an Optical Paradox*

H. W. LEE
Chiswick, England

(Received February 25, 1938)

DR. HERZBERGER'S "paradox" is obvious without analysis.

In the Fig. 1, A is a lens corrected for two colors which focus at b, where a second lens B is placed. A third color, focused by A at c, will emerge from B in a direction parallel to that of the first two rays if the focal length of B for the third color is equal to the common focal length of A for the first two colors, as stated by Dr. Herzberger.

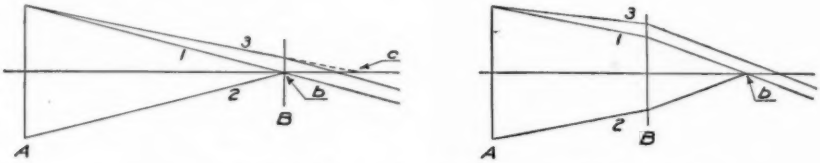

FIG. 1. The rays 1 and 2 are shown on opposite sides of the axis for clarity.

The theorem may be generalized. Suppose A and B both achromatized for two colors, which finally focus at b. A ray of a third color will emerge from B in a direction parallel to that of the first two rays if the separation of A and B (call it s) is equal to the focal length of B for the third color.

Let F_a, F_b be the powers of A and B for the first two colors, F_b', the power of B for the third color, F, the power of the complete system A and B. Then

$$s = 1/F_b'$$

and

$$F = F_a + F_b - s \cdot F_a \cdot F_b$$
$$= F_a + F_b - F_a \cdot F_b / F_b'.$$

We can write $F_b = (1+e) \cdot F_b'$ where e is small.

Then $F = F_b - e \cdot F_a$.

If F is given (as is usual in an optical problem), F_a and F_b are chosen to satisfy this equation, and this is always possible.

* M. Herzberger, "An Optical Paradox," J. O. S. A. **28**, 23 (1938).